Northumbria
University
NEWCASTLE

Metadata of the chapter that will be visualized in SpringerLink

Book Title	Dynamic Stability and Bifurcation in Nonconservative Mechanics	
Series Title		
Chapter Title	Classical Results and Modern Approaches to Nonconservative Stability	
Copyright Year	2019	
Copyright HolderName	CISM International Centre for Mechanical Sciences	
Corresponding Author	Family Name	**Kirillov**
	Particle	
	Given Name	**Oleg N.**
	Prefix	
	Suffix	
	Role	
	Division	
	Organization	Northumbria University
	Address	NE1 8ST, Newcastle upon Tyne, United Kingdom
	Email	oleg.kirillov@northumbria.ac.uk

Abstract	Stability of nonconservative systems is nontrivial already on the linear level, especially, if the system depends on multiple parameters. We present an overview of results and methods of stability theory that are specific for nonconservative applications. Special attention is given to the topics of flutter and divergence, reversible- and Hamiltonian-Hopf bifurcation, Krein signature, modes and waves of positive and negative energy, dissipation-induced instabilities, destabilization paradox, influence of structure of forces on stability and stability optimization.

Classical Results and Modern Approaches to Nonconservative Stability

Oleg N. Kirillov

Abstract Stability of nonconservative systems is nontrivial already on the linear level, especially, if the system depends on multiple parameters. We present an overview of results and methods of stability theory that are specific for nonconservative applications. Special attention is given to the topics of flutter and divergence, reversible- and Hamiltonian-Hopf bifurcation, Krein signature, modes and waves of positive and negative energy, dissipation-induced instabilities, destabilization paradox, influence of structure of forces on stability and stability optimization.

1 Introduction

1.1 "It was Greenhill who Started the Trouble...

...though he never knew it," remarked Gladwell (1990) in his historical account of the genesis of the field of nonconservative stability. As many of his scientific contemporaries, Greenhill successfully combined his interest to pure mathematical subjects, such as elliptic functions, with contributions to applied problems of ballistics (Greenhill 1879), hydrodynamics (Greenhill 1880), and elasticity (Greenhill 1881) coming from the flourishing industries of the British Empire. In particular, motivated by the problem of buckling of propeller-shafts of steamers he analyzed in Greenhill (1883) stability of an elastic shaft of a *circular* cross-section, length L, and mass per unit length m under the action of a compressive force, P, and an axial torque, M. Figure 1 taken from Gladwell (1990) illustrates five possible in this system boundary conditions:

I. Symmetric clamped-clamped shaft
II. Asymmetric clamped-clamped shaft
III. Clamped-free shaft

O. N. Kirillov (✉)
Northumbria University, NE1 8ST, Newcastle upon Tyne, United Kingdom
e-mail: oleg.kirillov@northumbria.ac.uk

D. Bigoni and O. Kirillov (eds.), *Dynamic Stability and Bifurcation in Nonconservative Mechanics*, CISM International Centre for Mechanical Sciences 586, https://doi.org/10.1007/978-3-319-93722-9_4

451277_1_En_4_Chapter ☑ TYPESET ☐ DISK ☐ LE ☑ CP Disp.:11/6/2018 Pages: 191 Layout: T1-Standard

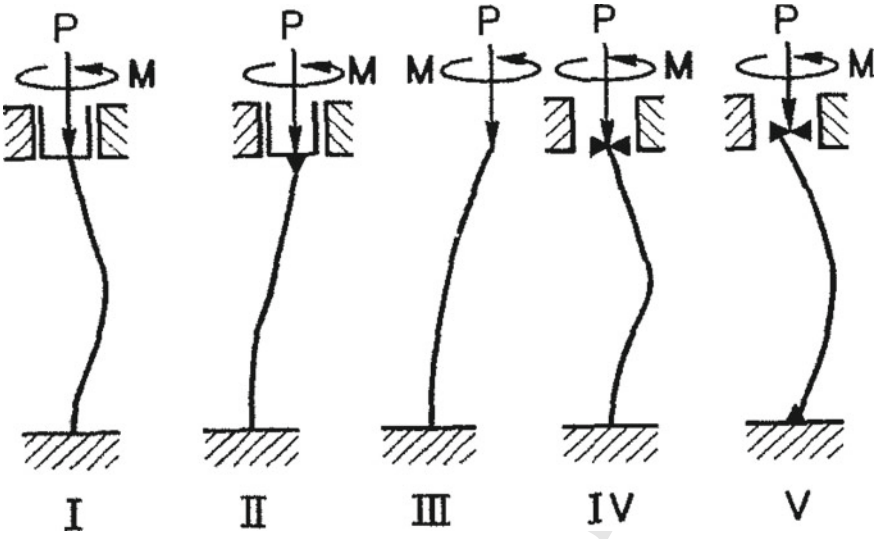

Fig. 1 Five realizations of Greenhill's elastic shaft loaded by a compressing force, P, and an axial torque, M, corresponding to five different boundary conditions (from Gladwell 1990)

IV. Clamped-hinged shaft
V. Hinged-hinged shaft

In the absence of the axial torque ($M = 0$), the Greenhill problem reduces to the famous Euler's buckling under compression of 1757. The critical load at the onset of the static instability can be found by the equilibrium method, which seeks values of the axial force, for which there are nontrivial equilibrium configurations. This yields the Euler formula for the critical buckling *force*

$$P_{cr} = k\frac{\pi^2 EI}{L^2}, \quad \text{where} \quad \begin{array}{c|c|c|c|c|c} \text{BC} & \text{I} & \text{II} & \text{III} & \text{IV} & \text{V} \\ \hline k & 4 & 1 & 1/4 & 2.046 & 1 \end{array}, \tag{1}$$

E is the Young modulus and I is the moment of inertia of a (circular) cross-section of the shaft.

In contrast to the Euler buckling case, Greenhill set $P = 0$ and tried to find the critical *torque* that causes buckling of the shaft. Using the equilibrium method, he managed to find the critical torque for the boundary conditions I, II, and V (Greenhill 1883; Ziegler 1953a, b; Gladwell 1990)

$$M_{cr} = k\frac{\pi EI}{L}, \quad \text{where} \quad \begin{array}{c|c|c|c|c|c} \text{BC} & \text{I} & \text{II} & \text{III} & \text{IV} & \text{V} \\ \hline k & 2.861 & 2 & ? & ? & 2 \end{array}. \tag{2}$$

The cases III and IV have not been analyzed by Greenhill and remained untreated until Nicolai (1928) reconsidered a variant of the case IV, in which the *axial* torque

is replaced with the *follower* torque, M, such that the vector of the torque is directed along the tangent to the deformed axis of the shaft at the end point (Gladwell 1990).

Nicolai (1928) had established that no nontrivial equilibrium configuration of the shaft exists different from the rectilinear one, meaning stability for all magnitudes, M, of the follower torque and thus $k = \infty$ in (2). Being unsatisfied with this overoptimistic result, Nicolai realized that the equilibrium method does not work properly in the case of the follower torque. He decided to study small oscillations of the shaft about its rectilinear configuration using what is now known as the Lyapunov stability theory (Lyapunov 1992) that, in particular, can predict instability via eigenvalues of the linearized problem.

Surprisingly, it turned out that there exist eigenvalues with positive real parts (instability) for all magnitudes of the torque, meaning that the critical value of the follower torque for an elastic shaft of a circular cross-section is actually $M_{cr} = 0$, i.e. $k = 0$ in (2). Because of its unusual behavior, this instability phenomenon received a name "Nicolai's paradox" (Nicolai 1928; Gladwell 1990).

In 1951-56 Ziegler re-considered the five original Greenhill problems with the Lyapunov approach and found that at $P = 0$ the shaft is unstable in cases III and IV for all values of the axial torque M, just as in Nicolai's problem with the follower torque (Ziegler 1951a, b, 1953a, b, 1956).

$$M_{cr} = k\frac{\pi E I}{L}, \quad \text{where} \quad \begin{array}{c|c|c|c|c|c} \text{BC} & \text{I} & \text{II} & \text{III} & \text{IV} & \text{V} \\ \hline \text{k} & 2.861 & 2 & 0 & 0 & 2 \end{array}. \tag{3}$$

Moreover, Ziegler realized that "Stability problem for a shaft loaded by an axial torque M, is generally *non-conservative*, as in the cases III, IV, and V, where the end slope is unconstrained. Only in exceptional cases the work of such torques in a virtual deformation can be represented as a variation of an integral" and the problem is conservative, as in cases I and II, where the equilibrium method gives the correct critical torque. "In any case", concluded Ziegler, "the results show that even very simple models are *not conservative* and, if they occur as stability problems, they should be treated dynamically", i.e. with the use of the Lyapunov approach (Ziegler 1951a, b).

Note that already Nicolai (1929) realized that the cases III and IV do not represent generic situations because it is possible to modify the end conditions, or consider a shaft with *unequal* stiffness (non-circular cross-section) yielding a nonzero critical torque (Bolotin 1963; Gladwell 1990). These conclusions were later confirmed by Ziegler (1956) and developed further in the recent works on the Nicolai paradox by Seyranian and Mailybaev (2011) and Luongo et al. (2016).

1.2 Greenhill's Shaft as a Non-self-adjoint Problem

Small vibrations of the Greenhill's shaft near its non-deformed rectilinear configuration are described by the following partial differential equation (Bolotin 1963)

$$\mathbf{l}_0\partial_z^4\mathbf{w}+\mathbf{l}_1\partial_z^3\mathbf{w}+\mathbf{l}_2\partial_z^2\mathbf{w}+m\partial_t^2\mathbf{w}=0,\quad z\in[0,L],\quad \mathbf{w}=\begin{pmatrix}w_1\\w_2\end{pmatrix} \tag{4}$$

where the matrices $\mathbf{l}_0$, $\mathbf{l}_1$, and $\mathbf{l}_2$ are

$$\mathbf{l}_0=\begin{pmatrix}EI&0\\0&EI\end{pmatrix},\quad \mathbf{l}_1=\begin{pmatrix}0&M\\-M&0\end{pmatrix},\quad \mathbf{l}_2=\begin{pmatrix}P&0\\0&P\end{pmatrix} \tag{5}$$

The nonconservative clamped-free case (III) is characterized by the following boundary conditions

$$\begin{aligned}\mathbf{w}(0)=\mathbf{w}'(0)&=0,\\ \mathbf{l}_0\mathbf{w}''(L)+\mathbf{l}_1\mathbf{w}'(L)&=0,\\ \mathbf{l}_0\mathbf{w}'''(L)+\mathbf{l}_1\mathbf{w}''(L)+\mathbf{l}_2\mathbf{w}'(L)&=0,\end{aligned} \tag{6}$$

corresponding to the constrained deflection and slope at the clamped end ($z=0$) and vanishing axial force and axial torque at the free end ($z=L$).

Separating time with $\mathbf{w}=\mathbf{u}e^{\lambda t}$, and introducing the matrix

$$\mathbf{l}_4(\lambda)=\lambda^2\begin{pmatrix}m&0\\0&m\end{pmatrix},$$

we come to the boundary eigenvalue problem

$$\mathbf{L}(\lambda)\mathbf{u}=\mathbf{l}_0\partial_z^4\mathbf{u}+\mathbf{l}_1\partial_z^3\mathbf{u}+\mathbf{l}_2\partial_z^2\mathbf{u}+\mathbf{l}_4(\lambda)\mathbf{u}=0 \tag{7}$$

with the boundary conditions

$$\begin{aligned}\mathbf{u}(0)=\mathbf{u}'(0)&=0,\\ \mathbf{l}_0\mathbf{u}''(L)+\mathbf{l}_1\mathbf{u}'(L)&=0,\\ \mathbf{l}_0\mathbf{u}'''(L)+\mathbf{l}_1\mathbf{u}''(L)+\mathbf{l}_2\mathbf{u}'(L)&=0,\end{aligned} \tag{8}$$

where prime denotes partial differentiation with respect to z. The equilibrium state is unstable if there is a value of λ with positive real part.

Integrating by parts the inner product

$$(\mathbf{Lu},\mathbf{v})=\overline{\mathbf{v}}^T\mathbf{L}(\lambda)\mathbf{u},$$

where the bar indicates complex conjugation, we obtain (Kirillov 2010)

$$\int_0^L\overline{\mathbf{v}}^T\mathbf{L}(\lambda)\mathbf{u}dx=\int_0^L(\overline{\mathbf{L}}^T(\overline{\lambda})\mathbf{v})^T\mathbf{u}dx+\mathfrak{v}^T\mathcal{L}\mathfrak{u}. \tag{9}$$

Here $\overline{\mathbf{L}}^T(\overline{\lambda})\mathbf{v}=:\mathbf{L}^\dagger(\overline{\lambda})\mathbf{v}$ is the *adjoint* differential expression (Kirillov 2010)

$$\mathbf{L}^{\dagger}(\overline{\lambda})\mathbf{v} = \sum_{q=0}^{4}(-1)^{4-q}\partial_z^{4-q}(\bar{\mathbf{l}}_q^T\mathbf{v}) = \mathbf{l}_0\partial_z^4\mathbf{v} + \mathbf{l}_1\partial_z^3\mathbf{v} + \mathbf{l}_2\partial_z^2\mathbf{v} + \mathbf{l}_4(\overline{\lambda})\mathbf{v}, \qquad (10)$$

the vectors $\mathfrak{u}$ and $\mathfrak{v}$ are

$$\mathfrak{u}^T = (\mathbf{u}^T(0), \mathbf{u}_z'^T(0), \mathbf{u}_z''^T(0), \mathbf{u}_z'''^T(0), \mathbf{u}^T(L), \mathbf{u}_z'^T(L), \mathbf{u}_z''^T(L), \mathbf{u}_z'''^T(L))$$
$$\mathfrak{v}^T = (\mathbf{v}^T(0), \mathbf{v}_z'^T(0), \mathbf{v}_z''^T(0), \mathbf{v}_z'''^T(0), \mathbf{v}^T(L), \mathbf{v}_z'^T(L), \mathbf{v}_z''^T(L), \mathbf{v}_z'''^T(L))$$

and the block matrix $\mathcal{L} := (\mathbf{l}_{ij})$

$$\mathcal{L} = \begin{pmatrix} -\mathfrak{L}(0) & 0 \\ 0 & \mathfrak{L}(L) \end{pmatrix}, \quad \mathfrak{L}(z) = \begin{pmatrix} \mathbf{l}_{00} & \mathbf{l}_{01} & \mathbf{l}_{02} & \mathbf{l}_{03} \\ \mathbf{l}_{10} & \mathbf{l}_{11} & \mathbf{l}_{12} & 0 \\ \mathbf{l}_{20} & \mathbf{l}_{21} & 0 & 0 \\ \mathbf{l}_{30} & 0 & 0 & 0 \end{pmatrix}.$$

The matrices $\mathbf{l}_{ij}$ are expressed through the matrices of the differential expression as (Kirillov 2010, 2013a)

$$\mathbf{l}_{ij} = \sum_{k=i}^{3-j}(-1)^k M_{ij}^k \partial_z^{k-i}\mathbf{l}_{3-j-k}, \quad M_{ij}^k := \begin{cases} \frac{k!}{(k-i)!i!}, & i+j \le 3 \bigcap k \ge i \ge 0 \\ 0, & i+j > 3 \bigcap k < i \end{cases}$$

which yields

$$\mathfrak{L}(z) = \begin{pmatrix} 0 & \mathbf{l}_2 & \mathbf{l}_1 & \mathbf{l}_0 \\ -\mathbf{l}_2 & -\mathbf{l}_1 & -\mathbf{l}_0 & 0 \\ \mathbf{l}_1 & \mathbf{l}_0 & 0 & 0 \\ -\mathbf{l}_0 & 0 & 0 & 0 \end{pmatrix},$$

where 0 denotes the 2×2 zero matrix.

Boundary conditions (8) can be written in the matrix form as

$$\mathbf{U}_k\mathbf{u} = \sum_{j=0}^{3}\mathbf{A}_{kj}\mathbf{u}_z^{(j)}(z=0) + \sum_{j=0}^{3}\mathbf{B}_{kj}\mathbf{u}_z^{(j)}(z=L) = 0, \quad k = 1, \ldots, 4$$

where

$$\mathbf{A}_{10} = \mathbf{A}_{21} = \mathbf{I}, \quad \mathbf{B}_{32} = \mathbf{l}_1, \quad \mathbf{B}_{33} = \mathbf{l}_0, \quad \mathbf{B}_{42} = \mathbf{l}_2, \quad \mathbf{B}_{43} = \mathbf{l}_1, \quad \mathbf{B}_{44} = \mathbf{l}_0$$

and all of other matrices $\mathbf{A}_{kj}$ and $\mathbf{B}_{kj}$ are zero. Introducing the matrices $\mathfrak{A} = (\mathbf{A}_{kj})\big|_{z=0}$ and $\mathfrak{B} = (\mathbf{B}_{kj})\big|_{z=L}$ and composing the block matrix $\mathfrak{U} = [\mathfrak{A}, \mathfrak{B}]$ we can finally write the boundary conditions (8) in the compact matrix form (Kirillov 2010, 2013a)

$$\mathfrak{U}\mathfrak{u} = [\mathfrak{A}, \mathfrak{B}]\mathfrak{u} = 0. \qquad (11)$$

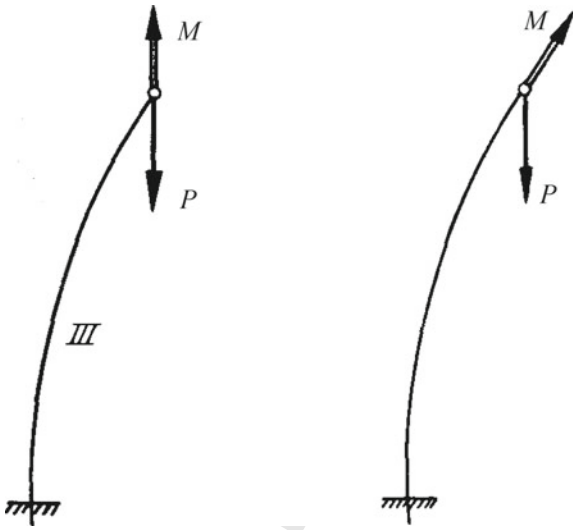

Fig. 2 (Left) Greenhill-III problem with the axial torque described by the problem (14). (Right) Nicolai's variant of the Greenhill-III problem with the follower torque described by the problem (13) which is adjoint to (14) (from Ziegler 1951a)

Extend the original matrix $\mathfrak{U}$ to a square non-degenerate matrix $\mathcal{U}$ by an appropriate choice of the auxiliary matrices $\widetilde{\mathfrak{A}}$ and $\widetilde{\mathfrak{B}}$

$$\mathfrak{U} = [\mathfrak{A}, \mathfrak{B}] \hookrightarrow \mathcal{U} = \begin{pmatrix} \mathfrak{A} & \mathfrak{B} \\ \widetilde{\mathfrak{A}} & \widetilde{\mathfrak{B}} \end{pmatrix}, \quad \det \mathcal{U} \neq 0.$$

Then, we can obtain the formula for calculation of the matrix $\mathfrak{V}$ of the boundary conditions for the adjoint differential expression (10)

$$\mathfrak{V}\mathfrak{v} = 0$$

and the auxiliary matrix $\widetilde{\mathfrak{V}}$

$$\overline{\begin{bmatrix} -\widetilde{\mathfrak{V}} \\ \mathfrak{V} \end{bmatrix}}^{T} = \mathcal{L}\mathcal{U}^{-1} = \begin{pmatrix} -\mathfrak{L}(0) & 0 \\ 0 & \mathfrak{L}(L) \end{pmatrix} \begin{pmatrix} \mathfrak{A} & \mathfrak{B} \\ \widetilde{\mathfrak{A}} & \widetilde{\mathfrak{B}} \end{pmatrix}^{-1} \tag{12}$$

Choosing

$$\widetilde{\mathfrak{A}} = \begin{pmatrix} 0\,0\,\mathbf{I}\,0 \\ 0\,0\,0\,\mathbf{I} \\ 0\,0\,0\,0 \\ 0\,0\,0\,0 \end{pmatrix}, \quad \widetilde{\mathfrak{B}} = \begin{pmatrix} 0\,0\,0\,0 \\ 0\,0\,0\,0 \\ 0\,\mathbf{I}\,0\,0 \\ \mathbf{I}\,0\,0\,0 \end{pmatrix},$$

where $\mathbf{I}$ is the 2×2 identity matrix and 0 denotes the 2×2 zero matrix, we find that $\det \mathcal{U} = (EI)^4 \neq 0$.

Then, the differential expression (10) and the relation (12) yield the adjoint boundary eigenvalue problem:

$$\begin{aligned}
\mathbf{l}_0\partial_z^4\mathbf{v}+\mathbf{l}_1\partial_z^3\mathbf{v}+\mathbf{l}_2\partial_z^2\mathbf{v}+\mathbf{l}_4(\overline{\lambda})\mathbf{v}&=0,\\
\mathbf{v}(0)=\mathbf{v}'(0)&=0,\\
\mathbf{v}''(L)&=0,\\
\mathbf{l}_0\mathbf{v}'''(L)+\mathbf{l}_2\mathbf{v}'(L)&=0,
\end{aligned}\tag{13}$$

which is instructive to compare with the original boundary eigenvalue problem (7), (8):

$$\begin{aligned}
\mathbf{l}_0\partial_z^4\mathbf{u}+\mathbf{l}_1\partial_z^3\mathbf{u}+\mathbf{l}_2\partial_z^2\mathbf{u}+\mathbf{l}_4(\lambda)\mathbf{u}&=0,\\
\mathbf{u}(0)=\mathbf{u}'(0)&=0,\\
\mathbf{l}_0\mathbf{u}''(L)+\mathbf{l}_1\mathbf{u}'(L)&=0,\\
\mathbf{l}_0\mathbf{u}'''(L)+\mathbf{l}_1\mathbf{u}''(L)+\mathbf{l}_2\mathbf{u}'(L)&=0.
\end{aligned}\tag{14}$$

It is easy to see that the differential expressions of the problems (14) and (13) are identical and the difference comes from the terms in the boundary conditions that contain the matrix $\mathbf{l}_1=\begin{pmatrix}0 & M\\ -M & 0\end{pmatrix}$ that is non-zero at nonzero torque M. Only if $M=0$ the matrix $\mathbf{l}_1=0$ and the boundary conditions of the original boundary eigenvalue problem and the adjoint boundary eigenvalue problem coincide.

Therefore, only in the absence of the torque ($M=0$), the problem (14) as well as its adjoint (13), is self-adjoint and represents a conservative system, which is not surprising in view that it is the Euler buckling problem for an elastic shaft.

In case when $M\neq 0$ the boundary conditions of the adjoint problem (13) do not coincide with the boundary conditions of the original problem (14), manifesting the non-self-adjoint nature of the non-conservative Greenhill-III problem (Ziegler 1951a, b, 1956).

It is well-known that adjoint problems have the same characteristic equation that determines eigenvalues. Hence, stability properties of (14) and (13) are identical despite they have different mechanical meaning.

The boundary value problem (14) corresponds to the original Greenhill-III clamped-free shaft loaded by the axial force and the axial torque, Fig. 2(left). It turns out that its adjoint given by (13) corresponds to the Nicolai's variant of the Greenhill-III problem with the axial force and the follower torque, Fig. 2(right), Bolotin (1963).

Both mechanical systems shown in Fig. 2 are nonconservative but have the same spectrum and, therefore, the same stability properties. In the both problems the critical value of the torque at $P=0$ is $M_{cr}=0$ (Nicolai's paradox) no matter whether the torque is axial or follower.

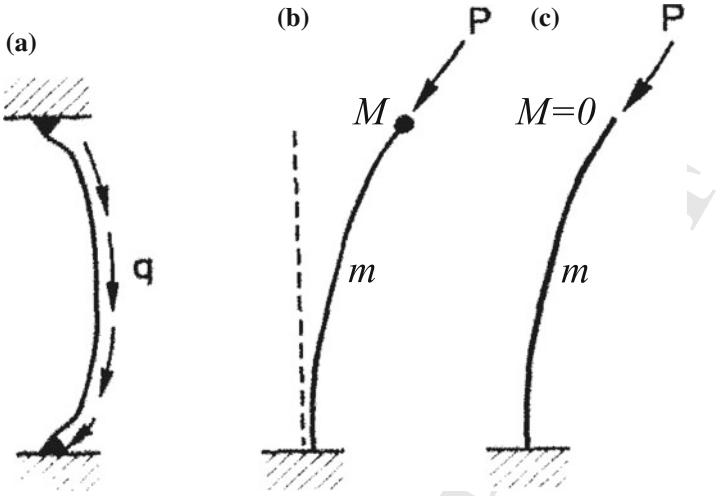

Fig. 3 **a** Pflüger's hinged-hinged column loaded by the distributed follower force (static instability, or divergence), **b** Pflüger's clamped-free column of the mass per unit length, m, carrying the end mass, M, and loaded by the concentrated follower force at the tip, **c** Beck's column loaded by the concentrated follower force is a particular case of **b** with the end mass $M = 0$ (dynamic instability, or flutter), from Gladwell (1990)

1.3 From Follower Torques to Follower Forces

A remarkable property of the Greenhill's five problems established by Nicolai and Ziegler is that, depending on boundary conditions, they could be both conservative and nonconservative. In conservative cases I and II, the Greenhill's shaft loses stability of the rectilinear equilibrium statically, i.e. without vibrations (*divergence* instability). In the nonconservative cases III and IV (and their Nicolai's variants with the *follower torque*), however, the mechanism of instability involves growing oscillations about the rectilinear equilibrium and is called *flutter*. Whereas divergence is the only possible type of instability in conservative systems, the nonconservative systems possess both flutter and divergence.

For instance, the nonconservative Greenhill-V shaft loses its stability by divergence (Greenhill 1883; Ziegler 1951a; Gladwell 1990). In 1950 Pflüger established divergence instability of a nonconservative hinged-hinged elastic column loaded by a distributed *follower force*, Fig. 3a.

Note that columns loaded by distributed follower forces provide a basis for mathematical modeling of some biomechanical objects. We mention, for instance, recent works on the human spine (Rohlmann et al. 2009), centipede locomotion (Aoi et al. 2013), and flutter of flagella under the action of distributed tangential follower forces caused by cytoskeletal motor proteins (Bayly and Dutcher 2016).

Immediately after the Pflüger's work, Beck (1952) has found flutter of a clamped-free elastic column of length, L, and mass per unit length, m, loaded by the

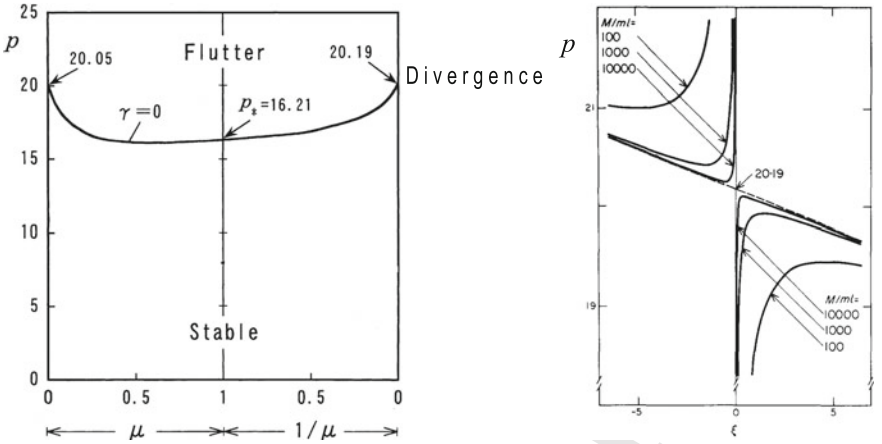

Fig. 4 (Left) Stability map for the elastic Pflüger column in the "load" - "mass ratio" plane (from Ryu and Sugiyama 2003). (Right) Load parameter $p = \frac{PL^2}{EI}$ versus dimensionless squared vibration frequency $\xi = \frac{m\omega^2 L^4}{EI}$ for the Pflüger column at different mass ratios μ when $1/\mu$ is close to zero (from Sugiyama et al. 1976)

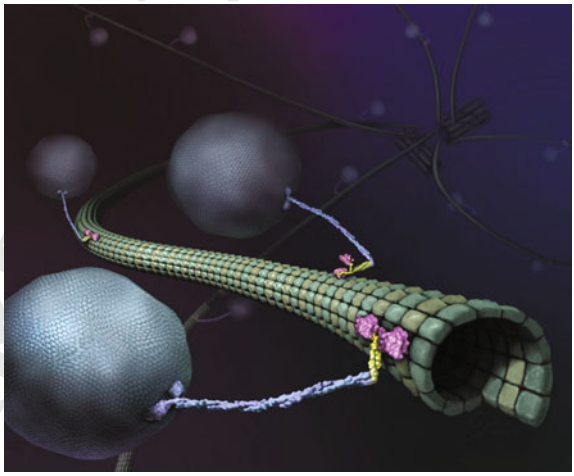

Fig. 5 Molecular motors (kinesin) transporting membranes along microtubules (cytoskeletal filaments) inside a cell cause tangential follower forces acting on the microtubules (from Vale Lab web site https://valelab4.ucsf.edu/external/moviepages/moviesMolecMotors.html)

concentrated follower force at its tip, Fig. 3c. In 1955 Pflüger re-considered the Beck's column with an end mass, M, (see Fig. 3b) and found it flutter-unstable for almost all mass ratios $\mu = \frac{M}{mL}$, except for the case when $m = 0$ or $\mu \to \infty$, Fig. 4(left).

Figure 4(right) shows the load parameter of the *Pflüger column* as a function of the squared dimensionless eigenfrequency at small values of μ^{-1}. The lower hyperbolic branch has its maximum at the critical flutter value of the load. The interval of loads

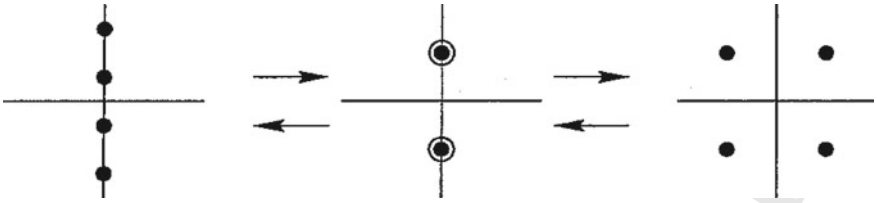

Fig. 6 Linear reversible-Hopf bifurcation: (Left) eigenvalues of a stable reversible system are all imaginary and semi-simple; (centre) a pair of two simple imaginary eigenvalues (as well as the complex conjugate pair) merges into a pair of double imaginary eigenvalues with the Jordan block at the flutter threshold; (right) the pair of the double non-semi-simple eigenvalues unfolds into a complex quadruplet inside the flutter domain (from Lamb and Roberts 1998)

corresponding to flutter is between the minimum of the upper hyperbolic branch and the maximum of the lower hyperbolic branch in Fig. 4(right). As μ increases, the size of the flutter interval tends to zero so that in the limit $\mu \to \infty$ the two hyperbolic branches merge and form a crossing at the load $p \approx 20.19$ (Sugiyama et al. 1976). Exactly at the crossing the eigenfrequency is double zero with the Jordan block, which corresponds to the onset of the divergence instability. In the $\mu \to \infty$ limit the Pflüger column is *weightless* and is known as the *Dzhanelidze column* (Bolotin 1963). The opposite limit, $\mu \to 0$, of the Pflüger column is known as the *Beck column* with the critical flutter load $p \approx 20.05$. It is instructive to note that the critical load reaches its local maxima exactly in these two limiting cases, Fig. 4(left).

Connection of a maximum of the critical load and a crossing in the load-frequency plane (Fig. 4(right)) is not a coincidence. Already Mahrenholtz and Bogacz (1981) emphasized that "In the case of complicated structures there may appear different shapes of characteristic curves, and only an analysis in the [load-frequency] plane may assure the correct results for the design of structures subjected to nonconservative loads". A general perturbation approach to local extrema associated with the crossings of characteristic curves has been developed in Kirillov and Seyranian (2002a, b).

The follower force problems of 1950-s are increasingly popular nowadays in the mathematical modeling of mechanics underlying complex cellular phenomena caused by molecular motors that translocate along cytoskeletal filaments, carrying cargo, Fig. 5. It turns out that molecular motors produce piconewton tangential follower forces acting on filaments and resulting in their flutter, which is well described by the classical continuous models of Beck and Pflüger and their discrete analogue — the *Ziegler pendulum* (Ziegler 1952; Saw and Wood 1975) — as is shown in the recent work by De Canio et al. (2017). Note that the Ziegler pendulum has been realized experimentally by Bigoni and Noselli (2011) and the Pflüger column by Bigoni et al. (2018).

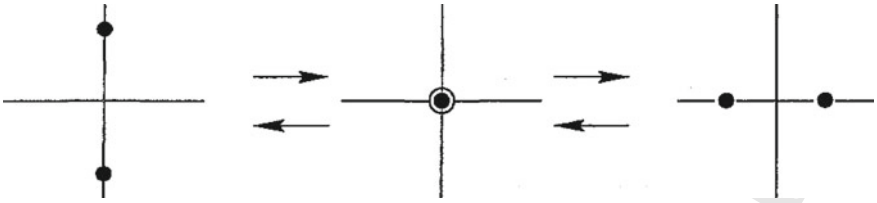

Fig. 7 Steady-state bifurcation in a reversible system: (left) eigenvalues of a stable reversible system are all imaginary and semi-simple; (centre) a conjugate pair of simple imaginary eigenvalues merges into a double zero eigenvalue with the Jordan block at the divergence threshold; (right) the double zero non-semi-simple eigenvalue splits into two real eigenvalues of opposite signs inside the divergence domain

2 Reversible and Circulatory Systems

O'Reilly, Malhotra and Namachchivaya (1995, 1996) observed that the governing equations of the classical structures with nonconservative follower loads possess a special type of symmetry, which largely determines their stability properties.

This symmetry, known as the *reversible symmetry*, can be defined with reference to the differential equation (Lamb and Roberts 1998)

$$\frac{d\mathbf{x}}{dt} = \mathbf{g}(\mathbf{x}), \quad \mathbf{x} \in \mathbb{R}^n$$

which is said to be $\mathbf{R}$-reversible ($\mathbf{R}^{-1} = \mathbf{R}$) if it is invariant with respect to the transformation $(\mathbf{x}, t) \mapsto (\mathbf{Rx}, -t)$, implying that the right hand side should satisfy $\mathbf{Rg}(\mathbf{x}) = -\mathbf{g}(\mathbf{Rx})$.

If $\mathbf{x} = \mathbf{x}_0$ is a *reversible equilibrium* such that $\mathbf{Rx}_0 = \mathbf{x}_0$, and $\mathbf{A} = \nabla\mathbf{g}$ is the linearization matrix about $\mathbf{x}_0$, then $\mathbf{A} = -\mathbf{RAR}$, and the characteristic polynomial

$$\det(\mathbf{A} - \lambda\mathbf{I}) = \det(-\mathbf{RAR} - \mathbf{R}\lambda\mathbf{R}) = (-1)^n \det(\mathbf{A} + \lambda\mathbf{I}),$$

implies that $\pm\lambda, \pm\overline{\lambda}$ are eigenvalues of $\mathbf{A}$ (Lamb and Roberts 1998). Due to the spectrum's symmetry with respect to both the real and imaginary axes of the complex plane, stability requires that *all* the eigenvalues of $\mathbf{A}$ stay on the imaginary axis, Fig. 6(left).

Transition from stability to flutter instability occurs through the *reversible-Hopf bifurcation* (Lamb and Roberts 1998) that requires the generation of a non-semi-simple double pair of imaginary eigenvalues and its subsequent separation into a complex quadruplet, Fig. 6.

Transition from stability to divergence instability is accompanied by the *steady-state bifurcation* in which two simple imaginary eigenvalues merge at zero and then split into a real couple with the opposite signs, Fig. 7.

An important for applications fact is that reversible are all equations of second order (Lamb and Roberts 1998):

$$\frac{d^2\mathbf{x}}{dt^2} = \mathbf{f}(\mathbf{x}). \tag{15}$$

Indeed, denoting $\mathbf{x}_1 = \mathbf{x}$ and $\mathbf{x}_2 = \frac{d\mathbf{x}}{dt}$ we can write the first-order system

$$\dot{\mathbf{x}}_1 = \mathbf{x}_2, \quad \dot{\mathbf{x}}_2 = \mathbf{f}(\mathbf{x}_1),$$

which is invariant under the transformation

$$\mathbf{x}_1 \to \mathbf{x}_1, \quad \mathbf{x}_2 \to -\mathbf{x}_2, \quad t \to -t.$$

The system (15) is reversible also in the case when the positional force $\mathbf{f}(\mathbf{x})$ has a non-trivial *curl*

$$\nabla \times \mathbf{f}(\mathbf{x}) \neq 0,$$

which makes the reversible system *nonconservative*. Such nonconservative *curl forces* (Berry and Shukla 2016) that cannot be derived from any potential appear in modern opto-mechanical applications, including optical tweezers (Wu et al. 2009; Simpson and Hanna 2010; Sukhov and Dogariu 2017) and *light robotics* (Phillips et al. 2017). In mechanics these nonconservative positional forces are known as *circulatory forces* for producing non-zero work along a closed circuit (Ziegler 1953a, b). A circulatory force acting on an elastic structure and remaining directed along the tangent line to the structure at the point of its application during deformation is the already familiar to us *follower force* (Ziegler 1952; Bolotin 1963).

We notice that in aeroelasticity the term 'circulatory' is frequently associated with the lift force in the Theodorsen lift model (Theodorsen 1935) that was developed to explain flutter instability occurring in aircrafts at high speeds. The Kutta–Joukowski theorem relates the lift on an airfoil to a circulatory component (circulation) of the flow around the airfoil. The circulation is the contour integral of the tangential velocity of the air on a closed loop (circuit) around the boundary of an airfoil. Hence the name *circulatory lift force*, see Pigolotti et al. (2017). Remarkably, the Theodorsen model is nonconservative and the non-potential positional forces arising in it due to the circulatory lift are simultaneously the circulatory forces in the sense of Ziegler (Pigolotti et al. 2017).

2.1 Zubov-Zhuravlev Decomposition of Non-potential Force Fields

Zubov (1970) established the following instructive result:

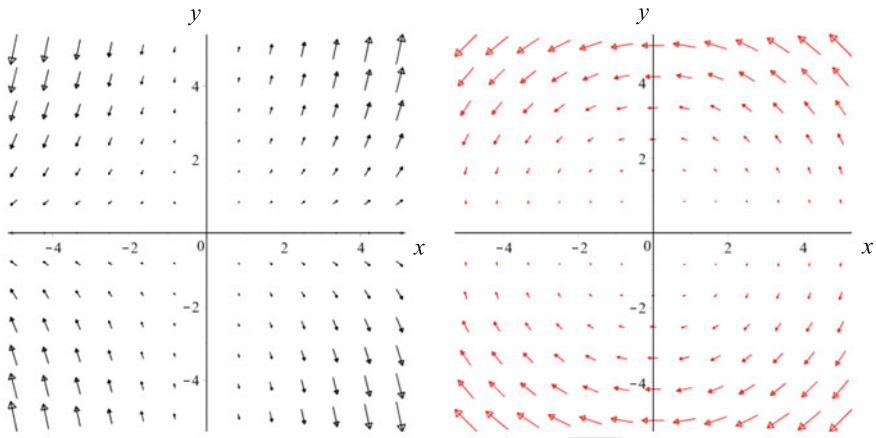

Fig. 8 (Left) The non-potential force field $\mathbf{f} = (x, xy)^T = \mathbf{f}' + \mathbf{f}''$; (right) its circulatory part $\mathbf{f}'' = \left(-\frac{y^2}{3}, \frac{xy}{3}\right)^T$

Theorem 2.1 (Zubov 1970) *Let $\boldsymbol{f}(t, \boldsymbol{x}) : \mathbb{R}_+ \times \mathbb{R}^n \to \mathbb{R}^n$ be a real-valued continuous vector-function and let $w(t, \boldsymbol{x}) = \boldsymbol{f}^T \boldsymbol{x} = \sum_{i=1}^n x_i f_i(t, \boldsymbol{x})$ be a continuously differentiable function with respect to components of $\boldsymbol{x}$. Then,*

(a) there exists a real-valued function $V(t, \boldsymbol{x}) : \mathbb{R}_+ \times \mathbb{R}^n \to \mathbb{R}$, which is continuous and continuously differentiable with respect to components of $\boldsymbol{x}$;

(b) $\boldsymbol{f}(t, \boldsymbol{x})$ possesses the following representation

$$\boldsymbol{f}(t, \boldsymbol{x}) = -\nabla_{\boldsymbol{x}} V(t, x) + \boldsymbol{P}\boldsymbol{x}, \tag{16}$$

where $\boldsymbol{P}(t, \boldsymbol{x})$ is an $n \times n$ skew-symmetric matrix ($\boldsymbol{P}^T = -\boldsymbol{P}$) with the elements that are continuous functions of t and components of $\boldsymbol{x}$.

Example: Let

$$\mathbf{f}(t, \mathbf{x}) = \begin{pmatrix} x \\ xy \end{pmatrix}, \quad \mathbf{x} = \begin{pmatrix} x \\ y \end{pmatrix} \tag{17}$$

According to Theorem 2.1, there exists the following decomposition

$$\begin{aligned} \mathbf{f}(t, \mathbf{x}) &= -\begin{pmatrix} \frac{\partial V}{\partial x} \\ \\ \frac{\partial V}{\partial y} \end{pmatrix} + \frac{y}{3}\begin{pmatrix} 0 & -1 \\ 1 & 0 \end{pmatrix}\begin{pmatrix} x \\ y \end{pmatrix} \\ &= \begin{pmatrix} x + \frac{y^2}{3} \\ \\ \frac{2xy}{3} \end{pmatrix} + \begin{pmatrix} -\frac{y^2}{3} \\ \\ \frac{xy}{3} \end{pmatrix} = \begin{pmatrix} x \\ xy \end{pmatrix}, \end{aligned} \tag{18}$$

where $V(t, \mathbf{x}) = -\frac{x^2}{2} - \frac{xy^2}{3}$, see Fig. 8. Notice that many examples of nonconservative force fields and their curls can be found in the modern literature on optical tweezers, see e.g. Wu et al. (2009), Simpson and Hanna (2010), Sukhov and Dogariu (2017), and light robotics (Phillips et al. 2017).

Zhuravlev (2007, 2008) proposed an algorithm for constructing the Zubov decomposition, in particular, of nonlinear generalized forces in the Lagrange equations. Here we are interested in positional forces only.

Let T denote kinetic energy of a mechanical system. Consider the Lagrange equations

$$\frac{d}{dt}\left(\frac{\partial T}{\partial \dot{q}_i}\right) - \frac{\partial T}{\partial q_i} = f_i(t, q_1, \ldots, q_n), \quad i = 1, \ldots, n.$$

We assume that the generalized forces f_i have positional character, being functions of time and generalized coordinates only.

Let us first assume that the generalized forces $\mathbf{f}$ are *linear*

$$\mathbf{f} = -\mathbf{A}\mathbf{q}, \quad \mathbf{A} \neq \mathbf{A}^T.$$

Recall that the $n \times n$ matrix $\mathbf{A}$ can be uniquely represented as the sum

$$\mathbf{A} = \frac{\mathbf{A} + \mathbf{A}^T}{2} + \frac{\mathbf{A} - \mathbf{A}^T}{2} = \mathbf{K} + \mathbf{N},$$

where $\mathbf{K} = \mathbf{K}^T$ is a real symmetric matrix and $\mathbf{N} = -\mathbf{N}^T$ is a real skew-symmetric matrix. Then, we can write the generalized positional force as

$$\mathbf{f} = -\mathbf{K}\mathbf{q} - \mathbf{N}\mathbf{q},$$

where the force $\mathbf{f}' = -\mathbf{K}\mathbf{q}$ is derived from the potential $V(\mathbf{q}) = \frac{1}{2}\mathbf{q}^T\mathbf{K}\mathbf{q}$:

$$\mathbf{f}' = -\nabla V(\mathbf{q})$$

and the circulatory force $\mathbf{f}'' = -\mathbf{N}\mathbf{q}$ is orthogonal to the vector of generalizes coordinates

$$\mathbf{q}^T\mathbf{f}'' = 0.$$

Indeed,

$$\mathbf{q}^T\mathbf{f}'' = -\mathbf{q}^T\mathbf{N}\mathbf{q} = (\mathbf{q}^T\mathbf{N}^T\mathbf{q})^T = \mathbf{q}^T\mathbf{N}\mathbf{q} \quad \Rightarrow \quad \mathbf{q}^T\mathbf{N}\mathbf{q} = 0.$$

A *linear circulatory system* is thus defined as (Ziegler 1953a, b, 1956)

$$\ddot{\mathbf{q}} + \mathbf{K}\mathbf{q} + \mathbf{N}\mathbf{q} = 0.$$

This is a reversible system (O'Reilly, Malhotra and Namachchivaya 1996).

Let us calculate the work of the linear positional force $\mathbf{f}$ on the displacement $\mathbf{q}$ with the frozen time

$$W = \int_0^1 \mathbf{q}^T \mathbf{f}(s\mathbf{q})ds = -\int_0^1 \mathbf{q}^T \mathbf{K}\mathbf{q}sds - \int_0^1 \mathbf{q}^T \mathbf{N}\mathbf{q}sds = -\frac{1}{2}\mathbf{q}^T \mathbf{K}\mathbf{q}$$

Therefore, the potential component of the linear positional force $\mathbf{f}$ is $\mathbf{f}' = \nabla W = -\nabla V$ and the circulatory component is just $\mathbf{f}'' = \mathbf{f} - \mathbf{f}'$. Zhuravlev (2007, 2008) employs this idea for the decomposition of *nonlinear* non-potential force fields into a potential and circulatory parts.

Following Zhuravlev (2007, 2008), we define the potential part of $\mathbf{f}$ as $\mathbf{f}' = -\nabla V$, where

$$V = -\int_0^1 \mathbf{q}^T \mathbf{f}(s\mathbf{q})ds.$$

Then, the circulatory part of the nonlinear force $\mathbf{f}$ is $\mathbf{f}'' = \mathbf{f} - \mathbf{f}'$, $\mathbf{f}'' \cdot \mathbf{q} = 0$.

Example: Decompose the non-potential vector field $\mathbf{f}$ into the potential and circulatory parts

$$\mathbf{f} = \begin{pmatrix} x \\ xy \end{pmatrix} = \mathbf{f}' + \mathbf{f}''.$$

First, construct the potential function V of the potential part of the field

$$V = -\int_0^1 [xf_x(sx, sy) + yf_y(sx, sy)]ds = -\int_0^1 (x^2 s + xy^2 s^2)ds$$

$$= -\frac{x^2}{2} - \frac{xy^2}{3}.$$

Then, find the potential part of $\mathbf{f}$

$$\mathbf{f}' = -\begin{pmatrix} \frac{\partial V}{\partial x} \\ \frac{\partial V}{\partial y} \end{pmatrix} = \begin{pmatrix} x + \frac{y^2}{3} \\ \frac{2xy}{3} \end{pmatrix}.$$

Finally, determine the circulatory part of $\mathbf{f}$

$$\mathbf{f}'' = \mathbf{f} - \mathbf{f}' = \begin{pmatrix} -\frac{y^2}{3} \\ \frac{xy}{3} \end{pmatrix} = \frac{y}{3}\begin{pmatrix} 0 & -1 \\ 1 & 0 \end{pmatrix}\begin{pmatrix} x \\ y \end{pmatrix}, \quad \mathbf{f}'' \cdot \mathbf{q} = 0,$$

in agreement with Theorem 2.1. Note that $\nabla \times \mathbf{f}'' = y\mathbf{e}_z \neq 0$.

The decomposition is unique up to the class of potential forces that are simultaneously orthogonal to the vector of coordinates: $\mathbf{q}^T \nabla V = 0$. For instance, the force derived from the potential $V(x, y) = x/(x + y)$ belongs to this class (Zhuravlev 2007, 2008)

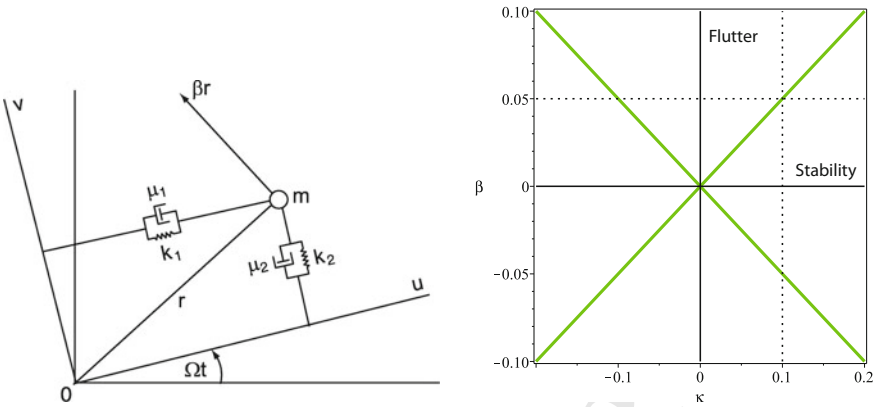

Fig. 9 (Left) Rotating shaft by Shieh and Masur (1968). (Right) Stability map of the model (21) with $k_1 = 1$ and $m = 1$

$$\mathbf{f} = -\begin{pmatrix} \frac{\partial V}{\partial x} \\ \\ \frac{\partial V}{\partial y} \end{pmatrix} = \frac{1}{(x+y)^2}\begin{pmatrix} -y \\ x \end{pmatrix}, \quad \mathbf{f}\cdot\mathbf{q} = 0.$$

In this case, obviously, $\nabla \times \mathbf{f} = -\nabla \times (\nabla V) = 0$.

2.2 Circulatory Forces in Rotor Dynamics

Non-potential circulatory forces historically originated in equations of rotor dynamics when dissipation both in rotor and stator was taken into account. The two types of damping were introduced by Kimball (1925) in order to explain a new type of instability observed in built-up rotors at high speeds in the early 1920s. Smith (1933) implemented this idea in a model of a rotor carried by a flexible shaft in flexible bearings with the linearization given by the equation

$$\ddot{\mathbf{z}} + \mathbf{D}\dot{\mathbf{z}} + 2\Omega\mathbf{G}\dot{\mathbf{z}} + (\mathbf{K} + (\Omega\mathbf{G})^2)\mathbf{z} + \beta\mathbf{N}\mathbf{z} = 0 \tag{19}$$

where $\mathbf{z}^T = (x, y)$ is the position vector in the frame rotating with the shaft's angular velocity Ω, $\mathbf{D} = \mathrm{diag}(\delta + \beta, \delta + \beta)$, $\mathbf{G} = \mathbf{J}$, $\mathbf{J} = \begin{pmatrix} 0 & -1 \\ 1 & 0 \end{pmatrix}$, $\mathbf{K} = \mathrm{diag}(k_1, k_2)$, and $\mathbf{N} = \Omega\mathbf{J}$. In Smith's model (19) the stationary (in the laboratory frame, and thus external with respect to the shaft) damping coefficient $\beta > 0$ represents the effect of viscous damping in bearing supports while the rotating damping coefficient $\delta > 0$ represents the effect of viscous damping in the shaft itself (internal damping). The term $\beta\mathbf{N}\mathbf{z}$ in Eq. (19) corresponds to circulatory forces.

In a more general model of the rotating shaft by Shieh and Masur (1968), the diagonal elements of the damping matrix in Eq. (19) are allowed to be different. In fact, Shieh and Masur (1968) model the shaft as the point mass m which is attached by two springs with the stiffness coefficients k_1 and $k_2 = k_1 + \kappa$ and two dampers with the coefficients μ_1 and μ_2 to a Cartesian coordinate system Ouv rotating at constant angular velocity Ω, Fig. 9 (left).

A non-conservative positional force which is proportional to the radial distance of the mass from the origin and perpendicular to the radius vector $\mathbf{f}'' = \begin{pmatrix} -\beta v \\ \beta u \end{pmatrix}$ acts on the mass. Such a force on the shaft in the bearings may arise in a rotating fluid or in an electromagnetic field. The linearized equations of motion of the shaft have the form (Shieh and Masur 1968; Kirillov 2013a, 2011a, b)

$$\begin{aligned} m\ddot{u} + \mu_1\dot{u} - 2m\Omega\dot{v} + (k_1 - m\Omega^2)u + \beta v = 0, \\ m\ddot{v} + \mu_2\dot{v} + 2m\Omega\dot{u} + (k_2 - m\Omega^2)v - \beta u = 0. \end{aligned} \tag{20}$$

Assuming that damping is absent ($\mu_1 = 0$, $\mu_2 = 0$) and that the shaft is not rotating $\Omega = 0$ we reduce the model (20) to the motion of the planar oscillator under the action of a nonconservative circulatory force

$$\begin{aligned} m\ddot{u} + k_1 u + \beta v = 0, \\ m\ddot{v} - \beta u + k_2 v = 0. \end{aligned} \tag{21}$$

Separating time in (21) with $u = \tilde{u}e^{\lambda t}$ and $v = \tilde{v}e^{\lambda t}$, introducing the stiffness anisotropy $\kappa = k_2 - k_1$, and writing the solvability condition for the resulting system of two algebraic equations we end up with the quadratic equation in λ^2. Its solutions

$$\lambda = \pm i\frac{\sqrt{2m(2k_1 + \kappa \pm \sqrt{-4\beta^2 + \kappa^2})}}{2m}$$

are imaginary (stability) if $\kappa^2 > 4\beta^2$ and form a complex quadruplet with negative and positive real parts (flutter) if

$$\beta^2 > \frac{\kappa^2}{4}. \tag{22}$$

This conical flutter domain is shown in Fig. 9(right) in the (κ, β)-plane of the stiffness anisotropy, κ, and magnitude of the circulatory force, β. Note that flutter instability occurs already at $\beta > 0$ if the stiffness is symmetric ($\kappa = 0$), similarly to the Nicolai paradox for the cantilever rod of circular cross-section under a follower or axial torque. However, stiffness anisotropy ($\kappa \neq 0$), no matter how small, increases the flutter threshold as $|\beta_f| = |\kappa|/2$. Again, similar to the disappearance of the Nicolai's paradox in rods of non-circular cross-section (Nicolai 1929). This is not just a coincidence. Indeed, the linearization of a two-degrees-of-freedom model of the

Greenhill-Nicolai problem considered recently by Luongo and Ferretti (2016) is described exactly by Eq. (21).

2.3 Stability Criteria for Circulatory Systems

Let us consider a circulatory system

$$\ddot{\mathbf{x}} + (\mathbf{K} + \mathbf{N})\mathbf{x} = 0 \tag{23}$$

where $\mathbf{K} = \mathbf{K}^T$ and $\mathbf{N} = -\mathbf{N}^T$ are real $m \times m$ matrices.

Separating time in (23) with the standard substitution $\mathbf{x} = \mathbf{u}e^{\lambda t}$, write the characteristic polynomial $p(\lambda) = \det(\lambda^2 + \mathbf{K} + \mathbf{N})$

$$p(\lambda) = a_0\lambda^{2m} + a_1\lambda^{2m-2} + a_2\lambda^{2m-4} + \ldots + \lambda^2 a_{m-1} + a_m.$$

Write the $2m \times 2m$ *discriminant matrix* for $p(\lambda)$

$$\Delta = \begin{pmatrix} a_0 & a_1 & a_2 & a_3 & \cdots & a_n & 0 & 0 & 0 \\ 0 & ma_0 & (m-1)a_1 & (m-2)a_2 & \cdots & a_{m-1} & 0 & 0 & 0 \\ 0 & a_0 & a_1 & a_2 & \cdots & a_{m-1} & a_m & 0 & 0 \\ 0 & 0 & ma_0 & (m-1)a_1 & \cdots & 2a_{m-2} & a_{m-1} & 0 & 0 \\ \cdots & \cdots & \cdots & \cdots & \cdots & \cdots & \cdots & \cdots & \cdots \\ \cdots & \cdots & \cdots & \cdots & \cdots & \cdots & \cdots & \cdots & \cdots \\ 0 & 0 & 0 & \cdots & 0 & a_0 & a_1 & \cdots & a_m \\ 0 & 0 & 0 & \cdots & 0 & 0 & ma_0 & \cdots & a_{m-1} \end{pmatrix} \tag{24}$$

Consider a sequence of determinants of all even-order submatrices along the main diagonal of Δ starting from the upper left corner

$$\det \Delta_1 = \det \begin{pmatrix} a_0 & a_1 \\ 0 & ma_0 \end{pmatrix}, \quad \det \Delta_2, \quad \cdots, \quad \det \Delta_m = \det \Delta \tag{25}$$

Theorem 2.2 (Gallina criterion Gallina 2003) *A necessary and sufficient condition for all the eigenvalues λ of the eigenvalue problem for the undamped circulatory system (23) to be imaginary is that the elements of the discriminant sequence corresponding to the discriminant matrix Δ are all nonnegative and that the coefficients of the polynomial $p(\lambda)$ are either all non-positive or all non-negative:*

$$\det \Delta_1 \geq 0, \quad \det \Delta_2 \geq 0, \quad \cdots, \quad \det \Delta_m = \det \Delta \geq 0,$$

$$a_0 \geq 0, \quad a_1 \geq 0, \quad a_2 \geq 0, \quad \ldots, \quad a_m \geq 0.$$

With the use of the Leverrier-Barnett algorithm, see e.g. Kirillov (2013a), one can write the characteristic polynomial of the system (23) as

$$p(\lambda) = \lambda^{2m} + \mathrm{tr}\mathbf{K}\lambda^{2m-2} + \frac{1}{2}\left((\mathrm{tr}\mathbf{K})^2 - \mathrm{tr}\mathbf{K}^2 - \mathrm{tr}\mathbf{N}^2\right)\lambda^{2m-4} + \dots \tag{26}$$

Since for the polynomial (26) we have $\det \Delta_1 = m > 0$, then, Gallina criterion gives a sufficient condition for instability if

$$a_0^2((a_1^2 - a_2a_0)m - a_1^2) < 0. \tag{27}$$

With the explicit expressions for the coefficients of the polynomial from (26), we re-write (27) as

$$\mathrm{tr}\mathbf{K}^2 + \mathrm{tr}\mathbf{N}^2 < \frac{1}{m}(\mathrm{tr}\mathbf{K})^2. \tag{28}$$

Taking into account that

$$\mathrm{tr}\mathbf{K}^2 = \mathrm{tr}(\mathbf{K}^T\mathbf{K}) = \|\mathbf{K}\|^2,$$

and

$$\mathrm{tr}\mathbf{N}^2 = \mathrm{tr}(-\mathbf{N}^T\mathbf{N}) = -\|\mathbf{N}\|^2,$$

where the norm is understood as the Frobenius norm, we represent (28) in the form

$$\|\mathbf{N}\|^2 > \|\mathbf{K}\|^2 - \frac{1}{m}(\mathrm{tr}\mathbf{K})^2. \tag{29}$$

The inequality (29) is known as the *Bulatovic flutter condition*.

Theorem 2.3 (Bulatovic flutter condition Bulatovic 2011, 2017) *If*

$$\|\boldsymbol{N}\|^2 > \|\boldsymbol{K}\|^2 - \frac{1}{m}(tr\boldsymbol{K})^2$$

the equilibrium of the circulatory system

$$\ddot{\boldsymbol{x}} + (\boldsymbol{K} + \boldsymbol{N})\boldsymbol{x} = \boldsymbol{F}(\boldsymbol{x}, \dot{\boldsymbol{x}}),$$

where $\boldsymbol{K} = \boldsymbol{K}^T$, $\boldsymbol{N} = -\boldsymbol{N}^T$, and $\boldsymbol{F}$ is a collection of terms of no lower than second order, is unstable.

In a particular case when the stiffness matrix is proportional to the identity matrix, $\mathbf{K} = \kappa\mathbf{I}$, we have $\mathrm{tr}\mathbf{K} = \kappa m$ and $\mathrm{tr}\mathbf{K}^2 = \|\mathbf{K}\|^2 = \kappa^2 m$. With this, the flutter condition (29) reduces to the inequality $\|\mathbf{N}\|^2 > 0$, which is always fulfilled if $\|\mathbf{N}\| \neq 0$. Instability in this degenerate case occurs at arbitrary small circulatory forces. This statement is the famous Merkin theorem, see e.g. Krechetnikov and Marsden (2007); Udwadia (2017).

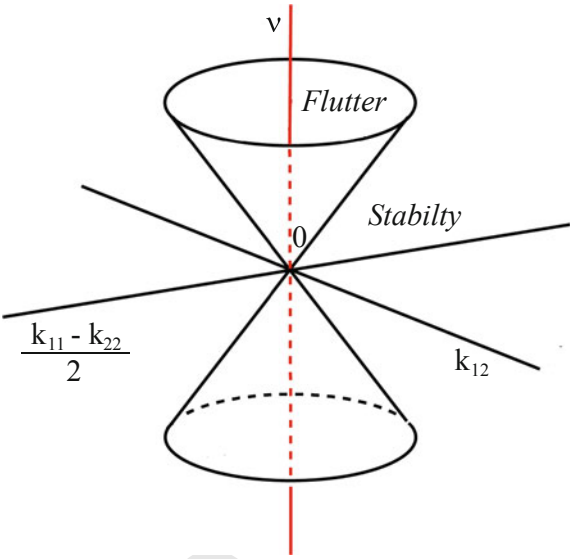

Fig. 10 Geometrical interpretation of the Bulatovic flutter condition and Merkin theorem for $m = 2$ degrees of freedom

Theorem 2.4 (Merkin Theorem (Merkin 1956)) *Perturbation by arbitrary linear circulatory forces of a stable pure potential system with eigenfrequencies coinciding into one with the algebraic multiplicity equal to the dimension of the system destroys the stability of the equilibrium regardless of the form of the nonlinear terms.*

2.4 Geometrical Interpretation for $m = 2$ Degrees of Freedom

Let us now assume that $m = 2$ in Eq. (23). Notice that the 2×2 matrix $\mathbf{A} = \mathbf{K} + \mathbf{N}$ has the following decomposition

$$\mathbf{A} = \frac{k_{11} + k_{22}}{2} \begin{pmatrix} 1 & 0 \\ 0 & 1 \end{pmatrix} + \frac{1}{2} \begin{pmatrix} k_{11} - k_{22} & 2k_{12} \\ 2k_{12} & k_{22} - k_{11} \end{pmatrix} + \begin{pmatrix} 0 & -\nu \\ \nu & 0 \end{pmatrix} = \mathbf{C} + \mathbf{H} + \mathbf{N}, \tag{30}$$

where the matrix $\mathbf{C}$ corresponds to potential forces of spherical type, $\mathbf{H}$ to potential forces of hyperbolic type, and $\mathbf{N}$ to circulatory forces (Zhuravlev 2007, 2008). When $\mathbf{H} = 0$ we are in the conditions of the Merkin theorem.

Calculating the eigenvalues of the corresponding eigenvalue problem, which are the roots of the polynomial $\det(\lambda^2\mathbf{I} + \mathbf{A})$, we find

$$\lambda^2 = -\frac{k_{11}+k_{22}}{2} \pm \frac{1}{2}\sqrt{(k_{11}-k_{22})^2 + 4k_{12}^2 - 4\nu^2}. \tag{31}$$

which is complex (flutter) if

$$\nu^2 > \frac{(k_{11}-k_{22})^2}{4} + k_{12}^2. \tag{32}$$

This condition determines an interior of a double cone in the space of parameters $\frac{k_{11}-k_{22}}{2}$, k_{12}, and ν, see Fig. 10.

Let us establish a connection between the stability diagram of Fig. 10 and already known to us Bulatovic's flutter condition and Merkin's theorem.

Observing that

$$\|\mathbf{K}\|^2 = k_{11}^2 + k_{22}^2 + 2k_{12}^2, \quad (\mathrm{tr}\mathbf{K})^2 = (k_{11}+k_{22})^2, \quad \|\mathbf{N}\|^2 = 2\nu^2$$

we find

$$\|\mathbf{K}\|^2 - \frac{1}{2}(\mathrm{tr}\mathbf{K})^2 = \frac{(k_{11}-k_{22})^2}{2} + 2k_{12}^2.$$

Hence,

$$\nu^2 > \frac{(k_{11}-k_{22})^2}{4} + k_{12}^2 \Leftrightarrow \|\mathbf{N}\|^2 > \|\mathbf{K}\|^2 - \frac{1}{m}(\mathrm{tr}\mathbf{K})^2.$$

and we establish the equivalence of the Bulatovic flutter condition (29) and (32). Therefore, the Bulatovic flutter condition determines the conical flutter domain in Fig. 10. The axis of the cone passing through the origin at $k_{11}-k_{22}=0, k_{12}=0$ and $\nu=0$ lies in the flutter domain, corresponding to the condition $\nu^2>0$ or $\|\mathbf{N}\|^2>0$ given by the Merkin theorem.

The apex of the cone at $k_{11}-k_{22}=0$, $k_{12}=0$ and $\nu=0$ corresponds to the potential system under the action of potential forces of spherical type, which is stable. Potential forces of spherical type and circulatory forces imply Merkin's instability at all values of $\nu \neq 0$. Potential forces of hyperbolic type stabilize the Merkin-unstable system at $\nu < \nu_{cr} = \frac{(k_{11}-k_{22})^2}{4} + k_{12}^2$. This is equivalent to the finite threshold for a torque in the Nicolai shaft with a non-circular cross-section (Nicolai 1929; Ziegler 1951a, b; Bolotin 1963; Seyranian and Mailybaev 2011; Luongo and Ferretti 2016).

2.5 *Approximating Flutter Cone by Perturbation of Eigenvalues*

Consider the matrix $\mathbf{A}$ defined by Eq. (30) as a function of three parameters $\mathbf{A} = \mathbf{A}(k_{22}, k_{12}, \nu)$, whereas the parameter k_{11} is fixed, and the eigenvalue problem for it

$$\mathbf{A}(k_{22}, k_{12}, \nu)\mathbf{u} = \sigma\mathbf{u}, \tag{33}$$

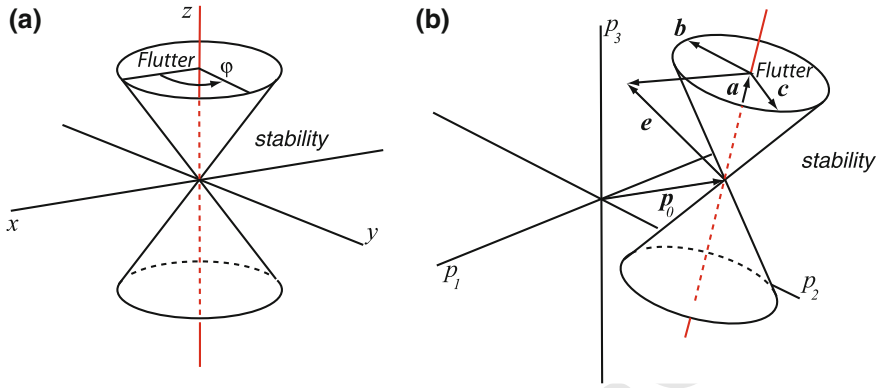

Fig. 11 Conical flutter domain of a circulatory system in the vicinity of a point in the parameter space corresponding to a semi-simple eigenvalue of the matrix $\mathbf{A} = \mathbf{K} + \mathbf{N}$. **a** Given by Eq. (39). **b** Given by Eq. (40)

where $\sigma = -\lambda^2$.

Let $\mathbf{A}_0 = \mathbf{A}(k_{22} = k_{11}, k_{12} = 0, \nu = 0)$. Then

$$\mathbf{A}_0 = \begin{pmatrix} k_{11} & 0 \\ 0 & k_{11} \end{pmatrix}. \tag{34}$$

This matrix has a *semi-simple* real eigenvalue $\sigma_0 = k_{11}$ with the two linearly-independent right eigenvectors $\mathbf{u}_1$ and $\mathbf{u}_2$ and two linearly-independent left eigenvectors, $\mathbf{v}_1$ and $\mathbf{v}_2$. In general, left and right eigenvectors of a non-symmetric matrix differ but in our example $\mathbf{A}_0$ is real and symmetric and we can choose

$$\mathbf{u}_1 = \mathbf{v}_1 = \begin{pmatrix} 0 \\ 1 \end{pmatrix}, \quad \mathbf{u}_2 = \mathbf{v}_2 = \begin{pmatrix} 1 \\ 0 \end{pmatrix}. \tag{35}$$

Let us introduce the vector of parameters $\mathbf{p} = (k_{22}, k_{12}, \nu)$ and denote $\mathbf{p}_0 = (k_{11}, 0, 0)$. Then, $\mathbf{A}(k_{22}, k_{12}, \nu) = \mathbf{A}(\mathbf{p})$ and $\mathbf{A}_0 = \mathbf{A}(\mathbf{p}_0)$.

In the following, we briefly consider a perturbative approach to the study of stability of circulatory systems following (Kirillov 2010, 2013a). We introduce a scalar parameter ε and consider a smooth path in the parameter space $\mathbf{p}(\varepsilon)$ and consider it in the vicinity of $\mathbf{p}_0 = \mathbf{p}(\varepsilon = 0)$

$$\mathbf{p}(\varepsilon) = \mathbf{p}_0 + \varepsilon \frac{d\mathbf{p}}{d\varepsilon} + o(\varepsilon).$$

Then, the matrix family $\mathbf{A}(\mathbf{p}(\varepsilon))$ takes an increment

$$\mathbf{A}(\mathbf{p}(\varepsilon)) = \mathbf{A}_0 + \varepsilon \mathbf{A}_1 + o(\varepsilon),$$

where $\mathbf{A}_1 = \sum_{s=1}^{n} \frac{\partial \mathbf{A}}{\partial p_s} \frac{dp_s}{d\varepsilon}$. In our example $n = 3$, $p_1 = k_{22}$, $p_2 = k_{12}$, and $p_3 = \nu$.

It can be shown by perturbation argument (Kirillov 2010, 2013a) that the double semi-simple eigenvalue σ_0 splits into two simple eigenvalues as follows

$$\sigma(\varepsilon) = \sigma_0 + \varepsilon \frac{(\mathbf{A}_1\mathbf{u}_1, \mathbf{v}_1) + (\mathbf{A}_1\mathbf{u}_2, \mathbf{v}_2)}{2} \pm \frac{\varepsilon}{2}\sqrt{D} + o(\varepsilon), \tag{36}$$

where $D = x^2 + y^2 - z^2$ and

$$x = \langle \mathbf{f}_*, \mathbf{e} \rangle, \quad y = \langle \mathbf{f}_+, \mathbf{e} \rangle, \quad z = \langle \mathbf{f}_-, \mathbf{e} \rangle. \tag{37}$$

The vector $\mathbf{e} = \left(\frac{dp_1}{d\varepsilon}, \ldots, \frac{dp_n}{d\varepsilon} \right)^T$. The components of the vectors $\mathbf{f}_*$, $\mathbf{f}_+$ and $\mathbf{f}_-$ are given by the expressions

$$\begin{aligned} f_{*,s} &= (\partial_{p_s}\mathbf{A}\mathbf{u}_1, \mathbf{v}_1) - (\partial_{p_s}\mathbf{A}\mathbf{u}_2, \mathbf{v}_2), \\ f_{\pm,s} &= (\partial_{p_s}\mathbf{A}\mathbf{u}_1, \mathbf{v}_2) \pm (\partial_{p_s}\mathbf{A}\mathbf{u}_2, \mathbf{v}_1). \end{aligned} \tag{38}$$

The brackets $\langle\ ,\ \rangle$ in (37) denote the inner product of vectors in n-dimensional space and the brackets $(,)$ in (38) denote the inner product of vectors in m-dimensional space. Recall that in our example $m = 2$ and $n = 3$.

The perturbed eigenvalues (36) are complex if

$$z^2 > x^2 + y^2, \tag{39}$$

that is, inside the conical surface in the (x, y, z)-space, see Fig. 11a.

In order to describe this conical flutter domain in the space of parameters $\mathbf{p}$, we introduce the vectors

$$\mathbf{a} = \mathbf{f}_* \times \mathbf{f}_+, \quad \mathbf{b} = \mathbf{f}_* \times \mathbf{f}_-, \quad \mathbf{c} = \mathbf{f}_- \times \mathbf{f}_+$$

and the polar angle φ through the relations $x = z\cos\varphi$ and $y = z\sin\varphi$. Then we can describe the flutter cone at the point $\mathbf{p}_0$ as the *tangent cone* to the flutter domain, i.e. as a set of directions $\mathbf{e}$ in which from the given point one can send a curve that lies in the flutter domain:

$$\{\mathbf{e} : \mathbf{e} = t(\mathbf{a} + d(\mathbf{b}\sin\phi + \mathbf{c}\cos\phi)),\ t \in \mathbb{R},\ \varphi \in [0, 2\pi],\ d \in [0, 1)\}. \tag{40}$$

Taking into account the eigenvectors (35) of the matrix (34) and constructing the gradient vector

$$\mathbf{e} = \begin{pmatrix} k_{22} - k_{11} \\ k_{12} \\ \nu \end{pmatrix}$$

we find the vectors

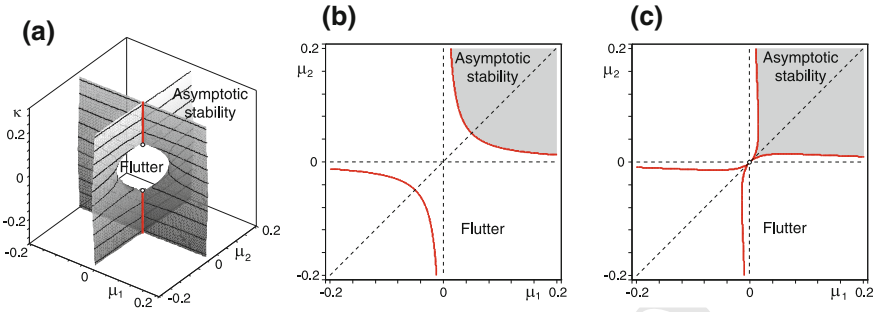

Fig. 12 Flutter instability of the shaft (41) at weak damping and weak stiffness anisotropy for $k_1 = 1$, $m = 1$ and $\beta = 0.05$. **a** Stability domain (42) with two Whitney umbrella singular points in the (μ_1, μ_2, κ)-space. **b** Instability at weak damping and zero stiffness anisotropy ($\kappa = 0$). **c** Stabilization by weak damping at large stiffness anisotropy ($\kappa = 2\beta = 0.1$)

$$\mathbf{f}_* = \begin{pmatrix} 1 \\ 0 \\ 0 \end{pmatrix}, \quad \mathbf{f}_+ = \begin{pmatrix} 0 \\ 2 \\ 0 \end{pmatrix}, \quad \mathbf{f}_- = \begin{pmatrix} 0 \\ 0 \\ -2 \end{pmatrix}.$$

Substituting these vectors into the flutter condition

$$\langle \mathbf{f}_*, \mathbf{e} \rangle^2 + \langle \mathbf{f}_+, \mathbf{e} \rangle^2 - \langle \mathbf{f}_-, \mathbf{e} \rangle^2 < 0,$$

we reproduce the flutter cone (32).

Note that the conical singularity is one of the eight generic singularities of codimension 3 that can occur on stability boundaries of circulatory systems with at least three parameters (Kirillov 2013a). In case of two parameters the number of generic singular points reduces to four, and in one-parameter families of circulatory systems we have only two singular points, corresponding to the reversible-Hopf bifurcation and to the steady-state bifurcation shown in Figs. 6 and 7, respectively.

3 Perturbing Circulatory Systems

3.1 Shieh–Masur Shaft with Dissipative Forces

Let us return to the model (20) of a rotating shaft by Shieh and Masur (1968) in the case when the shaft is non-rotating ($\Omega = 0$) and take into account damping

$$\begin{aligned} m\ddot{u} + \mu_1 \dot{u} + k_1 u + \beta v &= 0 \\ m\ddot{v} + \mu_2 \dot{v} + k_2 v - \beta u &= 0 \end{aligned} \qquad (41)$$

Separating time with $u = \tilde{u}e^{\lambda t}$ and $v = \tilde{v}e^{\lambda t}$ and applying to the characteristic polynomial of the resulting system of two algebraic equations the Hurwitz stability criterion, we find that the trivial solution $u = 0$, $v = 0$ is stable asymptotically, if and only if

$$(\mu_1 + \mu_2)^2(\mu_1\mu_2 k_1 - m\beta^2) + \mu_1\mu_2\kappa(\kappa m + \mu_1(\mu_1 + \mu_2)) > 0,$$
$$\mu_1 + \mu_2 > 0. \tag{42}$$

The stability conditions (42) ensure the exponential decay with time of all no-trivial solutions $u(t)$ and $v(t)$ of the Eq. (41).

The conditions (42) have a complicated form in contrast to the undamped case corresponding to $\mu_1 = 0$ and $\mu_2 = 0$ when the shaft is stable at $\beta^2 < \kappa^2/4$. How the damped and undamped cases are connected? Does the undamped flutter condition always follow from the damped one in the limit of vanishing damping coefficients? Let us investigate.

Equate the left side of Eq. $(42)_1$ to zero and solve the resulting equation with respect to κ. Then assume in the result $\mu_1 = b\mu_2$ and consider its limit as $\mu_2 \to 0$. This yields

$$\kappa(b) = \pm\beta\left(\sqrt{b} + \frac{1}{\sqrt{b}}\right), \quad b = \frac{\mu_1}{\mu_2}. \tag{43}$$

The function $\kappa(b)$ has a minimum equal to 2β and a maximum equal to -2β at $b = 1$. This means that the threshold of stability of the dissipative system coincides with the threshold of the undamped system ($\kappa^2 = 4\beta^2$) in the limit of vanishing dissipation only if $\mu_1 = \mu_2$, or $b = \mu_1/\mu_2 = 1$.

Let us expand $\kappa(b)$ in a Taylor series in the vicinity of $b = 1$

$$\kappa = \pm 2\beta \pm \beta\frac{(b-1)^2}{4} + o\left((b-1)^2\right). \tag{44}$$

Truncating the series and taking into account that $b = \mu_1/\mu_2$, we write

$$\kappa(\mu_1, \mu_2) = \pm 2\beta \pm \beta\frac{(\mu_1 - \mu_2)^2}{4\mu_2^2}. \tag{45}$$

Equation (45) is in the form $zy^2 = x^2$, which is the normal form of a surface in the $Oxyz$-space that has the Whitney umbrella singular point at the origin (Bottema 1956; Arnold 1972; Langford 2003; Kirillov and Verhulst 2010). The function $z(x, y) = x^2/y^2 > 0$ at all x, y except for the specific line $x = 0$, where $z(0, y) = 0$.

In our case the line $x = 0$ is the line $\mu_1 = \mu_2$ in the (μ_1, μ_2)-plane, see Fig. 12 where the stability domain (42) is shown with the two Whitney umbrella singular points situated on the κ-axis at $\kappa = \pm 2\beta$. It is remarkable that a weak stiffness anisotropy in the presence of weak damping does not prevent the system from flutter when circulatory forces are acting, Fig. 12b. Indeed, at $\kappa = 0$ criterion (42)

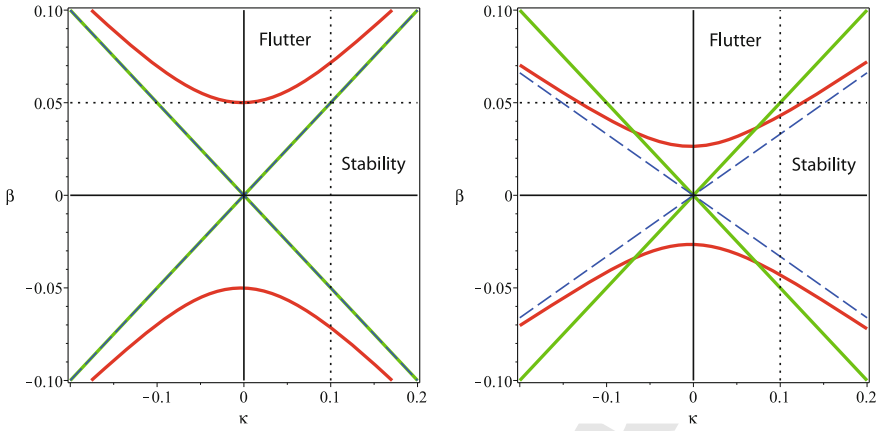

Fig. 13 Stability map of the rotating shaft with $k_1 = 1$, $m = 1$ (green lines) without dissipation and (red curves) with dissipation when (left) dissipation coefficients are equal, $\mu_1 = \mu_2 = 0.05$, (right) when $\mu_1 = 0.07$ and $\mu_2 = 0.01$. The asymptotic dashed lines are given by Eqs. (48) and (49), respectively

yields stability beyond a hyperbolic branch in the first quadrant of the (μ_1, μ_2)-plane

$$\mu_1\mu_2 k_1 - m\beta^2 > 0, \tag{46}$$

at some distance form the origin. Notice that stability condition (46) traces back to Kapitsa (1939) who derived it in his study of transition to supercritical speeds in a special high-frequency expansion turbine that he developed for liquefaction of air.

As soon as the absolute value of the stiffness anisotropy increases, the stability domain comes closer to the origin and touches it in a cuspidal point exactly when $\kappa = \pm 2\beta$, Fig. 12c, i.e. at the Whitney umbrella singular points. We observe that at $\kappa = \pm 2\beta$ there exists only one direction pointing to the stability domain from the origin, and this direction is along the line $\mu_1 = \mu_2$, in full agreement with (45). Decreasing dissipation along this line yields tending the critical flutter load smoothly to its values $\kappa = \pm 2\beta$ for the undamped shaft. However, this is not true for all other directions, i.e. damping ratios $b = \mu_1/\mu_2$ different from 1.

In fact, near the Whitney umbrella points the stability boundary behaves much like a *ruled surface*, which has exactly two rulers $\mu_1 = b_\pm \mu_2$, where

$$b_\pm = 1 + \frac{\kappa^2 - 4\beta^2}{2\beta^2} \pm \kappa \frac{\sqrt{\kappa^2 - 4\beta^2}}{2\beta^2}$$

at every κ such that $\kappa^2 > 4\beta^2$. Consequently, tending damping to zero along either of the two directions, $\mu_1 = b_\pm \mu_2$, will result in the value of κ that does not coincide with the undamped values $\pm 2\beta$. The flutter load of the damped shaft has therefore a singular zero-dissipation limit at the Whitney umbrella points. At every damping

ratio, except for 1, the flutter load in the limit of vanishing dissipation differs by a finite value from the flutter load of the undamped system. This is the famous *Ziegler–Bottema destabilization paradox* (Ziegler 1952; Bottema 1956).

Now we are prepared to answer how dissipation affects the conical flutter domain of the undamped shaft given by the Bulatovich flutter condition that is shown in Fig. (9)(right). From (43) an expression for the two lines in the (κ, β)-plane follows

$$\beta = \pm \frac{\sqrt{\mu_1 \mu_2}}{\mu_1 + \mu_2} \kappa. \tag{47}$$

The slope of the lines depends on the damping ratio in the manner dictated by the ruled surface geometry near the Whitney umbrella singularities. Indeed, for equal damping coefficients, $\mu_1 = \mu_2$, the lines (47) are

$$\beta = \pm \frac{\sqrt{\mu_1 \mu_2}}{\mu_1 + \mu_2} \kappa = \pm \frac{1}{2} \kappa. \tag{48}$$

They coincide with the flutter boundaries of the undamped system, Fig. 13(left). If we plot the stability domain (42) in the (κ, β)-plane for different damping coefficients that satisfy the constraint $\mu_1 = \mu_2$, we will see that the stability boundary is a hyperbolic curve with the asymptotes (48). In the limit of vanishing dissipation such that $\mu_1 = \mu_2$ the stability boundary of the dissipative system degenerates into the cone $\kappa^2 = 4\beta^2$.

However, taking the limit of vanishing dissipation at any other constraint on the damping coefficients, say, $\mu_1 = 7\mu_2$, results in the different conical domain with the boundaries

$$\beta = \pm \frac{\sqrt{\mu_1 \mu_2}}{\mu_1 + \mu_2} \kappa = \pm \frac{\sqrt{7}}{6} \kappa. \tag{49}$$

The flutter domain in the limit of vanishing dissipation given by the inequality $36\beta^2 > 7\kappa^2$ is therefore larger than the flutter domain of the undamped shaft, $\kappa^2 < 4\beta^2$, Fig. 13(right), providing an instructive example of a dissipation-induced instability (Bloch et al. 1994; Krechetnikov and Marsden 2007).

3.2 A Circulatory System Perturbed by Dissipative Forces

The Shieh and Masur (1968) shaft is a non-conservative system with two degrees of freedom illustrating the properties summarized in the remark by Leipholz (1987): "*Independent works of* Bottema (1956) *and* Bolotin (1963) *for* second-order *systems has shown that in the non-conservative case and for different damping coefficients the stability condition is discontinuous with respect to the undamped case.*"

Let us build a general theory proving this effect in a finite-dimensional mechanical system of *arbitrary order* under the action of positional conservative forces represented by a real symmetric matrix $\mathbf{K} = \mathbf{K}^T$ and positional non-conservative (or circulatory) forces with the real skew-symmetric matrix $\mathbf{N} = -\mathbf{N}^T$:

$$\mathbf{M}\ddot{\mathbf{x}} + (\mathbf{K} + \mathbf{N}(q))\mathbf{x} = 0. \tag{50}$$

The matrix of circulatory forces smoothly depends on a parameter q.

Assuming solution to the problem (50) in the form $\mathbf{x} = \mathbf{u}\exp\lambda t$, we arrive at the eigenvalue problem

$$\mathbf{L}(\lambda, q)\mathbf{u} := (\mathbf{K} + \mathbf{N}(q))\mathbf{u} + \lambda^2\mathbf{M}\mathbf{u} = 0. \tag{51}$$

Let at the value of the parameter $q = q_0$ there exist an algebraically double imaginary eigenvalue $\lambda_0 = i\omega_0$ with the Jordan block that satisfies the following equations

$$\begin{aligned}(\mathbf{K} + \mathbf{N}(q_0))\mathbf{u}_0 - \omega_0^2\mathbf{M}\mathbf{u}_0 &= 0\\ (\mathbf{K} + \mathbf{N}(q_0))\mathbf{u}_1 - \omega_0^2\mathbf{M}\mathbf{u}_1 &= -2i\omega_0\mathbf{M}\mathbf{u}_0,\end{aligned} \tag{52}$$

where $\mathbf{u}_0$ is an eigenfunction and $\mathbf{u}_1$ is an associated function at λ_0.

Note that the eigenfunction $\mathbf{v}_0$ and the associated function $\mathbf{v}_1$ at the eigenvalue $\overline{\lambda}_0 = -i\omega_0$ are governed by the adjoint equations

$$\begin{aligned}(\mathbf{K} - \mathbf{N}(q_0))\mathbf{v}_0 - \omega_0^2\mathbf{M}\mathbf{v}_0 &= 0\\ (\mathbf{K} - \mathbf{N}(q_0))\mathbf{v}_1 - \omega_0^2\mathbf{M}\mathbf{v}_1 &= 2i\omega_0\mathbf{M}\mathbf{v}_0.\end{aligned} \tag{53}$$

Let us perturb the parameter q in the vicinity of q_0 as

$$q(\varepsilon) = q_0 + \varepsilon q_1 + o(\varepsilon^2). \tag{54}$$

Then,

$$\mathbf{N}(q(\varepsilon)) = \mathbf{N}(q_0) + \varepsilon\mathbf{N}_1 + o(\varepsilon) \tag{55}$$

where $\mathbf{N}_1 = \frac{\partial\mathbf{N}}{\partial q}\frac{dq}{d\varepsilon}\Big|_{\varepsilon=0}$ and

$$\begin{aligned}\lambda(\varepsilon) &= \lambda_0 + \lambda_1\varepsilon^{1/2} + \lambda_2\varepsilon + o(\varepsilon),\\ \mathbf{u}(\varepsilon) &= \mathbf{u}_0 + \mathbf{z}_1\varepsilon^{1/2} + \mathbf{z}_2\varepsilon + o(\varepsilon).\end{aligned} \tag{56}$$

Substituting the expansions (55) and (56) into (51), we get

$$\begin{aligned}&(\mathbf{K} + \mathbf{N}(q_0) + \varepsilon\mathbf{N}_1 + o(\varepsilon))(\mathbf{u}_0 + \mathbf{z}_1\varepsilon^{1/2} + \mathbf{z}_2\varepsilon + o(\varepsilon))\\ &+ (\lambda_0^2 + 2\varepsilon^{1/2}\lambda_0\lambda_1 + \varepsilon(2\lambda_0\lambda_2 + \lambda_1^2) + o(\varepsilon))\mathbf{M}(\mathbf{u}_0 + \mathbf{z}_1\varepsilon^{1/2} + \mathbf{z}_2\varepsilon + o(\varepsilon))\\ &= 0.\end{aligned} \tag{57}$$

Collecting terms at ε^0, $\varepsilon^{1/2}$, and ε^1 we obtain the equations

$$\begin{aligned}
&(\mathbf{K}+\mathbf{N}(q_0))\mathbf{u}_0+\lambda_0^2\mathbf{M}\mathbf{u}_0=0\\
&(\mathbf{K}+\mathbf{N}(q_0))\mathbf{z}_1+\lambda_0^2\mathbf{M}\mathbf{z}_1=-2\lambda_0\mathbf{M}\lambda_1\mathbf{u}_0\\
&(\mathbf{K}+\mathbf{N}(q_0))\mathbf{z}_2+\lambda_0^2\mathbf{M}\mathbf{z}_2=-2\lambda_0\lambda_1\mathbf{M}\mathbf{z}_1-\mathbf{N}_1\mathbf{u}_0-(2\lambda_0\lambda_2+\lambda_1^2)\mathbf{M}\mathbf{u}_0.
\end{aligned}\tag{58}$$

Let $(\mathbf{a},\mathbf{b})=\overline{\mathbf{b}}^T\mathbf{a}$ be an inner product of vectors $\mathbf{a}$ and $\mathbf{b}$. Taking the inner product of the last of the Eq. (58) with the vector $\mathbf{v}_0$, we find

$$\begin{aligned}
((\mathbf{K}+\mathbf{N}(q_0))\mathbf{z}_2,\mathbf{v}_0)+\lambda_0^2(\mathbf{M}\mathbf{z}_2,\mathbf{v}_0)&=-2\lambda_0\lambda_1(\mathbf{M}\mathbf{z}_1,\mathbf{v}_0)-(\mathbf{N}_1\mathbf{u}_0,\mathbf{v}_0)\\
&\quad-(2\lambda_0\lambda_2+\lambda_1^2)(\mathbf{M}\mathbf{u}_0,\mathbf{v}_0).
\end{aligned}\tag{59}$$

In view of the property $(\mathbf{L}\mathbf{u},\mathbf{v})=(\mathbf{u},\mathbf{L}^\dagger\mathbf{v})$, where the adjoint matrix polynomial is just $\mathbf{L}^\dagger=\mathbf{K}-\mathbf{N}+\overline{\lambda}^2\mathbf{M}$, and taking into account that $\mathbf{L}^\dagger\mathbf{v}_0=0$, we find

$$2\lambda_0\lambda_1(\mathbf{M}\mathbf{z}_1,\mathbf{v}_0)+(\mathbf{N}_1\mathbf{u}_0,\mathbf{v}_0)+(2\lambda_0\lambda_2+\lambda_1^2)(\mathbf{M}\mathbf{u}_0,\mathbf{v}_0)=0.\tag{60}$$

Observing that $\mathbf{z}_1=\lambda_1\mathbf{u}_1+C_1\mathbf{u}_0$ and $(\mathbf{M}\mathbf{u}_0,\mathbf{v}_0)=0$ we arrive at the equation

$$2\lambda_0\lambda_1^2(\mathbf{M}\mathbf{u}_1,\mathbf{v}_0)+(\mathbf{N}_1\mathbf{u}_0,\mathbf{v}_0)=0.\tag{61}$$

Hence,

$$\lambda_1^2=\frac{i(\mathbf{N}_1\mathbf{u}_0,\mathbf{v}_0)}{2\omega_0(\mathbf{M}\mathbf{u}_1,\mathbf{v}_0)}.\tag{62}$$

In these conditions with $\varepsilon\mathbf{N}_1=\left.\frac{\partial\mathbf{N}}{\partial q}\frac{dq}{d\varepsilon}\right|_{\varepsilon=0}\varepsilon=\left.\frac{\partial\mathbf{N}}{\partial q}\right|_{q=q_0}\Delta q=\mathbf{N}'_q\Delta q$ we obtain

$$\lambda(q)=i\omega_0\pm\sqrt{\Delta q\frac{i(\mathbf{N}'_q\mathbf{u}_0,\mathbf{v}_0)}{2\omega_0(\mathbf{M}\mathbf{u}_1,\mathbf{v}_0)}}+o(\sqrt{|\Delta q|}),\tag{63}$$

$$\mathbf{u}(q)=\mathbf{u}_0\pm\mathbf{u}_1\sqrt{\Delta q\frac{i(\mathbf{N}'_q\mathbf{u}_0,\mathbf{v}_0)}{2\omega_0(\mathbf{M}\mathbf{u}_1,\mathbf{v}_0)}}+o(\sqrt{|\Delta q|}),\tag{64}$$

$$\mathbf{v}(q)=\mathbf{v}_0\pm\mathbf{v}_1\sqrt{\Delta q\frac{i(\mathbf{N}'_q\mathbf{u}_0,\mathbf{v}_0)}{2\omega_0(\mathbf{M}\mathbf{u}_1,\mathbf{v}_0)}}+o(\sqrt{|\Delta q|}).\tag{65}$$

Therefore, we have approximations to the eigenvalues and eigenvectors of the undamped circulatory system in the vicinity of $q=q_0$, i.e. in the vicinity of the flutter boundary corresponding to the reversible-Hopf bifurcation.

Assume that at $q<q_0$ the eigenvalues of the circulatory system are imaginary and at $q>q_0$ the eigenvalues are complex-conjugate (instability).

Let us study how simple imaginary eigenvalues of a circulatory system change due to dissipative perturbation with the matrix $\mathbf{D}(\mathbf{p})$ where $\mathbf{p} = (p_1, p_2, \ldots, p_n)^T$ and $\mathbf{D}(\mathbf{p} = 0) = 0$. Write the dissipatively perturbed eigenvalue problem (51)

$$\mathbf{L}(\lambda, q, \mathbf{p})\mathbf{u} := (\mathbf{K} + \mathbf{N}(q))\mathbf{u}(q) + \lambda(q)\mathbf{D}(\mathbf{p})\mathbf{u}(q) + \lambda^2(q)\mathbf{M}\mathbf{u}(q) = 0. \quad (66)$$

as well as its adjoint

$$\mathbf{L}^{\dagger}(\lambda, q, \mathbf{p})\mathbf{v} := (\mathbf{K} - \mathbf{N}(q))\mathbf{v}(q) + \overline{\lambda}(q)\mathbf{D}(\mathbf{p})\mathbf{v}(q) + \overline{\lambda}^2(q)\mathbf{M}\mathbf{v}(q) = 0. \quad (67)$$

We assume in the above equations that q is fixed such that $q < q_0$.

Let at $\mathbf{p} = 0$ the eigenvalue problem (66) has a simple eigenvalue $\lambda(q) = i\omega(q)$ with an eigenvector $\mathbf{u}(q)$. Assuming $\mathbf{p} = \mathbf{p}(\varepsilon)$, where $\mathbf{p}(\varepsilon) = \varepsilon\mathbf{p}_1 + o(\varepsilon)$, we obtain

$$\mathbf{D}(\mathbf{p}(\varepsilon)) = \varepsilon\mathbf{D}_1 + o(\varepsilon) \quad (68)$$

with $\mathbf{D}_1 = \sum_{s=1}^{n} \frac{\partial \mathbf{D}}{\partial p_s} \frac{dp_s}{d\varepsilon}\Big|_{\varepsilon=0}$. Then, the eigenvalues of (66) are

$$\lambda(\varepsilon) = \lambda(q) - \frac{(\mathbf{D}_1\mathbf{u}(q), \mathbf{v}(q))}{2(\mathbf{M}\mathbf{u}(q), \mathbf{v}(q))}\varepsilon + o(\varepsilon). \quad (69)$$

In other words

$$\lambda(q, \mathbf{p}) = \lambda(q) - \frac{\sum_{s=1}^{n}(\mathbf{D}'_{p_s}\mathbf{u}(q), \mathbf{v}(q))\Delta p_s}{2(\mathbf{M}\mathbf{u}(q), \mathbf{v}(q))} + o(\|\Delta\mathbf{p}\|). \quad (70)$$

Following Andreichikov and Yudovich (1974) we require

$$\sum_{s=1}^{n}(\mathbf{D}'_{p_s}\mathbf{u}(q), \mathbf{v}(q))\Delta p_s = 0 \quad (71)$$

as a condition for the imaginary eigenvalue remain imaginary after a dissipative perturbation. This means that we approximately stay on the neutral stability surface after the dissipative perturbation. Eq. (71) gives an exact linear approximation to the neutral stability surface at every $q < q_0$, if we know exactly the dependencies $\mathbf{u}(q)$, $\mathbf{v}(q)$ and $\lambda(q)$. Usually, however, these functions are determined numerically, see e.g. Andreichikov and Yudovich (1974); Luongo et al. (2016).

Kirillov (2007, 2013a) proposed to use in the method of Andreichikov and Yudovich (1974) approximations to $\mathbf{u}(q)$, $\mathbf{v}(q)$ and $\lambda(q)$ in the vicinity of $q = q_0$ such as those given by Eqs. (63), (64) and (65). Substituting them into (71), we express the approximate critical flutter load explicitly as

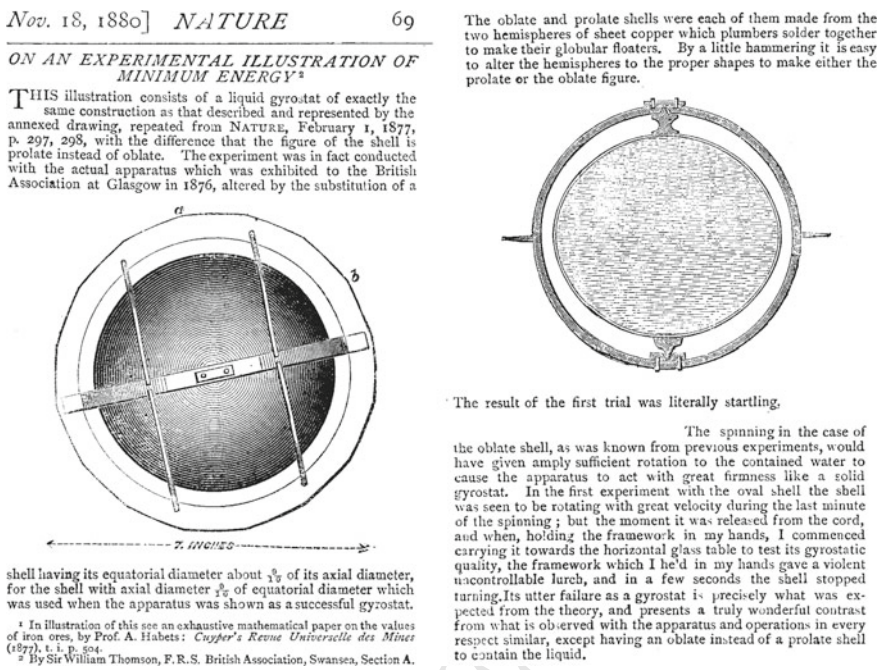

Nov. 18, 1880] NATURE 69

ON AN EXPERIMENTAL ILLUSTRATION OF MINIMUM ENERGY[1]

THIS illustration consists of a liquid gyrostat of exactly the same construction as that described and represented by the annexed drawing, repeated from NATURE, February 1, 1877, p. 297, 298, with the difference that the figure of the shell is prolate instead of oblate. The experiment was in fact conducted with the actual apparatus which was exhibited to the British Association at Glasgow in 1876, altered by the substitution of a

shell having its equatorial diameter about $\frac{8}{7}$ of its axial diameter, for the shell with axial diameter $\frac{8}{7}$ of equatorial diameter which was used when the apparatus was shown as a successful gyrostat.

[1] In illustration of this see an exhaustive mathematical paper on the values of iron ores, by Prof. A. Habets: *Cuyper's Revue Universelle des Mines* (1877), t. i. p. 504.

[2] By Sir William Thomson, F.R.S. British Association, Swansea, Section A.

The oblate and prolate shells were each of them made from the two hemispheres of sheet copper which plumbers solder together to make their globular floaters. By a little hammering it is easy to alter the hemispheres to the proper shapes to make either the prolate or the oblate figure.

The result of the first trial was literally startling.

The spinning in the case of the oblate shell, as was known from previous experiments, would have given amply sufficient rotation to the contained water to cause the apparatus to act with great firmness like a solid gyrostat. In the first experiment with the oval shell the shell was seen to be rotating with great velocity during the last minute of the spinning; but the moment it was released from the cord, and when, holding the framework in my hands, I commenced carrying it towards the horizontal glass table to test its gyrostatic quality, the framework which I held in my hands gave a violent uncontrollable lurch, and in a few seconds the shell stopped turning. Its utter failure as a gyrostat is precisely what was expected from the theory, and presents a truly wonderful contrast from what is observed with the apparatus and operations in every respect similar, except having an oblate instead of a prolate shell to contain the liquid.

Fig. 14 The Kelvin gyrostat (Thomson 1880)

$$q = q_0 + \frac{1}{\lambda_1^2}\left(\frac{\sum_{s=1}^{n}(\mathbf{D}'_{p_s}\mathbf{u}_0, \mathbf{v}_0)\Delta p_s}{\sum_{s=1}^{n}[(\mathbf{D}'_{p_s}\mathbf{u}_0, \mathbf{v}_1) + (\mathbf{D}'_{p_s}\mathbf{u}_1, \mathbf{v}_0)]\Delta p_s}\right)^2. \tag{72}$$

In the particular case of $n = 2$ parameters we assume that $\Delta p_1 = \beta \Delta p_2$. Introducing the quantity

$$\beta_0 = -\frac{(\mathbf{D}'_{p_2}\mathbf{u}_0, \mathbf{v}_0)}{(\mathbf{D}'_{p_1}\mathbf{u}_0, \mathbf{v}_0)}, \tag{73}$$

we can write $q(\beta)$ retaining only the terms of order $(\beta - \beta_0)^2$ and lower:

$$q = q_0 + \frac{\lambda_1^{-2}(\mathbf{D}'_{p_1}\mathbf{u}_0, \mathbf{v}_0)^2(\beta - \beta_0)^2}{[(\mathbf{D}'_{p_1}\mathbf{u}_0, \mathbf{v}_1)\beta_0 + (\mathbf{D}'_{p_1}\mathbf{u}_1, \mathbf{v}_0)\beta_0 + (\mathbf{D}'_{p_2}\mathbf{u}_0, \mathbf{v}_1) + (\mathbf{D}'_{p_2}\mathbf{u}_1, \mathbf{v}_0)]^2}. \tag{74}$$

Therefore, we have derived a general analogue of the expression (44), which gives the quadratic approximation to the vanishing-dissipation limit of the critical flutter load, $q(\beta)$, in the vicinity of $\beta = \beta_0$ in a rigorous sense. This approximation is sufficient to capture the Whitney umbrella singularity that is responsible for the Ziegler–Bottema destabilization paradox.

4 Krein Signature and Stability of Hamiltonian Systems

An attempt to spin a hard-boiled egg always ends up successfully: when spun sufficiently rapidly, its symmetry axis can even rise to the vertical position demonstrating a gyroscopic stabilization. The mathematical model of this effect is the rotating solid prolate spheroid known as Jellett's egg, see e.g. Kirillov (2013a). In contrast, trying to spin a raw egg containing a yolk inside, surrounded by a liquid, will generally lead to its slow wobbling motion.

Thomson (1880) experimentally demonstrated that a thin-walled and slightly oblate spheroid completely filled with liquid remains stable if rotated fast enough about a fixed point, which does not happen if the spheroid is slightly prolate, Fig. 14. In the same year this observation was confirmed theoretically by Greenhill (1880), who found that rotation around the center of gravity of the top in the form of a weightless ellipsoidal shell completely filled with an ideal and incompressible fluid, is unstable when $a < c < 3a$, where c is the length of the semiaxis of the ellipsoid along the axis of rotation and the lengths of the two other semiaxes are equal to a (Greenhill 1880).

Quite similarly, bullets and projectiles fired from the rifled weapons can relatively easily be stabilized by rotation, if they are solid inside. In contrast, the shells, containing a liquid substance inside, have a tendency to turn over despite seemingly revolved fast enough to be gyroscopically stabilized. Motivated by such artillery applications, in 1942 Sobolev, then director of the Steklov Mathematical Institute in Moscow, considered stability of a rotating heavy top with a cavity entirely filled with an ideal incompressible fluid (Moiseyev and Rumyantsev 1968; Ramodanov and Sidorenko 2017)—a problem that is directly connected to the classical XIXth century models of astronomical bodies with a crust surrounding a molten core (Stewartson 1959).

For simplicity, the solid shell of the top and the domain V occupied by the cavity inside it, can be assumed to have a shape of a solid of revolution. They have a common symmetry axis where the fixed point of the top is located. The velocity profile of the stationary unperturbed motion of the fluid is that of a solid body rotating with the same angular velocity Ω as the shell around the symmetry axis.

Following Sobolev, we denote by M_1 the mass of the shell, M_2 the mass of the fluid, ρ and p the density and the pressure of the fluid, g the gravity acceleration, and l_1 and l_2 the distances from the fixed point to the centers of mass of the shell and the fluid, respectively. The moments of inertia of the shell and the 'frozen' fluid with respect to the symmetry axis are C_1 and C_2, respectively; A_1 (A_2) stands for the moment of inertia of the shell (fluid) with respect to any axis that is orthogonal to the symmetry axis and passes through the fixed point. Let, additionally,

$$L = C_1 + C_2 - A_1 - A_2 - \frac{K}{\Omega^2}, \quad K = g(l_1 M_1 + l_2 M_2). \tag{75}$$

The solenoidal ($\operatorname{div} \mathbf{v} = 0$) velocity field $\mathbf{v}$ of the fluid is assumed to satisfy the no-flow condition on the boundary of the cavity: $\mathbf{v}_n|_{\partial V} = 0$.

Stability of the stationary rotation of the top around its vertically oriented symmetry axis is determined by the system of linear equations derived by Sobolev in the frame (x, y, z) that has its origin at the fixed point of the top and rotates with respect to an inertial frame around the vertical z-axis with the angular velocity of the unperturbed top, Ω. If the real and imaginary part of the complex number Z describe the deviation of the unit vector of the symmetry axis of the top in the coordinates x, y, and z, then these equations are, see e.g. Kopachevskii and Krein (2001); Kirillov (2013a):

$$\begin{aligned}
\frac{dZ}{dt} &= i\Omega W,\\
(A_1+\rho\kappa^2)\frac{dW}{dt} &= i\Omega L Z + i\Omega(C_1-2A_1+\rho E)W\\
&\quad + i\rho\int_V\left(v_x\frac{\partial\chi}{\partial y} - v_y\frac{\partial\chi}{\partial x}\right)dV,\\
\partial_t v_x &= 2\Omega v_y - \rho^{-1}\partial_x p + 2i\Omega^2 W\partial_y\overline{\chi},\\
\partial_t v_y &= -2\Omega v_x - \rho^{-1}\partial_y p - 2i\Omega^2 W\partial_x\overline{\chi},\\
\partial_t v_z &= -\rho^{-1}\partial_z p,
\end{aligned} \tag{76}$$

where $2\kappa^2 = \int_V |\nabla\chi|^2 dV$, $E = i\int_V \left(\partial_x\overline{\chi}\partial_y\chi - \partial_y\overline{\chi}\partial_x\chi\right)dV$, and the function χ is determined by the conditions

$$\nabla^2\chi = 0, \quad \partial_n\chi|_{\partial V} = z(\cos nx + i\cos ny) - (x+iy)\cos nz, \tag{77}$$

with n the absolute value of a vector $\mathbf{n}$, normal to the boundary of the cavity.

Sobolev realized that some qualitative conclusions on the stability of the top can be drawn with the use of the bilinear form

$$Q(R_1, R_2) = L\Omega Z_1\overline{Z}_2 + (A_1+\rho\kappa^2)W_1\overline{W}_2 + \frac{\rho}{2\Omega^2}\int_V \overline{\mathbf{v}}_2^T\mathbf{v}_1 dV \tag{78}$$

on the elements R_1 and R_2 of the space $\{R\} = \{Z, W, \mathbf{v}\}$. The linear operator B defined by Eq. (76) that can be written as $\frac{dR}{dt} = iBR$ has all its eigenvalues real when $L > 0$, which yields Lyapunov stability of the top. The number of pairs of complex-conjugate eigenvalues of B (counting multiplicities) does not exceed the number of negative squares of the quadratic form $Q(R, R)$, which can be equal only to one when $L < 0$. Hence, for $L < 0$ an unstable solution $R = e^{i\lambda_0 t}R_0$ can exist with $\mathrm{Im}\lambda_0 < 0$; all real eigenvalues are simple except for maybe one (Kopachevskii and Krein 2001).

In the particular case when the cavity is an ellipsoid of rotation with the semi-axes a, a, and c, the space of the velocity fields of the fluid can be decomposed into a direct sum of subspaces, one of which is finite-dimensional. Only the movements from this subspace interact with the movements of the rigid shell, which yields a finite-dimensional system of ordinary differential equations that describes coupling between the shell and the fluid.

Calculating the moments of inertia of the fluid in the ellipsoidal container

$$C_2 = \frac{8\pi\rho}{15}a^4 c, \quad A_2 = l_2^2 M_2 + \frac{4\pi\rho}{15}a^2 c(a^2 + c^2),$$

denoting $m = \frac{c^2-a^2}{c^2+a^2}$, and assuming the field $\mathbf{v} = (v_x, v_y, v_z)^T$ in the form

$$v_x = (z - l_2)a^2 m\xi, \quad v_y = -i(z - l_2)a^2 m\xi, \quad v_z = -(x - iy)c^2 m\xi,$$

one can eliminate the pressure in Eq. (76) and obtain the reduced model

$$\frac{d\mathbf{x}}{dt} = i\Omega\mathbf{A}^{-1}\mathbf{C}\mathbf{x} = i\Omega\mathbf{B}\mathbf{x}, \tag{79}$$

where $\mathbf{x} = (Z, W, \xi)^T \in \mathbb{C}^3$ and

$$\mathbf{A} = \begin{pmatrix} 1 & 0 & 0 \\ 0 & A_1 + l_2^2 M_2 + \frac{4\pi\rho}{15}a^2 c\frac{(c^2-a^2)^2}{c^2+a^2} & 0 \\ 0 & 0 & c^2 + a^2 \end{pmatrix},$$

$$\mathbf{C} = \begin{pmatrix} 0 & 1 & 0 \\ L & C_1 - 2A_1 - 2l_2^2 M_2 - \frac{8\pi\rho}{15}a^2 c^3 m^2 & -\frac{8\pi\rho}{15}a^4 c^3 m^2 \\ 0 & -2 & -2a^2 \end{pmatrix}. \tag{80}$$

The matrix $\mathbf{B} \neq \mathbf{B}^T$ in Eq. (79) after multiplication by a symmetric matrix

$$\mathbf{G} = \begin{pmatrix} L & 0 & 0 \\ 0 & A_1 + l_2^2 M_2 + \frac{4\pi\rho}{15}a^2 c\frac{(c^2-a^2)^2}{c^2+a^2} & 0 \\ 0 & 0 & \frac{4\pi\rho}{15}a^4 c^3 \frac{(c^2-a^2)^2}{c^2+a^2} \end{pmatrix} \tag{81}$$

yields a Hermitian matrix $\mathbf{GB} = \overline{(\mathbf{GB})}^T$, i.e. $\mathbf{B}$ is a self-adjoint operator in the space $\mathbb{C}^3$ endowed with the metric

$$[\mathbf{u}, \mathbf{u}] := (\mathbf{G}\mathbf{u}, \mathbf{u}) = \overline{\mathbf{u}}^T\mathbf{G}\mathbf{u}, \quad \mathbf{u} \in \mathbb{C}^3, \tag{82}$$

which is *definite* when $L > 0$ and *indefinite* with one negative square when $L < 0$. If λ is an eigenvalue of the matrix $\mathbf{B}$, i.e. $\mathbf{B}\mathbf{u} = \lambda\mathbf{u}$, then $\overline{\mathbf{u}}^T\mathbf{G}\mathbf{B}\mathbf{u} = \lambda\overline{\mathbf{u}}^T\mathbf{G}\mathbf{u}$. On the other hand, $\overline{\mathbf{u}}^T(\overline{\mathbf{G}\mathbf{B}})^T\mathbf{u} = \overline{\lambda}\,\overline{\overline{\mathbf{u}}^T\mathbf{G}\mathbf{u}} = \overline{\lambda}\,\overline{\mathbf{u}}^T\mathbf{G}\mathbf{u}$. Hence,

$$(\lambda - \overline{\lambda})\overline{\mathbf{u}}^T\mathbf{G}\mathbf{u} = 0,$$

implying $\overline{\mathbf{u}}^T\mathbf{G}\mathbf{u} = 0$ on the eigenvector $\mathbf{u}$ of the complex $\lambda \neq \overline{\lambda}$. For real eigenvalues $\lambda = \overline{\lambda}$ and $\overline{\mathbf{u}}^T\mathbf{G}\mathbf{u} \neq 0$. The sign of the quantity $\overline{\mathbf{u}}^T\mathbf{G}\mathbf{u}$ can be different for different real eigenvalues.

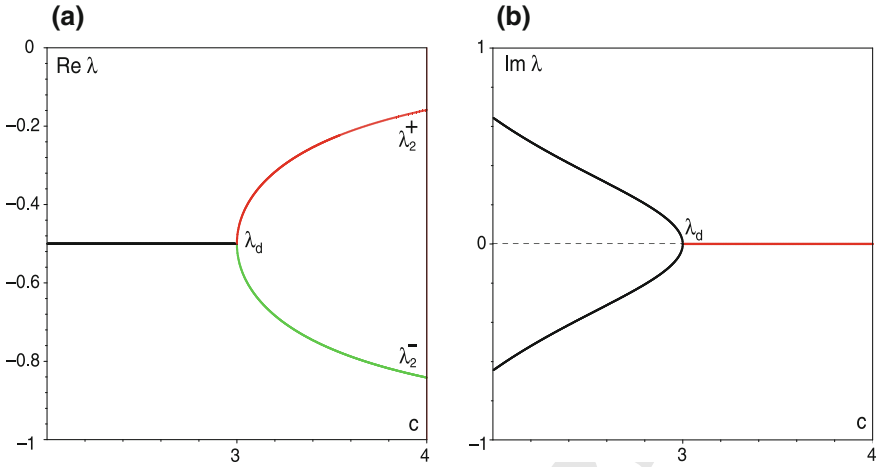

Fig. 15 **a** Simple real eigenvalues (83) of the Sobolev's top in the Greenhill's case for $a = 1$ with (red) $\bar{\mathbf{u}}^T \mathbf{G}\mathbf{u} > 0$ and (green) $\bar{\mathbf{u}}^T \mathbf{G}\mathbf{u} < 0$. **b** At simple complex-conjugate eigenvalues (black) and at the double real eigenvalue λ_d we have $\bar{\mathbf{u}}^T \mathbf{G}\mathbf{u} = 0$

For example, when the ellipsoidal shell is massless and the supporting point is at the center of mass of the system, then $A_1 = 0, C_1 = 0, M_1 = 0, l_2 = 0$. The matrix $\mathbf{B}$ has thus one real eigenvalue ($\lambda_1^+ = -1$, $\bar{\mathbf{u}}_1^{+T} \mathbf{G}\mathbf{u}_1^+ > 0$) and the pair of eigenvalues

$$\lambda_2^{\pm} = -\frac{1}{2} \pm \frac{1}{2}\sqrt{1 + \frac{32\pi\rho}{15}\frac{ca^4}{L}}, \quad L = \frac{4\pi\rho}{15} a^2 c(a^2 - c^2), \tag{83}$$

which are real if $L > 0$ and can be complex if $L < 0$. The latter condition together with the requirement that the radicand in Eq. (83) is negative, reproduces the Greenhill's instability zone: $a < c < 3a$ (Greenhill 1880). With the change in c, the real eigenvalue λ_2^+ with $\bar{\mathbf{u}}_2^{+T} \mathbf{G}\mathbf{u}_2^+ > 0$ collides at $c = 3a$ with the real eigenvalue λ_2^- with $\bar{\mathbf{u}}_2^{-T} \mathbf{G}\mathbf{u}_2^- < 0$ into a real double defective eigenvalue λ_d with the algebraic multiplicity two and geometric multiplicity one, see Fig. 15. Note that $\bar{\mathbf{u}}_d{}^T \mathbf{G}\mathbf{u}_d = 0$, where $\mathbf{u}_d$ is the eigenvector at λ_d.

Therefore, in the case of the ellipsoidal shapes of the shell and the cavity, the Hilbert space $\{R\} = \{Z, W, \mathbf{v}\}$ of the Sobolev's problem endowed with the indefinite metric ($L < 0$) decomposes into the three-dimensional space of the reduced model (79), where the self-adjoint operator B can have complex eigenvalues and real defective eigenvalues, and a complementary infinite-dimensional space, which is free of these complications. The very idea that the signature of the indefinite metric can serve for counting unstable eigenvalues of an operator that is self-adjoint in a functional space equipped with such a metric, turned out to be a concept of a rather universal character possessing powerful generalizations that were initiated by Pontryagin in 1944 (Yakubovich and Starzhinskii 1975; Kopachevskii and Krein 2001).

4.1 Canonical and Hamiltonian Equations

Following Yakubovich and Starzhinskii (1975), we consider a complex vector space $\mathbb{C}^n$ with the inner product $(\mathbf{x}, \mathbf{y}) = \overline{\mathbf{y}}^T \mathbf{x}$. Define an indefinite inner product in $\mathbb{C}^n$ as

$$[\mathbf{x}, \mathbf{y}] = (\mathbf{G}\mathbf{x}, \mathbf{y}) = \overline{\mathbf{y}}^T \mathbf{G}\mathbf{x}, \tag{84}$$

where $\mathbf{G} = \overline{\mathbf{G}}^T$ ($\det \mathbf{G} \neq 0$) is an arbitrary (neither positive nor negative definite) Hermitian $n \times n$ matrix. Hence, $[\mathbf{x}, \mathbf{x}]$ is real but in contrast to $(\mathbf{x}, \mathbf{x})$ it can be positive, negative, or zero for $\mathbf{x} \neq 0$.

The matrix $\mathbf{A}^+$ with the property

$$[\mathbf{A}\mathbf{x}, \mathbf{y}] = [\mathbf{x}, \mathbf{A}^+\mathbf{y}] \tag{85}$$

is said to be $\mathbf{G}$-adjoint to $\mathbf{A}$. From Eq. (85) it follows that

$$\mathbf{A}^+ = \mathbf{G}^{-1}\overline{\mathbf{A}}^T\mathbf{G}. \tag{86}$$

A differential equation

$$i^{-1}\mathbf{G}\frac{d\mathbf{z}}{dt} = \mathbf{H}\mathbf{z}, \tag{87}$$

where $\mathbf{H}$ is Hermitian, is called *Hamiltonian equation*. The matrix $\mathbf{A} = i\mathbf{G}^{-1}\mathbf{H}$ yields

$$[\mathbf{A}\mathbf{x}, \mathbf{y}] = -[\mathbf{x}, \mathbf{A}\mathbf{y}], \tag{88}$$

i.e. $\mathbf{A}^+ = -\mathbf{A}$, and is called the $\mathbf{G}$-Hamiltonian matrix (Yakubovich and Starzhinskii 1975; Zhang et al. 2016). In terms of the $\mathbf{G}$-Hamiltonian matrix $\mathbf{A}$, the Hamiltonian system (87) takes the form

$$\frac{d\mathbf{z}}{dt} = \mathbf{A}\mathbf{z}. \tag{89}$$

Since $\mathbf{A} = -\mathbf{G}^{-1}\overline{\mathbf{A}}^T\mathbf{G}$, the matrices $-\overline{\mathbf{A}}^T$ and $\mathbf{A}$ have the same spectrum. Consequently, if λ is an eigenvalue of $\mathbf{A}$, then so is $-\overline{\lambda}$. Hence, the spectrum of a $\mathbf{G}$-Hamiltonian matrix is symmetric about the imaginary axis. The eigenvalue λ lies on the imaginary axis if and only if $\lambda = -\overline{\lambda}$ (Yakubovich and Starzhinskii 1975).

Let $\mathbf{I}$ be the unit $k \times k$-matrix and

$$\mathbf{J} = \begin{pmatrix} 0 & -\mathbf{I} \\ \mathbf{I} & 0 \end{pmatrix} = -\mathbf{J}^{-1}, \tag{90}$$

the canonical *symplectic matrix*. The $n \times n$ matrix $\mathbf{G} = i\mathbf{J}$, where $n = 2k$, is Hermitian: $\overline{\mathbf{G}}^T = i\overline{\mathbf{J}^T} = -i(-\mathbf{J}) = i\mathbf{J} = \mathbf{G}$. With $\mathbf{G} = i\mathbf{J}$ and $\mathbf{H} = \mathbf{H}^T$ real, the Hamiltonian equation (87) reduces to

$$\mathbf{J}\frac{d\mathbf{x}}{dt} = \mathbf{H}\mathbf{x} \tag{91}$$

that is referred to as the *canonical equation*, whereas the indefinite inner product takes the form (Yakubovich and Starzhinskii 1975).

$$[\mathbf{x}, \mathbf{y}] = \overline{\mathbf{y}}^T (i\mathbf{J})\mathbf{x} = i\overline{\mathbf{y}}^T \mathbf{J}\mathbf{x}. \tag{92}$$

The canonical Hamiltonian linear equation (91) describe motion of a system with k degrees of freedom

$$\frac{dx_s}{dt} = \frac{\partial H}{\partial x_{k+s}}, \quad \frac{dx_{k+s}}{dt} = -\frac{\partial H}{\partial x_s}, \quad s = 1, \ldots, k, \tag{93}$$

where x_s are *generalized coordinates* and x_{k+s} are *generalized momenta*. The quadratic form $H = \frac{1}{2}(\mathbf{H}\mathbf{x}, \mathbf{x})$, where $\mathbf{x}^T = (x_1, \ldots, x_{2k})$, is referred to as a *Hamiltonian function*. The real symmetric $2k \times 2k$-matrix $\mathbf{H}$ of the quadratic form H is called the *Hamiltonian* (Yakubovich and Starzhinskii 1975).

Seeking for the solution to Eq. (91) in the form $\mathbf{x} = \mathbf{u}\exp(\lambda t)$, we find

$$\mathbf{H}\mathbf{u} = \lambda\mathbf{J}\mathbf{u}. \tag{94}$$

From Eqs. (92) and (94) it follows that if λ is a pure imaginary eigenvalue with the eigenvector $\mathbf{u}$ of the $(i\mathbf{J})$-Hamiltonian matrix $\mathbf{J}^{-1}\mathbf{H}$, then

$$(\mathbf{H}\mathbf{u}, \mathbf{u}) = \mathrm{Im}\lambda\,[\mathbf{u}, \mathbf{u}]. \tag{95}$$

Since $\mathbf{J}$ and $\mathbf{H}$ are real matrices and the eigenvalues of a $(i\mathbf{J})$-Hamiltonian matrix are symmetric with respect to the imaginary axis, the spectrum of the matrix $\mathbf{J}^{-1}\mathbf{H}$ is symmetric with respect to both real and imaginary axes of the complex plane.

Theorem 4.1 *Let λ be an eigenvalue of the eigenvalue problem (94). Then so is its complex conjugate, $\overline{\lambda}$, and $-\lambda$. Hence, for a canonical Hamiltonian linear equation (91) the eigenvalues come in singlets $\{0\}$, doublets $\{\lambda, -\lambda\}$ with $\lambda \in \mathbb{R}$ or $\lambda \in i\mathbb{R}$, or quadruplets $\{\lambda, -\lambda, \overline{\lambda}, -\overline{\lambda}\}$. The algebraic multiplicity of the eigenvalue $\lambda = 0$ is even.*

Consequently, the equilibrium $\mathbf{x} = 0$ of the system (91) is Lyapunov stable, if and only if the eigenvalues λ of the eigenvalue problem (94) are pure imaginary and semi-simple (Yakubovich and Starzhinskii 1975).

4.2 Krein Signature of Eigenvalues

Let λ ($\mathrm{Re}\lambda = 0$) be a simple pure imaginary eigenvalue of a $\mathbf{G}$-Hamiltonian matrix $\mathbf{A}$ and $\mathbf{u}$ be a corresponding eigenvector:

$$\mathbf{A}\mathbf{u} = \lambda\mathbf{u}. \tag{96}$$

Definition: *A simple pure imaginary eigenvalue* $\lambda = i\omega$ *with the eigenvector* $\mathbf{u}$ *is said to have positive Krein signature if* $[\mathbf{u}, \mathbf{u}] > 0$ and *negative Krein signature if* $[\mathbf{u}, \mathbf{u}] < 0$.

Let, further, λ ($\mathrm{Re}\lambda = 0$) be a multiple pure imaginary eigenvalue of a **G**-Hamiltonian matrix $\mathbf{A}$, and let $\mathbf{L}_\lambda$ be the eigensubspace of $\mathbf{A}$ belonging to the eigenvalue λ, i.e. the set of all $\mathbf{u} \in \mathbb{C}^n$ satisfying Eq. (96). If $[\mathbf{u}, \mathbf{u}] > 0$ for any $\mathbf{u} \in \mathbf{L}_\lambda$ ($\mathbf{u} \neq 0$), then λ is a multiple eigenvalue with positive Krein signature and the eigensubspace $\mathbf{L}_\lambda$ is positive definite; if $[\mathbf{u}, \mathbf{u}] < 0$, λ is a multiple eigenvalue with negative Krein signature and the eigensubspace $\mathbf{L}_\lambda$ is negative definite. In such cases the multiple eigenvalue is said to have *definite Krein signature*. If there exists a vector $\mathbf{u} \in \mathbf{L}_\lambda$ ($\mathbf{u} \neq 0$) such that $[\mathbf{u}, \mathbf{u}] = 0$, the multiple pure imaginary eigenvalue λ is said to have *mixed Krein signature* (Yakubovich and Starzhinskii 1975).

Note that in case when a multiple pure imaginary eigenvalue λ_0 of $\mathbf{A}$ has geometric multiplicity that is less than its algebraic multiplicity, then there is an eigenvector $\mathbf{u}_0$ at λ_0 such that $[\mathbf{u}_0, \mathbf{u}_0] = 0$, i.e. λ_0 has mixed Krein signature. Indeed, there exists at least one *associated vector* $\mathbf{u}_1$: $\mathbf{A}\mathbf{u}_1 = \lambda_0\mathbf{u}_1 + \mathbf{u}_0$, where $\mathbf{A}\mathbf{u}_0 = \lambda_0\mathbf{u}_0$. Taking into account the property (88), we obtain (Kirillov 2013a)

$$\begin{aligned}[\mathbf{A}\mathbf{u}_0, \mathbf{A}\mathbf{u}_1] &= -\left[\mathbf{u}_0, \mathbf{A}^2\mathbf{u}_1\right] = -\overline{\lambda}_0^2[\mathbf{u}_0, \mathbf{u}_1] - 2\overline{\lambda}_0[\mathbf{u}_0, \mathbf{u}_0] \\ &= \lambda_0\overline{\lambda}_0\,[\mathbf{u}_0, \mathbf{u}_1] + \lambda_0\,[\mathbf{u}_0, \mathbf{u}_0]\,,\end{aligned} \tag{97}$$

which yields

$$[\mathbf{u}_0, \mathbf{u}_0] = 0 \tag{98}$$

since $\lambda_0 = -\overline{\lambda}_0$ (Yakubovich and Starzhinskii 1975). On the other hand, if $\lambda_0 \neq -\overline{\lambda}_0$ then $[\mathbf{u}_0, \mathbf{u}_0] = 0$ for any eigenvector $\mathbf{u}_0$ at λ_0, which follows from the identity

$$[\mathbf{A}\mathbf{u}_0, \mathbf{A}\mathbf{u}_0] = \lambda_0\overline{\lambda}_0\,[\mathbf{u}_0, \mathbf{u}_0] = -\left[\mathbf{u}_0, \mathbf{A}^2\mathbf{u}_0\right] = \overline{\lambda}_0^2\,[\mathbf{u}_0, \mathbf{u}_0]\,.$$

Therefore, a multiple pure imaginary eigenvalue can have definite Krein signature only if it is semi-simple.

4.3 Krein Collision or Linear Hamiltonian-Hopf Bifurcation

Let in the eigenvalue problem (94) the matrix $\mathbf{H}$ smoothly depend on a vector of real parameters $\mathbf{p} \in \mathbb{R}^m$: $\mathbf{H} = \mathbf{H}(\mathbf{p})$. Let at $\mathbf{p} = \mathbf{p}_0$ the matrix $\mathbf{H}_0 = \mathbf{H}(\mathbf{p}_0)$ has a double pure imaginary eigenvalue $\lambda = i\omega_0$ ($\omega_0 \geq 0$) with the Jordan chain consisting of the eigenvector $\mathbf{u}_0$ and the associated vector $\mathbf{u}_1$. Hence,

$$\mathbf{H}_0\mathbf{u}_0 = i\omega_0\mathbf{J}\mathbf{u}_0, \quad \mathbf{H}_0\mathbf{u}_1 = i\omega_0\mathbf{J}\mathbf{u}_1 + \mathbf{J}\mathbf{u}_0. \tag{99}$$

Transposing Eq. (99) and applying the complex conjugation yields

$$\overline{\mathbf{u}}_0^T\mathbf{H}_0 = i\omega_0\overline{\mathbf{u}}_0^T\mathbf{J}, \quad \overline{\mathbf{u}}_1^T\mathbf{H}_0 = i\omega_0\overline{\mathbf{u}}_1^T\mathbf{J} - \overline{\mathbf{u}}_0^T\mathbf{J}. \tag{100}$$

As a consequence, $\overline{\mathbf{u}}_1^T\mathbf{J}\mathbf{u}_0 + \overline{\mathbf{u}}_0^T\mathbf{J}\mathbf{u}_1 = 0$, i.e.

$$[\mathbf{u}_0, \mathbf{u}_1] = -[\mathbf{u}_1, \mathbf{u}_0]. \tag{101}$$

Varying the vector of parameters along the curve $\mathbf{p} = \mathbf{p}(\varepsilon)$ ($\mathbf{p}(0) = \mathbf{p}_0$) and applying the perturbation formulas for double eigenvalues that can be found e.g. in Kirillov (2013a, 2017), we obtain

$$\lambda_\pm = i\omega_0 \pm i\omega_1\sqrt{\varepsilon} + o(\varepsilon^{1/2}), \quad \mathbf{u}_\pm = \mathbf{u}_0 \pm i\omega_1\mathbf{u}_1\sqrt{\varepsilon} + o(\varepsilon^{1/2}) \tag{102}$$

under the assumption

$$\omega_1 = \sqrt{\frac{\overline{\mathbf{u}}_0^T\mathbf{H}_1\mathbf{u}_0}{\overline{\mathbf{u}}_1^T\mathbf{J}\mathbf{u}_0}} > 0, \tag{103}$$

where

$$\mathbf{H}_1 = \sum_{s=1}^{m} \frac{\partial\mathbf{H}}{\partial p_s}\frac{dp_s}{d\varepsilon}\bigg|_{\varepsilon=0}. \tag{104}$$

When $\varepsilon > 0$, the double eigenvalue $i\omega_0$ splits into two pure imaginary ones according to the formulas (102). Calculating the indefinite inner product for the perturbed eigenvectors $\mathbf{u}_\pm$ by Eq. (92) and taking into account the conditions (98) and (101), we find (Kirillov 2013a, 2017)

$$[\mathbf{u}_\pm, \mathbf{u}_\pm] = \pm 2\omega_1\overline{\mathbf{u}}_1^T\mathbf{J}\mathbf{u}_0\sqrt{\varepsilon} + o(\varepsilon^{1/2}), \tag{105}$$

i.e. the simple pure imaginary eigenvalues λ_+ and λ_- have opposite Krein signatures. When ε decreases from positive values to negative ones, the pure imaginary eigenvalues of opposite Krein signatures merge at $\varepsilon = 0$ to the double pure imaginary eigenvalue $i\omega_0$ with the Jordan chain of length 2 that further splits into two complex eigenvalues, one of them with the positive real part.

When $\omega_0 \neq 0$, this process is known as the linear Hamiltonian-Hopf bifurcation (Langford 2003), the onset of flutter, non-semi-simple $1:1$ resonance or the Krein collision (Kirillov 2013a).

When $\omega_0 = 0$, a pair of pure imaginary eigenvalues of opposite Krein signatures colliding at zero and splitting then into a pair of real eigenvalues of different sign means the onset of the non-oscillatory instability or divergence known also as the linear *steady-state bifurcation*.

5 Dissipation-Induced Instabilities of Hamiltonian Systems

5.1 The Kelvin-Tait-Chetaev Theorem

Potential system of the form $\mathbf{M}\ddot{\mathbf{x}} + \mathbf{K}\mathbf{x} = 0$ with the mass matrix, $\mathbf{M} = \mathbf{M}^T$, and the stiffness matrix, $\mathbf{K} = \mathbf{K}^T$, can be transformed to the Hamiltonian form (91). Furthermore, this can be done also in the presence of velocity-dependent *gyroscopic forces* with the matrix $\mathbf{G} = -\mathbf{G}^T$ for the *gyroscopic system* $\mathbf{M}\ddot{\mathbf{x}} + \mathbf{G}\dot{\mathbf{x}} + \mathbf{K}\mathbf{x} = 0$. Gyroscopic forces can stabilize the otherwise unstable static equilibrium. This *gyroscopic stabilization* can be lost in the presence of dissipation, as we all know from observing the behavior of rotating tops.

This *dissipation-induced instability* of gyroscopic systems is formalized by the Kelvin-Tait-Chetaev theorem (Thomson and Tait 1879; Bloch et al. 1994; Krechetnikov and Marsden 2007).

Theorem 5.1 (Kelvin-Tait-Chetaev Theorem) *Stability of solutions of the equation*

$$\boldsymbol{M}\ddot{\boldsymbol{x}} + (\boldsymbol{G} + \boldsymbol{D})\dot{\boldsymbol{x}} + \boldsymbol{K}\boldsymbol{x} = 0, \tag{106}$$

where $\boldsymbol{M} > 0$, $\boldsymbol{D} = \boldsymbol{D}^T > 0$ *and* $\boldsymbol{K}$ *nondegenerate is the same as the stability of solutions of the corresponding potential system,* $\boldsymbol{M}\ddot{\boldsymbol{x}} + \boldsymbol{K}\boldsymbol{x} = 0$. *In particular, if all the eigenvalues of the real symmetric matrix* $\boldsymbol{K}$ *are positive (negative) then the system (106) is asymptotically stable (unstable).*

The number of eigenvalues with positive real parts of the system (106) is equal to the number of negative eigenvalues of the matrix $\mathbf{K}$ (Zajac Theorem, 1964). If the number of negative eigenvalues of $\mathbf{K}$ (known also as the *Poincaré instability degree*) is even, then the equilibrium of the corresponding potential system can be stabilized by the gyroscopic forces. However, this gyroscopic stabilization is destroyed when dissipative forces with full dissipation ($\mathbf{D} > 0$) are added, no matter how weak they are Kirillov (2013a).

Remarkably, the origin of the Kelvin-Tait-Chetaev theorem is in the centuries-old problem (going back to Newton) on the stability of rotating and self-gravitating masses of fluid motivated by the question of the actual shape of the Earth (Lebovitz 1998; Borisov et al. 2009).

5.2 Secular Instability of the Maclaurin Spheroids

In 1742 Maclaurin has found that an oblate spheroid

$$\frac{x^2}{a_1^2} + \frac{y^2}{a_2^2} + \frac{z^2}{a_3^2} = 1, \quad a_3 < a_2 = a_1$$

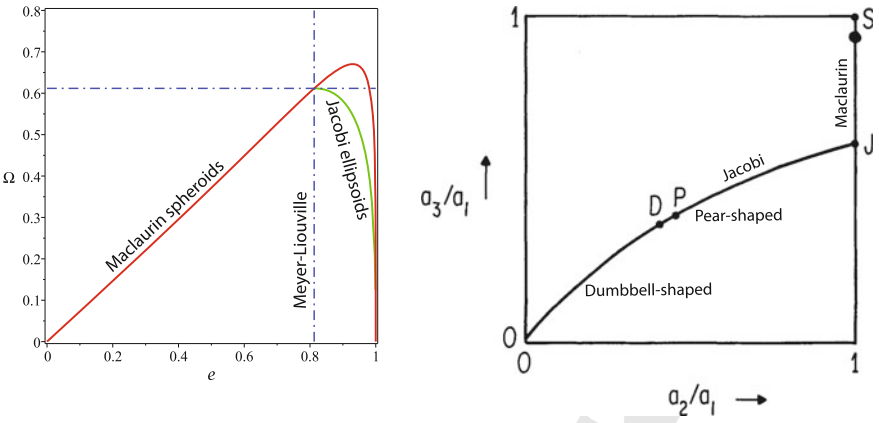

Fig. 16 (Left) Families of Maclaurin spheroids and Jacobian ellipsoids in the plane of angular velocity versus eccentricity with the common point at $e \approx 0.8127$. (Right) Sequence of bifurcations proposed by the fission theory of binary stars (Lebovitz 1987)

is a shape of relative equilibrium of a self-gravitating mass of inviscid fluid in a solid-body rotation about the z-axis, provided that the rate of rotation, Ω, is related to the eccentricity $e = \sqrt{1 - \frac{a_3^2}{a_1^2}}$ through the formula (Lebovitz 1998)

$$\Omega^2(e) = 2e^{-3}(3 - 2e^2)\sin^{-1}(e)\sqrt{1 - e^2} - 6e^{-2}(1 - e^2). \tag{107}$$

A century later, Jacobi (1834) has discovered less symmetric shapes of relative equilibria in this problem that are tri-axial ellipsoids

$$\frac{x^2}{a_1^2} + \frac{y^2}{a_2^2} + \frac{z^2}{a_3^2} = 1, \quad a_3 < a_2 < a_1.$$

Later on Meyer (1842) and Liouville (1846) have shown that the family of Jacobi's ellipsoids has one member in common with the family of Maclaurin's spheroids at $e \approx 0.8127$, see Fig. 16. The equilibrium with the Meyer-Liouville eccentricity is neutrally stable, Fig. 17.

In 1860 Riemann established neutral stability of inviscid Maclaurin's spheroids on the interval of eccentricities ($0 < e < 0.9529..$). At the Riemann point with the critical eccentricity $e \approx 0.9529$ the Hamilton-Hopf bifurcation sets in and causes dynamical instability with respect to ellipsoidal perturbations beyond this point.

A century later Chandrasekhar (1969) proposed a virial method to reduce the problem to a finite-dimensional system, which stability is governed by the eigenvalues of the matrix polynomial

$$\mathbf{L}_i(\lambda) = \lambda^2 \begin{pmatrix} 1 & 0 \\ 0 & 1 \end{pmatrix} + \lambda \begin{pmatrix} 0 & -4\Omega \\ \Omega & 0 \end{pmatrix} + \begin{pmatrix} 4b - 2\Omega^2 & 0 \\ 0 & 4b - 2\Omega^2 \end{pmatrix}, \tag{108}$$

where $\Omega(e)$ is given by the Maclaurin law (107) and $b(e)$ is as follows

$$b = \frac{\sqrt{1-e^2}}{4e^5} \left\{ e(3-2e^2)\sqrt{1-e^2} + (4e^2-3)\left(\frac{\pi}{2} - \tan^{-1}(e^{-1}\sqrt{1-e^2})\right)\right\}. \tag{109}$$

The eigenvalues of the matrix polynomial (108) are

$$\lambda = \pm\left(i\Omega \pm i\sqrt{4b - \Omega^2}\right). \tag{110}$$

Requiring $\lambda = 0$ we can determine the critical Meyer-Liouville eccentricity by solving with respect to e the equation (Chandrasekhar 1969)

$$4b(e) = 2\Omega^2(e).$$

The critical eccentricity at the Riemann point follows from requiring the radicand in (110) to vanish:

$$4b(e) = \Omega^2(e).$$

Remarkably, when

$$\Omega^2(e) < 4b(e) < 2\Omega^2(e) \tag{111}$$

both eigenvalues of the stiffness matrix

$$\begin{pmatrix} 4b - 2\Omega^2 & 0 \\ 0 & 4b - 2\Omega^2 \end{pmatrix}$$

are negative, i.e. the Poincaré instability degree of the equilibrium is even and equal to 2. Hence, the interval (111) corresponding to $0.8127.. < e < 0.9529..$, which is stable according to Riemann, is, in fact, the interval of gyroscopic stabilization of the Maclaurin spheroids, Fig. 17.

According to the Theorem 5.1 the gyroscopic stabilization of the equilibrium with nonzero Poincaré instability degree can be destroyed even by the infinitely small dissipation with the positive-definite damping matrix. In the words by Thomson and Tait (1879), "If there be any viscosity, however slight, in the liquid, the equilibrium [beyond $e \approx 0.8127$] in any case of energy either a minimax or a maximum cannot be secularly stable".

The prediction made by Thomson and Tait (1879) has been verified quantitatively only in the XX-th century by Roberts and Stewartson (1963). Using the virial approach Chandrasekhar (1969) reduced the linear stability problem to the study of eigenvalues of the matrix polynomial

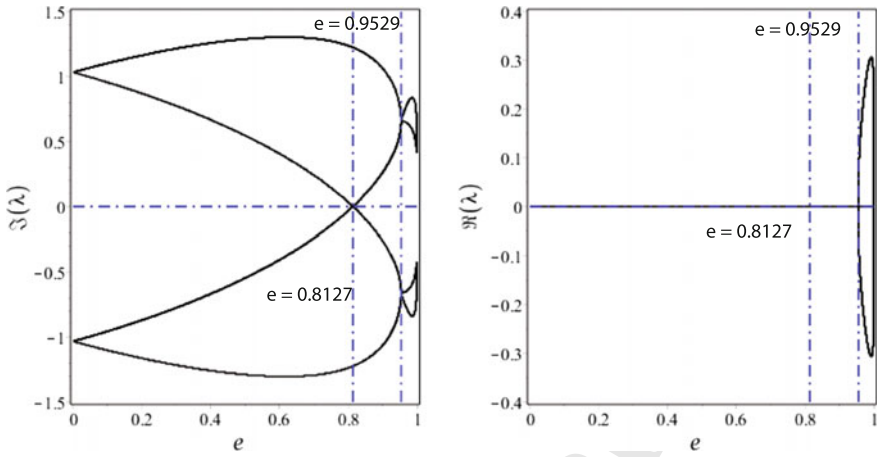

Fig. 17 (Left) Frequencies and (right) growth rates of the eigenvalues of the inviscid eigenvalue problem $\mathbf{L}_i(\lambda)\mathbf{u} = 0$ demonstrating the Hamilton-Hopf bifurcation at the Riemann critical value of the eccentricity, $e \approx 0.9529$ and neutral stability at the Meyer-Liouville point, $e \approx 0.8127$

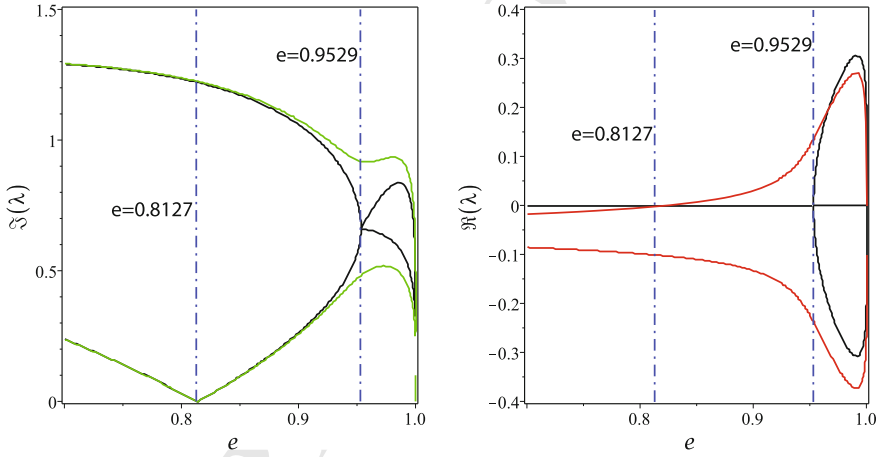

Fig. 18 (Left) Frequencies and (right) growth rates of the (black lines) inviscid Maclaurin spheroids and (green and red lines) viscous ones with $\mu = \frac{\nu}{a_1^2} = 0.01$. Viscosity destabilizes the gyroscopic stabilization of the Maclaurin spheroids on the interval $0.8127\ldots < e < 0.9529\ldots$, which is stable in the inviscid case (Roberts and Stewartson 1963; Chandrasekhar 1969; Chandresekhar 1984)

$$\mathbf{L}_v(\lambda) = \lambda^2 \begin{pmatrix} 1 & 0 \\ 0 & 1 \end{pmatrix} + \lambda \begin{pmatrix} 10\mu & -4\Omega \\ \Omega & 10\mu \end{pmatrix} + \begin{pmatrix} 4b - 2\Omega^2 & 0 \\ 0 & 4b - 2\Omega^2 \end{pmatrix}, \qquad (112)$$

where $\mu = \frac{\nu}{a_1^2}$ and ν is the viscosity of the fluid. The operator $\mathbf{L}_v(\lambda)$ differs from the operator of the ideal system, $\mathbf{L}_i(\lambda)$, by the matrix of dissipative forces $10\lambda\mu\mathbf{I}$, where $\mathbf{I}$ is the 2×2 unit matrix.

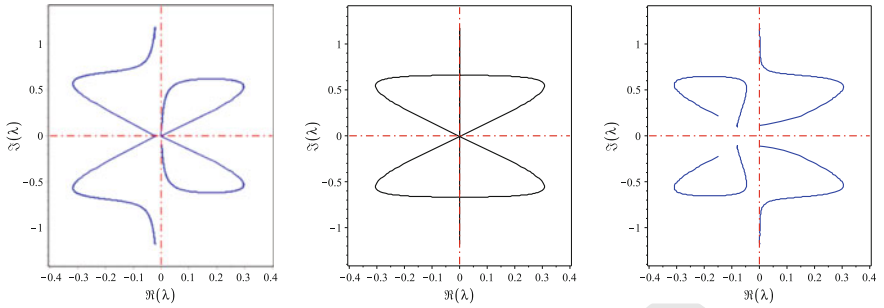

Fig. 19 Paths of the eigenvalues in the complex plane for (left) viscous Maclaurin spheroids with $\mu = \frac{\nu}{a_1^2} = 0.002$, (centre) Maclaurin spheroids without dissipation, and (right) inviscid Maclaurin spheroids with radiative losses for $\delta = 0.05$. The Krein collision of two modes of the non-dissipative Hamiltonian system shown in the centre occurs at the Rieman critical value $e \approx 0.9529$. Both types of dissipation destroy the Krein collision and destabilize one of the two interacting modes at the Meyer-Liuoville critical value $e \approx 0.8127$

The characteristic polynomial written for $\mathbf{L}_v(\lambda)$ yields the equation governing the growth rates of ellipsoidal perturbations in the presence of viscosity:

$$25\Omega^2\mu^2 + (\mathrm{Re}\lambda + 5\mu)^2(\Omega^2 - \mathrm{Re}\lambda^2 - 10\mathrm{Re}\lambda\mu - 4b) = 0. \qquad (113)$$

The right panel of Fig. 18 shows that the growth rates (113) become positive beyond the Meyer-Liouville point. Indeed, assuming $\mathrm{Re}\lambda = 0$ in (113), we reduce it to $50\mu^2(\Omega^2 - 2b) = 0$, meaning that the growth rate vanishes when $\Omega^2 = 2b$ no matter how small the viscosity coefficient μ is. But, as we already know, the equation $\Omega^2(e) = 2b(e)$ determines exactly the Meyer-Liouville point, $e \approx 0.8127$.

It turns out, that the critical eccentricity of the viscous Maclaurin spheroid is equal to the Meyer-Liouville value, $e \approx 0.8127$, even in the limit of vanishing viscosity, $\mu \to 0$, and thus does not converge to the inviscid Riemann value $e \approx 0.9529$. This is nothing else but the Ziegler–Bottema destabilization paradox in a near-Hamiltonian dissipative system (Langford 2003; Krechetnikov and Marsden 2007; Kirillov 2007, 2013a).

Viscous dissipation destroys the Krein interaction of two modes at the Riemann critical point and destabilizes one of them beyond the Meyer-Liouville point, showing a typical for the destabilization paradox *avoided crossing* in the complex plane, Fig. 19(left).

Thomson and Tait (1879) hypothesised that the instability, which is stimulated by the presence of viscosity in the fluid, will result in a slow, or *secular*, departure of the system from the unperturbed equilibrium of the Maclaurin family at the Meyer-Liouville point and subsequent evolution along the Jacobi family, as long as the latter is stable (Lebovitz 1998).

Therefore, a rotating, self-gravitating fluid mass, initially symmetric about the axis of rotation, can undergo an axisymmetric evolution in which it first loses stability

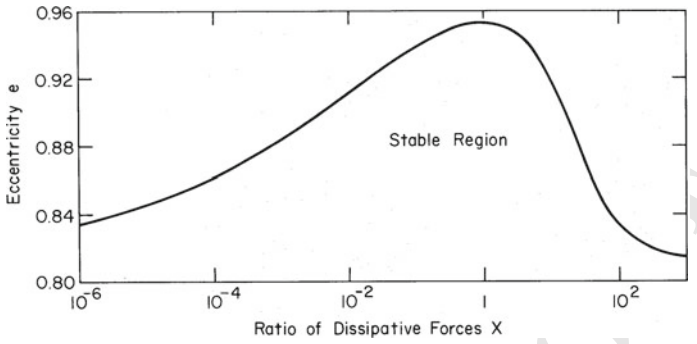

Fig. 20 Critical eccentricity in the limit of vanishing dissipation depends on the damping ratio, X, and attains its maximum (Riemann) value, $e \approx 0.9529$ exactly at $X = 1$. As X tends to zero or infinity, the critical value tends to the Meyer-Liouville value $e \approx 0.8127$, (Lindblom and Detweiler 1977; Chandresekhar 1984)

to a nonaxisymmetric disturbance, and continues for a while evolving along a nonaxisymmetric family toward greater departure from axial symmetry, Fig. 16; then it undergoes a further loss of stability to a disturbance tending toward splitting into two parts (Lebovitz 1998).

Rigorous mathematical treatment of the fission theory of binary stars proposed by Thomson and Tait (1879) by Lyapunov and Poincaré has laid a foundation to modern nonlinear analysis. In particular, it has led Lyapunov to the development of a general theory of stability of motion (Borisov et al. 2009). As we remember, it is the Lyapunov stability theory that helped Nicolai and Ziegler to shed light on stability of nonconservative systems under circulatory forces.

Chandrasekhar (1970) demonstrated that there exists another mechanism making the Maclaurin spheroid unstable beyond the Meyer-Liouville point of bifurcation, namely, the radiative losses due to emission of gravitational waves. However, the mode that is made unstable by the radiation reaction is not the same one that is made unstable by viscosity, Fig. 19(right).

In the case of the radiative damping mechanism stability is determined by the spectrum of the following matrix polynomial (Chandrasekhar 1970)

$$\mathbf{L}_g(\lambda) = \lambda^2 + \lambda(\mathbf{G} + \mathbf{D}) + \mathbf{K} + \mathbf{N}$$

that contains the matrices of gyroscopic, **G**, damping, **D**, potential, **K**, and nonconservative positional, **N**, forces

$$\mathbf{G} = \frac{5}{2}\begin{pmatrix} 0 & -\Omega \\ \Omega & 0 \end{pmatrix}, \quad \mathbf{D} = \begin{pmatrix} \delta 16\Omega^2(6b - \Omega^2) & -3\Omega/2 \\ -3\Omega/2 & \delta 16\Omega^2(6b - \Omega^2) \end{pmatrix}$$

$$\mathbf{K} = \begin{pmatrix} 4b - \Omega^2 & 0 \\ 0 & 4b - \Omega^2 \end{pmatrix}, \quad \mathbf{N} = \delta\begin{pmatrix} 2q_1 & 2q_2 \\ -q_2/2 & 2q_1 \end{pmatrix},$$

where $\Omega(e)$ and $b(e)$ are given by Eqs. (107) and (109). Explicit expressions for q_1 and q_2 can be found in Chandrasekhar (1970).

Lindblom and Detweiler (1977) studied the combined effects of gravitational radiation reaction and of viscosity on the stability of the Maclaurin spheroids. As we know, each of these dissipative effects induces a secular instability in the Maclaurin sequence past the Meyer-Liouville point of bifurcation. However, when both effects are considered together, the sequence of stable Maclaurin spheroids therefore reaches past the bifurcation point to a new point determined by the *ratio* of the strengths of the viscous and the radiative forces.

Figure 20 shows the limit of the critical eccentricity as a function of the damping ratio in the limit of vanishing dissipation. This limit coincides with the inviscid Riemann point only at a particular damping ratio. At any other ratio, the critical value is below the Riemann one and tends to the Meyer-Liouville value as this ratio tends either to zero or infinity. Lindblom and Detweiler (1977) correctly attributed the cancellation of the secular instabilities to the fact that viscous dissipation and radiation reaction cause different modes to become unstable, see Fig. 19.

Andersson (2003) relates the mode destabilized by the fluid viscosity to the prograde moving spherical harmonic that appears to be retrograde in the frame rotating with the fluid mass and the mode destabilized by the radiative losses to the retrograde moving spherical harmonic when it appears to be prograde in the inertial frame. This gives a link to destabilization of positive- and negative energy modes (Ostrovsky et al. 1986; Kirillov 2009, 2013a) as well as to the theory of the anomalous Doppler effect (Nezlin 1976; Ginzburg and Tsytovich 1979; Vesnitskii and Metrikin 1996). It is known (Nezlin 1976) that to excite the positive energy mode one must provide additional energy to the mode, while to excite the negative energy mode one must extract energy from the mode. The latter can be done by dissipation and the former by the nonconservative positional (curl) forces. Both are presented in the model by Lindblom and Detweiler (1977).

The destabilization of a Hamiltonian system in the presence of two different types of non-Hamiltonian perturbations can be understood on the example of the general two-dimensional system

$$\ddot{\mathbf{x}}(t) + (\delta\mathbf{D} + \Omega\mathbf{G})\dot{\mathbf{x}}(t) + (\mathbf{K} + \nu\mathbf{N})\mathbf{x}(t) = 0, \quad \mathbf{x} \in \mathbb{R}^2 \tag{114}$$

where δ, Ω, ν are scalar coefficients and matrices $\mathbf{D} > 0$, $\mathbf{K} > 0$ are real and symmetric, while matrices $\mathbf{G}$ and $\mathbf{N}$ are skew-symmetric as follows

$$\mathbf{G} = \mathbf{N} = \begin{pmatrix} 0 & -1 \\ 1 & 0 \end{pmatrix}.$$

This system is a conservative Hamiltonian system if $\delta = 0$, $\Omega = 0$, and $\nu = 0$, which is statically unstable for $\mathbf{K} < 0$ with the even Poincaré instability degree equal to 2. Adding gyroscopic forces with $\Omega > 0$, keeps this system Hamiltonian and yields its stabilization if $\Omega > \Omega_f = \sqrt{-\kappa_1} + \sqrt{-\kappa_2}$, where $\kappa_{1,2} < 0$ are eigenvalues of $\mathbf{K}$.

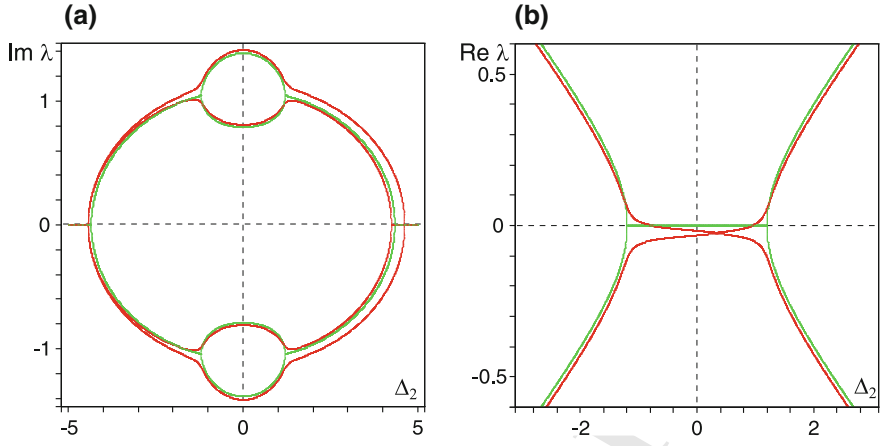

Fig. 21 Given $\Omega = 0.3$, the green lines depict (a) imaginary and (b) real parts of the eigenvalues of the PT - symmetric problem with indefinite damping (116) as functions of the parameter $\Delta_2 = \mu_1 - \mu_2 = 2\mu$ when $k = 1$. Red lines correspond to the eigenvalues of the problem (41) with $k_1 = 1$, $\kappa = k_2 - k_1 = 0.1$ and $\Delta_1 = \mu_1 + \mu_2 = 0.1$

Owing to the 'reversible' symmetry of its spectrum (MacKay 1991; Bloch et al. 1994), the Hamiltonian system displays flutter instability via the collision of imaginary eigenvalues at $\Omega = \Omega_f$ and their subsequent splitting into a complex quadruplet as soon as Ω decreases below Ω_f. This is the already familiar to us linear Hamilton-Hopf bifurcation.

If $\delta > 0$, $\nu > 0$ the gyroscopic stability is destroyed at the threshold of the classical-Hopf bifurcation (Kirillov 2007, 2013a)

$$\Omega_H \approx \Omega_f + \frac{2\Omega_f}{(\omega_f \mathrm{tr}\mathbf{D})^2}\left(\frac{\nu}{\delta} - \frac{\mathrm{tr}(\mathbf{KD} + (\Omega_f^2 - \omega_f^2)\mathbf{D})}{2\Omega_f}\right)^2,$$

where $\omega_f^2 = \sqrt{\kappa_1 \kappa_2}$ and $\mathbf{D} > 0$.

The dependency of the new gyroscopic stabilization threshold just on the ratio ν/δ implies that the limit of Ω_H as both ν and $\delta \to 0$ is higher than Ω_f for all ratios except a unique one. Similarly to the case of nonconservative reversible systems, this happens because the classical Hopf and the Hamilton-Hopf bifurcations meet in the Whitney umbrella singularity that exists on the stability boundary of a nearly-Hamiltonian dissipative system and corresponds to the onset of the Hamilton-Hopf bifurcation (Bottema 1956; Arnold 1972; Langford 2003; Kirillov 2007, 2013a; Krechetnikov and Marsden 2007; Kirillov and Verhulst 2010).

6 Stability in the Presence of Potential, Circulatory, Gyroscopic and Dissipative Forces

Beletsky (1995) remarked that when potential, circulatory and gyroscopic forces are present simultaneously, it becomes nontrivial to judge about stability. "The pairwise interaction of arbitrary two of these [forces] results in the existence of stable domains in the parameter space. However, the simultaneous action of all three effects always results in instability!" (Beletsky 1995). Addition of dissipation entangles stability analysis even more (Kirillov 2013a; Hagedorn et al. 2014; Kliem and Pommer 2017). Here we present several examples illustrating these statements.

6.1 *Rotating Shaft by Shieh and Masur (1968)*

Let us return once again to the model (20) of a rotating shaft by Shieh and Masur (1968) with damping but without circulatory forces

$$\begin{aligned} m\ddot{u} + \mu_1\dot{u} - 2\Omega\dot{v} + (k_1 - \Omega^2)u = 0 \\ m\ddot{v} + \mu_2\dot{v} + 2\Omega\dot{u} + (k_2 - \Omega^2)v = 0. \end{aligned} \tag{115}$$

Although the literal meaning of the word 'damping' prescribes the coefficients μ_1 and μ_2 to be nonnegative, it is instructive to relax this sign convention Kirillov (2013b). Therefore, we consider the gyroscopic system (115) where the negative sign of the damping coefficient corresponds to a gain and the positive one to a loss (Karami and Inman 2011; Schindler et al 2011).

In mechanics, negative damping terms enter the equations of motion of moving continua in frictional contact when the dependence of the frictional coefficient on the relative velocity has a negative slope, which can be observed already in the tabletop experiments with the singing wine glass (Kirillov 2009, 2013a). In physics, a pair of coupled oscillators, one with gain and the other with loss, can naturally be implemented as an LRC-circuit (Schindler et al 2011).

When $\mu_1 = -\mu_2 = \mu > 0$ the gain and loss in Eq. (41) are in perfect balance. Let us further assume that $k_1 = k_2 = k$:

$$\begin{aligned} m\ddot{u} + \mu\dot{u} - 2\Omega\dot{v} + (k - \Omega^2)u = 0 \\ m\ddot{v} - \mu\dot{v} + 2\Omega\dot{u} + (k - \Omega^2)v = 0. \end{aligned} \tag{116}$$

Let us look at what happens with these equations when we change the direction of time, assuming $t \to -t$. Then,

$$\begin{aligned} m\ddot{u} - \mu\dot{u} + 2\Omega\dot{v} + (k - \Omega^2)u = 0 \\ m\ddot{v} + \mu\dot{v} - 2\Omega\dot{u} + (k - \Omega^2)v = 0 \end{aligned} \tag{117}$$

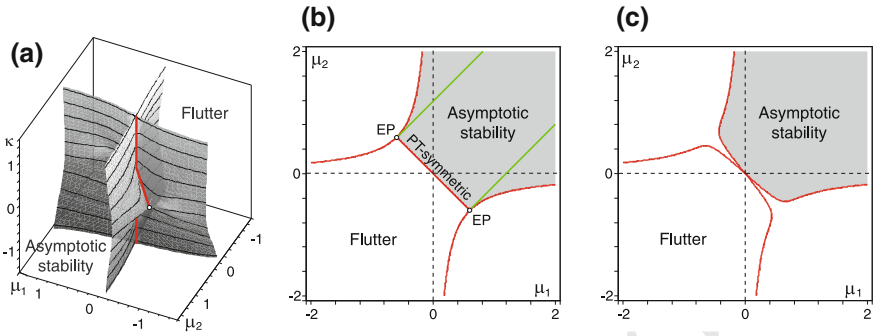

Fig. 22 Stability domain of the rotating shaft by Shieh and Masur for $k_1 = 1$, $\Omega = 0.3$, and $\beta = 0$. **a** The Plücker conoid in the (μ_1, μ_2, κ)-space and its slices in the μ_1, μ_2-plane with **b** $\kappa = 0$ and **c** $\kappa = 0.1$. Open circles show locations of exceptional points (EPs) where pure imaginary eigenvalues of the ideal PT -symmetric system (116) experience the nonsemisimple 1 : 1 resonance; green lines are locations of the exceptional points where double nonsemisimple eigenvalues have negative real parts

and we see that Eq. (116) are not invariant to the time reversal transformation (T). The interchange of the coordinates as $x \leftrightarrow y$ in Eq. (116) results again in Eq. (117), which do not coincide with the original. Hence, the Eq. (116) are not invariant with respect to the parity transformation (P).

Nevertheless, two negatives make an affirmative, and the combined PT-transformation leaves the Eq. (116) invariant despite the T-symmetry and P-symmetry not being respected separately. The spectrum of the PT-symmetric system (116) with indefinite damping is symmetrical with respect to the imaginary axis on the complex plane as it happens in Hamiltonian and reversible systems.

To see this, let us consider the eigenvalues λ of the problem (41) introducing the new parameters $\Delta_1 = \mu_1 + \mu_2$, $\Delta_2 = \mu_1 - \mu_2$ and $\kappa = k_2 - k_1$. At $\Delta_1 = 0$ and $\kappa = 0$ they represent the spectrum of the problem (116)

$$\lambda = \pm\frac{1}{4}\sqrt{2\Delta_2^2 - 16k_1 - 16\Omega^2 \pm 2\sqrt{(16\Omega^2 - \Delta_2^2)(16k_1 - \Delta_2^2)}}$$

where $k_1 = k$ and $\Delta_2 = 2\mu$. In Fig. 21 the eigenvalues are shown by the green lines. They are pure imaginary when $|\Delta_2| < 4|\Omega|$. At the exceptional points (EPs), $\Delta_2 = \pm 4\Omega$, the pure imaginary eigenvalues collide into a double defective one which with the further increase in Δ_2 splits into a complex-conjugate pair (flutter instability).

PT - symmetry can be violated by the asymmetry both in the stiffness distribution $\kappa \neq 0$ and in the balance of gain and loss $\Delta_1 \neq 0$. In such a situation, the merging of eigenvalues that was perfect for the PT-symmetric system (116) is destroyed. The red eigencurves in Fig. 21 demonstrate the imperfect merging of modes that causes a decrease of the stability interval with respect to that of the symmetric system (the effect similar to the Ziegler–Bottema destabilization paradox in circulatory systems).

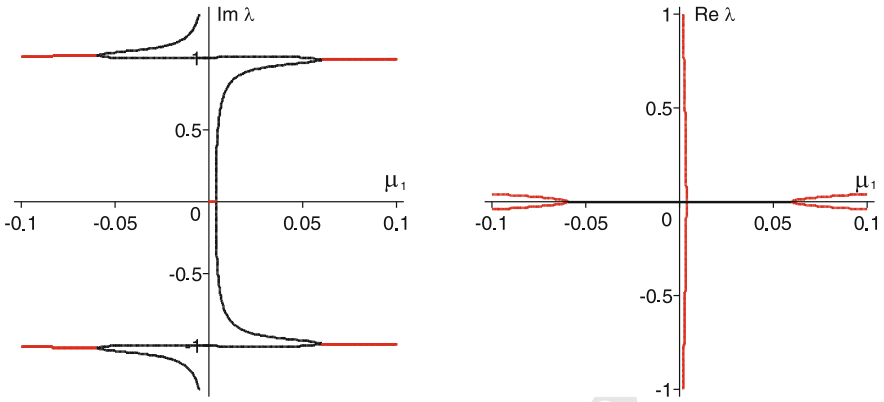

Fig. 23 Imaginary and real parts of the roots of the characteristic equation (118) as a function of the damping coefficient μ_1 under the constraints (119) for $k_1 = 1$, $\Omega = 0.03$ and $\beta = 0.03$

The Routh–Hurwitz conditions applied to the characteristic polynomial of the system (1.60) yield the domain of the asymptotic stability

$$\mu_1\mu_2\kappa^2 + (\mu_1+\mu_2)(\mu_1\mu_2 + 4\Omega^2)(\mu_1\kappa + (\mu_1+\mu_2)(k_1-\Omega^2)) > 0$$
$$\mu_1 + \mu_2 > 0,$$

shown in Fig. 22a in the (μ_1, μ_2, κ)-space. The surface has a self-intersection along the κ-axis that corresponds to a marginally stable conservative gyroscopic (Hamiltonian) system. More intriguing is that in the $(\kappa = 0)$ - plane there exists another self-intersection along the interval of the line $\mu_1 + \mu_2 = 0$ with the ends at the exceptional points $(\mu_1 = 2\Omega, \mu_2 = -2\Omega)$ and $(\mu_1 = -2\Omega, \mu_2 = 2\Omega)$, see Fig. 22b. This is the interval of marginal stability of the oscillatory damped (PT-symmetric) gyroscopic system (116) with the perfect gain/loss balance. At the exceptional points, the stability boundary has the Whitney umbrella singularities.

In the $(\kappa = 0)$ - plane the range of stability is growing with the increase of the distance from the line $\mu_1 + \mu_2 = 0$, which is accompanied by detuning of the gain/loss balance, Fig. 22b. Indeed, in this slice the boundary of the domain of asymptotic stability is the hyperbola

$$(\mu_1 - \mu_2)^2 - (\mu_1 + \mu_2)^2 = 16\Omega^2.$$

At $\mu_1 + \mu_2 = 0$ it touches the two straight lines $\mu_1 - \mu_2 = \pm 4\Omega$, every point of which corresponds to a pair of double defective complex-conjugate eigenvalues with real parts that are negative when $\mu_1 + \mu_2 > 0$, positive when $\mu_1 + \mu_2 < 0$, and zero when $\mu_1 + \mu_2 = 0$:

$$\lambda = -\frac{\mu_1+\mu_2}{4} \pm \frac{1}{4}\sqrt{(\mu_1+\mu_2)^2 - 16(k_1-\Omega^2)}$$

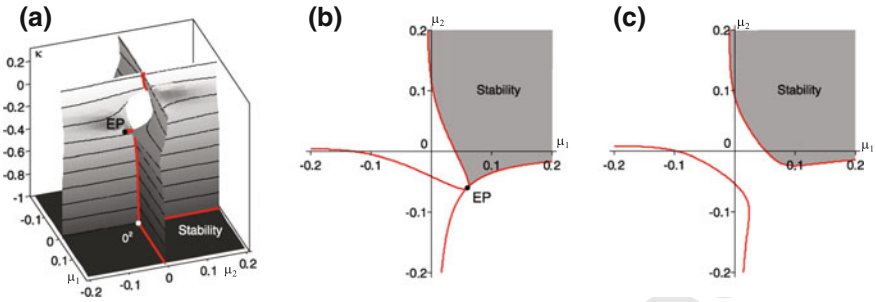

Fig. 24 Stability domain of the rotating shaft by Shieh and Masur for $k_1 = 1, \Omega = 0.03, \beta = 0.03$. **a** The 'Viaduct' in the (μ_1, μ_2, κ)-space and its slices in the (μ_1, μ_2)-plane with **b** $\kappa = 0.06$ and **c** $\kappa = 0.03$ (Kirillov 2011a, b)

The two lines of exceptional points stem from the end points of the interval of marginal stability of the PT - symmetric system and continue inside the asymptotic stability domain of the near-PT-symmetric one (green lines in Fig. 22b).

The proximity of a set of defective eigenvalues to the boundary of the asymptotic stability, that generically is characterized by simple pure imaginary eigenvalues, plays an important role in modern nonconservative physical and mechanical problems. Near this set the eigenvalues can dramatically change their trajectories in the complex plane. For this reason, encountering double eigenvalues with the Jordan block and negative real parts is considered as a precursor to instability.

The full model of Shieh and Masur (20) provides even more non-trivial example. Indeed, its characteristic equation has the form

$$\lambda^4 + (\mu_1 + \mu_2)\lambda^3 + (\mu_1\mu_2 + k_1 + k_2 + 2\Omega^2)\lambda^2 \qquad (118)$$
$$+(k_1\mu_2 + \mu_1 k_2 + 4\Omega\beta - (\mu_1 + \mu_2)\Omega^2)\lambda + (\Omega^2 - k_1)(\Omega^2 - k_2) + \beta^2 = 0.$$

Equation (118) is biquadratic in the case when

$$\mu_1 + \mu_2 = 0, \quad \kappa = -\frac{4\Omega\beta}{\mu_1}, \qquad (119)$$

with $\kappa = k_2 - k_1$. If $k_1 > \Omega^2$ and $\beta > 0$ then all the roots of Eq. (118) are imaginary when

$$2\Omega \le \mu_1 < 0, \quad \frac{4\Omega\beta(k_1 - \Omega^2)}{\beta^2 + (k_1 - \Omega^2)^2} < \mu_1 \le 2\Omega. \qquad (120)$$

In Fig. 23 the imaginary eigenvalues are shown by black lines as functions of the damping parameter μ_1. At

$$\mu_1 = \mu_d := \frac{4\Omega\beta(k_1 - \Omega^2)}{\beta^2 + (k_1 - \Omega^2)^2}, \quad \kappa = \kappa_d := -k_1 + \Omega^2 - \frac{\beta^2}{k_1 - \Omega^2} \qquad (121)$$

there exists a double zero eigenvalue with the Jordan block, see Figs. 23 and 24a. In the interval $0 < \mu_1 < \mu_d$ there exist one positive and one negative real eigenvalue. In Fig. 23 the eigenvalues with non-zero real parts are shown in red. In the (μ_1, μ_2, κ)-space the exceptional points (EPs)

$$(-2\Omega, 2\Omega, 2\beta), \quad (2\Omega, -2\Omega, -2\beta)$$

correspond to the double imaginary eigenvalues with the Jordan block

$$\lambda_{-2\Omega} = \pm i\sqrt{k_1 - \Omega^2 + \beta}, \quad \lambda_{2\Omega} = \pm i\sqrt{k_1 - \Omega^2 - \beta},$$

for $\mu_1 = -2\Omega$ and $\mu_1 = 2\Omega$, respectively.

We see in Fig. 23 that changing the damping parameter μ_1 we migrate from the marginal stability domain to that of flutter instability by means of the collision of the two simple pure imaginary eigenvalues as it happens in gyroscopic or circulatory systems without dissipation. It is remarkable that such a behavior of eigenvalues is observed in the gyroscopic system in the presence of dissipative and non-conservative positional forces.

Let us now establish how in the (μ_1, μ_2, κ)-space the domain of marginal stability given by the expressions (119) and (120) is connected to the domain of asymptotic stability of the Eq. (118). Writing the Liénard and Chipart conditions for asymptotic stability of the polynomial (118) we find

$$\begin{aligned}
p_1 &:= \mu_1 + \mu_2 > 0,\\
p_2 &:= \mu_1\mu_2 + k_1 + k_2 + 2\Omega^2 > 0,\\
p_4 &:= (\Omega^2 - k_1)(\Omega^2 - k_2) + \beta^2 > 0,\\
H_3 &:= (\mu_1 + \mu_2)(\mu_1\mu_2 + k_1 + k_2 + 2\Omega^2)\\
&\quad \times \left(k_1\mu_2 + \mu_1 k_2 + 4\Omega\beta - (\mu_1 + \mu_2)\Omega^2\right)\\
&\quad - (\mu_1 + \mu_2)^2((\Omega^2 - k_1)(\Omega^2 - k_2) + \beta^2)\\
&\quad - (k_1\mu_2 + \mu_1 k_2 + 4\Omega\beta - (\mu_1 + \mu_2)\Omega^2)^2 > 0.
\end{aligned} \tag{122}$$

The surfaces $p_4 = 0$ and $H_3 = 0$ are plotted in Fig. 24a. The former is simply a horizontal plane that passes through the point of the double zero eigenvalue with the coordinates $(\mu_d, -\mu_d, \kappa_d)$ and thus bounds the stability domain from below. The surface $H_3 = 0$ is singular because it has self-intersections along the portions of the hyperbolic curves (119) selected by the inequalities (120). The curve of self-intersection that corresponds to $\kappa > 0$ ends up at the EP with the double pure imaginary eigenvalue $\lambda_{-2\Omega}$.

Another curve of self-intersection has at its ends the EP with the double pure imaginary eigenvalue $\lambda_{2\Omega}$ and the point of the double zero eigenvalue, 0^2. In Fig. 24a the curves of self-intersection are shown in red and the EP and 0^2 are marked by the black and white circles, respectively. At the point 0^2 the surfaces $p_4 = 0$ and $H_3 = 0$ intersect each other forming a trihedral angle singularity of the stability boundary

with its edges depicted by red lines in Fig. 24a. The surface $H_3 = 0$ is symmetric with respect to the plane $p_1 = 0$. Thus, a part of it that belongs to the subspace $p_1 > 0$ bounds the domain of asymptotic stability.

At the EPs, the boundary of the asymptotic stability domain has singular points that are locally equivalent to the Whitney umbrella singularity. Between the two EPs the surface $H_3 = 0$ has an opening around the origin that separates its two sheets. This window allows the flutter instability to exist in the vicinity of the origin for small damping coefficients and small separation of the stiffness coefficients κ.

In Fig. 24b a cross-section of the surface $H_3 = 0$ by the horizontal plane that passes through the lower exceptional point is shown. The domain in grey indicates the area of asymptotic stability. Its boundary has a cuspidal point singularity at the EP. Although the very singular shape of the planar stability domain is typical in the vicinity of the EP with the pure imaginary double eigenvalue with the Jordan block, the unusual feature is the location of the EP that corresponds to non-vanishing damping coefficients, Fig. 24b.

According to the theorems of (Bottema, 1955; Lakhadanov, 1975) the undamped gyroscopic system with non-conservative positional forces is generically unstable, see e.g. Beletsky (1995), Kirillov (2013a). By examining the slices of the surface $H_3 = 0$ at various values of κ one can see that the origin is indeed always unstable, Fig. 24b, c. At $\kappa = 0$ the origin is unstable in the presence of the non-conservative positional forces even when the rotation is absent ($\Omega = 0$) according to the Merkin theorem. Contrary to the situation known as the Ziegler–Bottema destabilization paradox, in the Shieh–Masur model the tending of the damping coefficients to zero along a path in the (μ_1, μ_2)-plane cannot lead to the set of pure imaginary spectrum of the undamped system because in this model such a set corresponds to the non-vanishing damping coefficients.

Therefore, the Shieh–Masur model provides a nontrivial example of a gyroscopic system that can have all its eigenvalues pure imaginary in the presence of dissipative and circulatory forces. The highly non-trivial shape of the discovered stability boundary illustrates the peculiarities of stability of a system loaded by non-conservative positional forces in their interplay with the dissipative, gyroscopic and potential ones.

6.2 *Two-Mass-Skate (TMS) Model of a Bicycle*

Kooijman et al. (2011) considered a reduced model of a bicycle with vanishing radii of the wheels (that are replaced by skates), known under the name of the two-mass-scate (TMS) bicycle. The deviation from the straight vertical equilibrium is described by the leaning angle of the frame and the steering angle of the front wheel/skate that are governed by the following system of two linear equations

$$\mathbf{M}\ddot{\mathbf{x}} + v\mathbf{D}\dot{\mathbf{x}} + g\mathbf{K}\mathbf{x} + v^2\mathbf{N}\mathbf{x} = 0, \tag{123}$$

where dot denotes time differentiation,

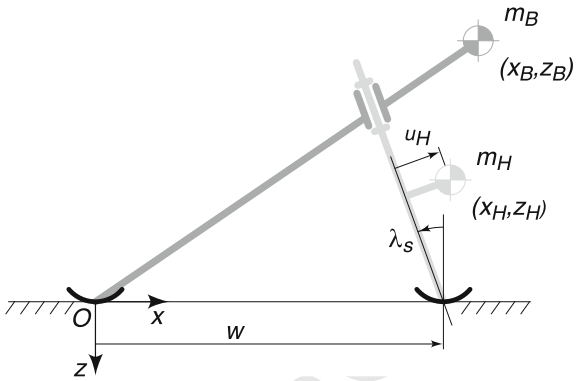

Fig. 25 The two-mass-skate bicycle model (Kooijman et al. 2011)

$$\mathbf{M} = \begin{pmatrix} m_B z_B^2 + m_H z_H^2 & -m_H u_H z_H \\ -m_H u_H z_H & m_H u_H^2 \end{pmatrix},$$

$$\mathbf{D} = \begin{pmatrix} 0 & -(m_B x_B z_B + m_H x_H z_H)/\hat{w} \\ 0 & (m_H u_H x_H)/\hat{w} \end{pmatrix},$$

$$\mathbf{K} = \begin{pmatrix} m_B z_B + m_H z_H & -m_H u_H \\ -m_H u_H & -m_H u_H sin\lambda_s \end{pmatrix},$$

$$\mathbf{N} = \begin{pmatrix} 0 & -(m_B z_B + m_H z_H)/\hat{w} \\ 0 & (m_H u_H)/\hat{w} \end{pmatrix}, \tag{124}$$

$u_H = (x_H - w)\cos\lambda_s - z_H \sin\lambda_s$, $\hat{w} = w/\cos\lambda_s$ and g denotes the gravity acceleration.

The model (123), (124) is nonconservative, containing dissipative, gyroscopic, potential and circulatory forces. Curiously enough, Eq. (123) has a form that is typical in many *fluid-structure interactions* problems, where the parameter v would correspond to the velocity of the flow either inside of a flexible pipe or around a flexible structure (Mandre and Mahadevan 2010; Paidoussis 2016). This similarity in the mathematical description suggests an analogy between the *weaving bicycle* and *fluttering flag*, which is not very obvious.

In fact, Eq. (123) depends on 9 dimensional parameters:

$$w, \quad v, \quad \lambda_s, \quad m_B, \quad x_B, \quad z_B, \quad m_H, \quad x_H, \quad z_H$$

that represent, respectively, the wheel base, velocity of the bicycle, steer axis tilt, rear frame assembly (B) mass, horizontal and vertical coordinates of the rear frame assembly center of mass, front fork and handlebar assembly (H) mass, and horizontal and vertical coordinates of the front fork and handlebar assembly center of mass.

Choosing the wheelbase, w, as a unit of length, and introducing the Froude number, Fr, we find that, actually, the model depends on the following *seven* dimensionless parameters:

$$\mathrm{Fr} = \frac{v}{\sqrt{gw}}, \quad \mu = \frac{m_H}{m_B}, \quad \xi_B = \frac{x_B}{w}, \quad \xi_H = \frac{x_H}{w}, \quad \zeta_B = \frac{z_B}{w}, \quad \zeta_H = \frac{z_H}{w}, \quad \lambda_s.$$

We can assume that for realistic bicycles $0 \le \mu \le 1$. Notice that $\zeta_B \le 0$ and $\zeta_H \le 0$ due to choice of the system of coordinates, Fig. 25.

Assuming the solution $\sim \exp(\sigma t)$ and introducing the dimensionless time $\tau = \sqrt{\frac{g}{w}}t$ such that the dimensionless eigenvalue is $s = \sigma\sqrt{\frac{w}{g}}$, we write the characteristic polynomial of the TMS bicycle model:

$$p(s) = a_0 s^4 + a_1 s^3 + a_2 s^2 + a_3 s + a_4,$$

with the coefficients

$$\begin{aligned}
a_0 &= -(\zeta_H \tan\lambda_s - \xi_H + 1)\zeta_B^2,\\
a_1 &= \mathrm{Fr}(\zeta_B\xi_H - \zeta_H\xi_B)\zeta_B,\\
a_2 &= \mathrm{Fr}^2(\zeta_B - \zeta_H)\zeta_B - \zeta_B(\zeta_B + \zeta_H)\tan\lambda_s - (\xi_H - 1)(\mu\zeta_H - \zeta_B),\\
a_3 &= -\mathrm{Fr}(\xi_B - \xi_H)\zeta_B,\\
a_4 &= -\zeta_B \tan\lambda_s - \mu(\xi_H - 1).
\end{aligned} \tag{125}$$

Notice that in the case when the coordinates of the masses m_B and m_H coincide:

$$\xi_H = \xi_B, \quad \zeta_H = \zeta_B$$

the characteristic polynomial simplifies and factorizes as

$$p(s) = -(s^2\zeta_B + 1)(\zeta_B(\zeta_B \tan\lambda_s - \xi_B + 1)s^2 + \zeta_B \tan\lambda_s + \mu(\xi_B - 1)).$$

Since $\zeta_B < 0$ by definition, this immediately yields static instability (growth of the leaning angle yielding *capsizing* of the bike).

Asymptotic Stability and Critical Froude Number

We study linear stability of the TMS bicycle with the Lienard–Chipart version of the Routh–Hurwitz criterion (Kirillov 2013a). First, compute the Hurwitz determinants of the characteristic polynomial

$$\begin{aligned}
h_1 &= \mathrm{Fr}(\zeta_B\xi_H - \zeta_H\xi_B)\zeta_B,\\
h_2 &= \mathrm{Fr}\zeta_B f,\\
h_3 &= -\mathrm{Fr}^2\zeta_B^2(\zeta_B - \zeta_H)h,\\
h_4 &= \mathrm{Fr}^2\zeta_B^2(\zeta_B - \zeta_H)(\tan(\lambda_s)\zeta_B + \mu\xi_H - \mu)h,
\end{aligned} \tag{126}$$

where

$$f = -\zeta_B(\zeta_B^2\xi_H - \zeta_H^2\xi_B)\tan\lambda_s - \zeta_H(\xi_H - 1)(\zeta_B\xi_H - \zeta_H\xi_B)\mu + \zeta_B(\zeta_B - \zeta_H)(\zeta_B\xi_H - \zeta_H\xi_B)\mathrm{Fr}^2 + \zeta_B\xi_B(\xi_H - 1)(\zeta_B - \zeta_H) \quad (127)$$

and

$$h = -\zeta_B\xi_B\xi_H(\zeta_B - \zeta_H)\tan\lambda_s - \xi_H(\xi_H - 1)(\zeta_B\xi_H - \zeta_H\xi_B)\mu + \zeta_B(\xi_B - \xi_H)(\zeta_B\xi_H - \zeta_H\xi_B)\mathrm{Fr}^2 + \zeta_B\xi_B(\xi_H - 1)(\xi_B - \xi_H). \quad (128)$$

The Lienard–Chipart criterion requires that

$$a_4 > 0, \quad a_3 > 0, \quad a_1 > 0, \quad a_0 > 0, \quad h_1 > 0, \quad h_3 > 0.$$

The relation $h_1 = a_1$ eliminates one of the inequalities and in view of that $\mu > 0$, $\zeta_B < 0$, and $\xi_B > 0$ yields the following explicit conditions

$$\begin{aligned} \xi_H &> 1 + \zeta_H \tan\lambda_s \\ \xi_H &< 1 - \frac{\zeta_B}{\mu}\tan\lambda_s \\ \xi_H &< \xi_B \\ \zeta_H &> \zeta_B \\ \mathrm{Fr} &> \mathrm{Fr}_c > 0, \end{aligned} \quad (129)$$

where the critical Froude number at the stability boundary is given by the expression

$$\mathrm{Fr}_c^2 = \frac{\zeta_B - \zeta_H}{\xi_B - \xi_H}\frac{\xi_B\xi_H}{\zeta_B\xi_H - \zeta_H\xi_B}\tan\lambda_s + \frac{\xi_H - 1}{\xi_B - \xi_H}\frac{\xi_H}{\zeta_B}\mu - \frac{(\xi_H - 1)\xi_B}{\zeta_B\xi_H - \zeta_H\xi_B} \quad (130)$$

that follows from the condition $h = 0$.

At $0 \le \mathrm{Fr} < \mathrm{Fr}_c$ the bicycle is unstable by flutter demonstrating the *weaving* motion (Kooijman et al. 2011)

Critical Fr for the Benchmark Bikes of Kooijman et al. (2011)

For the design determined by

$$w = 1\,\mathrm{m}, \quad \lambda_s = \frac{5\pi}{180}\,\mathrm{rad}, \quad m_H = 1\,\mathrm{kg}, \quad m_B = 10\,\mathrm{kg},$$

$$x_B = 1.2\,\mathrm{m}, \quad x_H = 1.02\,\mathrm{m}, \quad z_B = -0.4\,\mathrm{m}, \quad z_H = -0.2\,\mathrm{m}$$

the critical Froude number is

$$\mathrm{Fr}_1 = 0.9070641497, \quad (131)$$

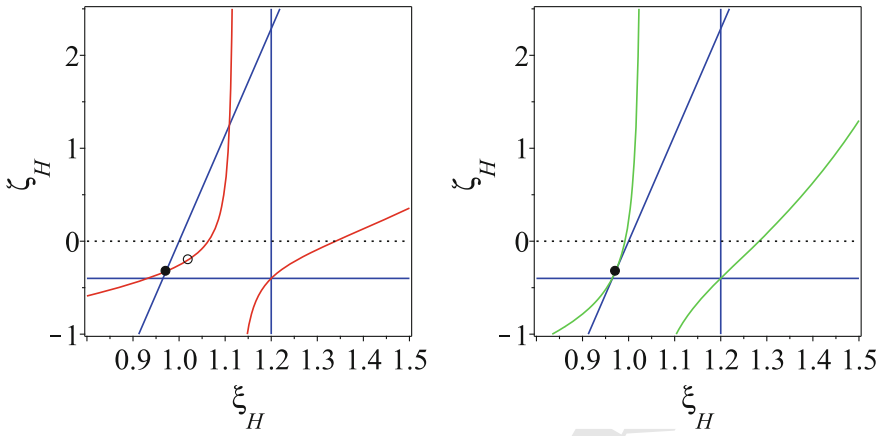

Fig. 26 For $w = 1\,\text{m}$, $\lambda_s = \frac{5\pi}{180}\,\text{rad}$, $m_H = 1\,\text{kg}$, $m_B = 10\,\text{kg}, x_B = 1.2\,\text{m}, z_B = -0.4\,\text{m}$ (left) stability diagram at $\text{Fr} = \text{Fr}_1 = 0.9070641497$ with the circle corresponding to $x_H = 1.02\,\text{m}$ and $z_H = -0.2\,\text{m}$; (right) stability diagram at $\text{Fr} = \text{Fr}_{min} = 0.6999527422$. Black circle denotes a point with the coordinates (0.9716634870,–0.3238878290) given by (135)

which corresponds to the critical velocity of weaving

$$v_1 = 2.841008324\,\text{m/s} \tag{132}$$

in accordance with the original result by Kooijman et al. (2011).

For the alternative design determined by

$$w = 1\,\text{m}, \quad \lambda_s = -\frac{5\pi}{180}\,\text{rad}, \quad m_H = 1\,\text{kg}, \quad m_B = 10\,\text{kg},$$

$$x_B = 0.85\,\text{m}, \quad x_H = 1\,\text{m}, \quad z_B = -0.2\,\text{m}, \quad z_H = -0.4\,\text{m}$$

the critical Froude number is

$$\text{Fr}_2 = 0.8415708896, \tag{133}$$

which corresponds to the critical velocity of weaving

$$v_2 = 2.635877411\,\text{m/s} \tag{134}$$

in accordance with the original result by Kooijman et al. (2011). Notice that careful analysis of the Lienard-Chipart criteria for the TMS bicycle proves the existence of just two classes of self-stable TMS bikes that differ by the sign of λ_s, see Austin Sydes (2018).

Finding Designs that Minimize the Critical Fr

Let us fix λ_s, ξ_B, ζ_B, and μ and plot the stability domain specified by Eq. (129) in the (ξ_H, ζ_H) - plane at different values of Fr, Fig. 26.

This yields a vertical line $\xi_H = \xi_B$, a horizontal line $\zeta_H = \zeta_B$ and an inclined line $\xi_H = 1 + \zeta_H \tan\lambda_s$ that form a rectangular triangle in the (ξ_H, ζ_H) - plane, Fig. 26. There is no stability outside of this triangle. On the other hand the condition $\mathrm{Fr} = \mathrm{Fr}_c$ defines two hyperbola-like curves, one of which always passes through the right lower corner of the triangle and the other one always passes through a point on the hypotenuse of the triangle shown by a black circle in Fig. 26. Solving simultaneously equations $\xi_H = 1 + \zeta_H \tan\lambda_s$ and $\mathrm{Fr} = \mathrm{Fr}_c$ we find the coordinates of this point to be

$$\xi_H = \frac{-\xi_B}{\zeta_B \tan\lambda_s - \xi_B}, \quad \zeta_H = \frac{-\zeta_B}{\zeta_B \tan\lambda_s - \xi_B}. \tag{135}$$

If we take, for instance

$$\begin{array}{lll} w = 1\,\mathrm{m}, & \lambda_s = \frac{5\pi}{180}\,\mathrm{rad}, & m_H = 1\,\mathrm{kg}, \qquad m_B = 10kg, \\ & x_B = 1.2\,\mathrm{m}, & z_B = -0.4\,\mathrm{m}, \end{array} \tag{136}$$

the branch of the curve $\mathrm{Fr} = \mathrm{Fr}_c$ passing through the point (135) with the coordinates $(0.9716634870, -0.3238878290)$ lies partially inside the triangle, Fig. 26(left). The area between this part and the hypotenuse is the stability domain, which for the TMS bicycle is further restricted by the condition $\zeta_H < 0$.

Can we change the design in order to minimize the critical Froude number? If we plot the curve $\mathrm{Fr}_c(\xi_H, \zeta_H) = \mathrm{Fr}$ at different values of Fr, we will see that the portion of its branch passing through the point (135) and lying in the triangle tends to get smaller as Fr decreases. At some Fr_{min} the branch is tangent to the hypotenuse at the point (135), and the stability domain disappears, Fig. 26(right).

Therefore, the design specified by the conditions (135) gives the minimum possible Froude number, beyond which the TMS bike becomes stable:

$$\mathrm{Fr}^2_{min} = \frac{(\zeta_B \tan\lambda_s - \xi_B)^2 + \mu}{(\zeta_B \tan\lambda_s - \xi_B)(\zeta_B \tan\lambda_s - \xi_B + 1)} \tan\lambda_s.$$

For instance, if we take parameters as in (136) and use (135) to find $x_H = 0.9716634870\,\mathrm{m}$ and $z_H = -0.3238878290\,\mathrm{m}$, then we obtain the minimal Froude number and the corresponding velocity of weaving

$$\mathrm{Fr}_{min} = 0.6999527422, \quad v_{min} = 2.192316351\,\mathrm{m/s}$$

that indeed are smaller then that given by (131) and (132) for the benchmark TMS bike in Kooijman et al. (2011).

References

N. Andersson, Gravitational waves from instabilities in relativistic stars. Class. Quantum Grav. **20**, R105–R144 (2003)

I.P. Andreichikov, V.I. Yudovich, The stability of visco-elastic rods. Izv. Akad. Nauk SSSR. Mekhanika Tverdogo Tela. **9**(2), 78–87 (1974)

S. Aoi, Y. Egi, K. Tsuchiya, Instability-based mechanism for body undulations in centipede locomotion. Phys. Rev. E **87**, 012717 (2013)

V.I. Arnold, Lectures on bifurcations in versal families. Russ. Math. Surv. **27**, 54–123 (1972)

G.L. Austin Sydes, *Self-stable bicycles*. Bsc (Hons) mathematics final year project report. (Northumbria University, Newcastle upon Tyne, UK, 2018)

P.V. Bayly, S.K. Dutcher, Steady dynein forces induce flutter instability and propagating waves in mathematical models of flagella. J. R. Soc. Interface **13**, 20160523 (2016)

M. Beck, Die Knicklast des einseitig eingespannten, tangential gedruckten Stabes. Z. angew. Math. Phys. **3**, 225–228 (1952)

V.V. Beletsky, Some stability problems in applied mechanics. Appl. Math. Comput. **70**, 117–141 (1995)

M.V. Berry, P. Shukla, Curl force dynamics: symmetries, chaos and constants of motion. New J. Phys. **18**, 063018 (2016)

D. Bigoni, G. Noselli, Experimental evidence of flutter and divergence instabilities induced by dry friction. J. Mech. Phys. Sol. **59**, 2208–2226 (2011)

D. Bigoni, D. Misseroni, M. Tommasini, O.N. Kirillov, G. Noselli, Detecting singular weak-dissipation limit for flutter onset in reversible systems. Phys. Rev. E **97**(2), 023003 (2018)

A.M. Bloch, P.S. Krishnaprasad, J.E. Marsden, T.S. Ratiu, Dissipation induced instabilities. Annales de L'Institut Henri Poincare - Analyse Non Lineaire **11**, 37–90 (1994)

V.V. Bolotin, *Nonconservative Problems of the Theory of Elastic Stability* (Pergamon Press, Oxford, 1963)

A.V. Borisov, A.A. Kilin, I.S. Mamaev, The Hamiltonian dynamics of self-gravitating liquid and gas ellipsoids. Reg. Chaotic Dyn. **14**(2), 179–217 (2009)

O. Bottema, On the stability of the equilibrium of a linear mechanical system, ZAMP Z. Angew. Math. Phys. **6**, 97–104 (1955)

O. Bottema, The Routh-Hurwitz condition for the biquadratic equation. Indag. Math. (Proc.) **59**, 403–406 (1956)

R.M. Bulatovic, A sufficient condition for instability of equilibrium of nonconservative undamped systems. Phys. Lett. A **375**, 3826–3828 (2011)

R.M. Bulatovic, A stability criterion for circulatory systems. Acta Mech. **228**(7), 2713–2718 (2017)

S. Chandrasekhar, *Ellipsoidal Figures of Equilibrium* (Yale University Press, New Haven, 1969)

S. Chandrasekhar, Solutions of two problems in the theory of gravitational radiation. Phys. Rev. Lett. **24**(11), 611–615 (1970)

S. Chandrasekhar, On stars, their evolution and their stability. Science **226**(4674), 497–505 (1984)

G. De Canio, E. Lauga, R.E. Goldstein, Spontaneous oscillations of elastic filaments induced by molecular motors. J. R. Soc. Interface **14**, 20170491 (2017)

P. Gallina, About the stability of non-conservative undamped systems. J. Sound Vibr. **262**, 977–988 (2003)

V.L. Ginzburg, V.N. Tsytovich, Several problems of the theory of transition radiation and transition scattering. Phys. Rep. **49**(1), 1–89 (1979)

G. Gladwell, Follower forces - Leipholz early researches in elastic stability. Can. J. Civil Eng. **17**, 277–286 (1990)

A.G. Greenhill, On the rotation required for the stability of an elongated projectile. Min. Proc. R. Artill. Inst. **X**(7), 577–593 (1879)

A.G. Greenhill, On the general motion of a liquid ellipsoid under the gravitation of its own parts. Proc. Camb. Philos. Soc. **4**, 4–14 (1880)

A.G. Greenhill, Determination of the greatest height consistent with stability that a vertical pole or must can be made, and of the greatest height to which a tree of given proportions can grow. Proc. Camb. Philos. Soc. **4**, 65–73 (1881)
A.G. Greenhill, On the strength of shafting when exposed both to torsion and to end thrust. Proc. Inst. Mech. Eng. **34**, 182–225 (1883)
P. Hagedorn, E. Heffel, P. Lancaster, P.C. Müller, S. Kapuria, Some recent results on MDGKN-systems. ZAMM - Z. Angew. Math. Mech. **95**(7), 695–702 (2014)
P.L. Kapitsa, Stability and passage through the critical speed of the fast spinning rotors in the presence of damping. Z. Tech. Phys. **9**, 124–147 (1939)
M.A. Karami, D.J. Inman, Equivalent damping and frequency change for linear and nonlinear hybrid vibrational energy harvesting systems. J. Sound Vibr. **330**, 5583–5597 (2011)
A.L. Kimball, Internal friction as a cause of shaft whirling. Phil. Mag. **49**, 724–727 (1925)
O.N. Kirillov, Gyroscopic stabilization in the presence of nonconservative forces. Doklady Math. **76**(2), 780–785 (2007)
O.N. Kirillov, Campbell diagrams of weakly anisotropic flexible rotors. Proc. R. Soc. A **465**(2109), 2703–2723 (2009)
O.N. Kirillov, Eigenvalue bifurcation in multiparameter families of non-self-adjoint operator matrices. ZAMP - Z. Angew. Math. Phys. **61**, 221–234 (2010)
O.N. Kirillov, Sensitivity of sub-critical mode-coupling instabilities in non-conservative rotating continua to stiffness and damping modifications. Int. J. Vehicle Struct. Syst. **3**(1), 1–13 (2011a)
O.N. Kirillov, Brouwer's problem on a heavy particle in a rotating vessel: wave propagation, ion traps, and rotor dynamics. Phys. Lett. A **375**, 1653–1660 (2011b)
O.N. Kirillov, *Nonconservative Stability Problems of Modern Physics* (De Gruyter, Berlin, 2013)
O.N. Kirillov, Stabilizing and destabilizing perturbations of PT-symmetric indefinitely damped systems. Phil. Trans. R. Soc. A **371**, 20120051 (2013)
O.N. Kirillov, Singular diffusionless limits of double-diffusive instabilities in magnetohydrodynamics. Proc. R. Soc. A **473**(2205), 20170344 (2017)
O.N. Kirillov, A.P. Seyranian, Metamorphoses of characteristic curves in circulatory systems. J. Appl. Math. Mech. **66**, 371–385 (2002a)
O.N. Kirillov, A.P. Seyranian, A nonsmooth optimization problem. Moscow Univ. Mech. Bull. **57**, 1–6 (2002b)
O.N. Kirillov, F. Verhulst, Paradoxes of dissipation-induced destabilization or who opened Whitney's umbrella? ZAMM - Z. Angew. Math. Mech. **90**(6), 462–488 (2010)
W. Kliem, C. Pommer, A note on circulatory systems: old and new results. Z. Angew. Math. Mech. **97**, 92–97 (2017)
J.D.G. Kooijman, J.P. Meijaard, J.M. Papadopoulos, A. Ruina, A.L. Schwab, A bicycle can be self-stable without gyroscopic or caster effects. Science **332**(6027), 339–342 (2011)
N.D. Kopachevskii, S.G. Krein, *Operator Approach in Linear Problems of Hydrodynamics. Self-adjoint Problems for an Ideal Fluid*, Operator Theory: Advances and Applications, vol. 1 (Birkhauser, Basel, 2001)
R. Krechetnikov, J.E. Marsden, Dissipation-induced instabilities in finite dimensions. Rev. Mod. Phys. **79**, 519–553 (2007)
V. Lakhadanov, On stabilization of potential systems, Prikl. Mat. Mekh. **39**, 53–58 (1975)
J.S.W. Lamb, J.A.G. Roberts, Time-reversal symmetry in dynamical systems: a survey. Phys. D **112**, 1–39 (1998)
W.F. Langford, Hopf meets Hamilton under Whitneys umbrella, in *IUTAM Symposium on Nonlinear Stochastic Dynamics. Proceedings of the IUTAM Symposium, Monticello, IL, USA, Augsut 26–30, 2002, Solid Mech. Appl.*, vol. 110, ed. S.N. Namachchivaya, pp. 157–165 (Kluwer, Dordrecht, 2003)
N.R. Lebovitz, Binary fission via inviscid trajectories. Geoph. Astroph. Fluid. Dyn. **38**(1), 15–24 (1987)
N.R. Lebovitz, The mathematical development of the classical ellipsoids. Int. J. Eng. Sci. **36**(12), 1407–1420 (1998)

H. Leipholz, *Stability Theory: an Introduction to the Stability of Dynamic Systems and Rigid Bodies*, 2nd edn. (Teubner, Stuttgart, 1987)
L. Lindblom, S.L. Detweiler, On the secular instabilities of the Maclaurin spheroids. Astrophys. J. **211**, 565–567 (1977)
A. Luongo, M. Ferretti, Postcritical behavior of a discrete Nicolai column. Nonlin. Dyn. **86**, 2231–2243 (2016)
A. Luongo, M. Ferretti, F. D'Annibale, Paradoxes in dynamic stability of mechanical systems: investigating the causes and detecting the nonlinear behaviors. Springer Plus **5**, 60 (2016)
A.M. Lyapunov, The general problem of the stability of motion (translated into English by A. T. Fuller). Int. J. Control **55**, 531–773 (1992)
R.S. MacKay, Movement of eigenvalues of Hamiltonian equilibria under non-Hamiltonian perturbation. Phys. Lett. A **155**, 266–268 (1991)
O. Mahrenholtz, R. Bogacz, On the shape of characteristic curves for optimal structures under non-conservative loads. Arch. Appl. Mech. **50**, 141–148 (1981)
S. Mandre, L. Mahadevan, A generalized theory of viscous and inviscid flutter. Proc. R. Soc. Lond. A **466**, 141–156 (2010)
D.R. Merkin, *Gyroscopic Systems* (Gostekhizdat, Moscow, 1956) [in Russian]
N.N. Moiseyev, V.V. Rumyantsev, *Dynamic Stability of Bodies Containing Fluid* (Springer, New York, 1968)
M.V. Nezlin, Negative-energy waves and the anomalous Doppler effect. Sov. Phys. Uspekhi **19**, 946–954 (1976)
E.L. Nicolai, On the stability of the rectilinear form of equilibrium of a bar in compression and torsion. Izvestia Leningradskogo Politechnicheskogo Instituta **31**, 201–231 (1928)
E.L. Nicolai, On the problem of the stability of a bar in torsion. Vestnik Mechaniki i Prikladnoi Matematiki **1**, 41–58 (1929)
O.M. O'Reilly, N.K. Malhotra, N.S. Namachchivaya, Reversible dynamical systems - dissipation-induced destabilization and follower forces. Appl. Math. Comput. **70**, 273–282 (1995)
O.M. O'Reilly, N.K. Malhotra, N.S. Namachchivaya, Some aspects of destabilization in reversible dynamical systems with application to follower forces. Nonlinear Dyn. **10**, 63–87 (1996)
L.A. Ostrovskii, S.A. Rybak, L.S. Tsimring, Negative energy waves in hydrodynamics. Sov. Phys. Usp. **29**, 1040–1052 (1986)
M.P. Païdoussis, *Fluid-Structure Interactions*, 2nd edn. (Academic Press, Oxford, 2016)
D. Phillips, S. Simpson, S. Hanna, Chapter 3 - optomechanical microtools and shape-induced forces, in *Light Robotics: Structure-Mediated Nanobiophotonics*, ed. by J. Glückstad, D. Palima (Elsevier, Amsterdam, 2017), pp. 65–98
L. Pigolotti, C. Mannini, G. Bartoli, Destabilizing effect of damping on the post-critical flutter oscillations of flat plates. Meccanica **52**(13), 3149–3164 (2017)
S.M. Ramodanov, V.V. Sidorenko, Dynamics of a rigid body with an ellipsoidal cavity filled with viscous fluid. Int. J. Non-Lin. Mech. **95**, 42–46 (2017)
P.H. Roberts, K. Stewartson, On the stability of a Maclaurin spheroid with small viscosity. Astrophys. J. **139**, 777–790 (1963)
A. Rohlmann, T. Zander, M. Rao, G. Bergmann, Applying a follower load delivers realistic results for simulating standing. J. Biomech. **42**, 1520–1526 (2009)
S. Ryu, Y. Sugiyama, Computational dynamics approach to the effect of damping on stability of a cantilevered column subjected to a follower force. Comput. Struct. **81**, 265–271 (2003)
S.S. Saw, W.G. Wood, The stability of a damped elastic system with a follower force. J. Mech. Eng. Sci. **17**(3), 163–176 (1975)
J. Schindler, A. Li, M.C. Zheng, F.M. Ellis, T. Kottos, Experimental study of active LRC circuits with PT symmetries. Phys. Rev. A **84**, 040101(R) (2011)
A.P. Seyranian, A.A. Mailybaev, Paradox of Nicolai and related effects. Z. angew. Math. Phys. **62**, 539–548 (2011)
R.C. Shieh, E.F. Masur, Some general principles of dynamic instability of solid bodies. Z. Angew. Math. Phys. **19**, 927–941 (1968)

S.H. Simpson, S. Hanna, First-order nonconservative motion of optically trapped nonspherical particles. Phys. Rev. E. **82**, 031141 (2010)
D.M. Smith, The motion of a rotor carried by a flexible shaft in flexible bearings. Proc. R. Soc. Lond. A **142**, 92–118 (1933)
K. Stewartson, On the stability of a spinning top containing liquid. J. Fluid Mech. **5**, 577–592 (1959)
Y. Sugiyama, K. Kashima, H. Kawagoe, On an unduly simplified model in the non-conservative problems of elastic stability. J. Sound Vib. **45**(2), 237–247 (1976)
S. Sukhov, A. Dogariu, Non-conservative optical forces. Rep. Prog. Phys. **80**, 112001 (2017)
T. Theodorsen, General theory of aerodynamic instability and the mechanism of flutter. Technical Report no. 496. National Advisory Commitee for Aeronautics (NACA) (1935)
W. Thomson, On an experimental illustration of minimum energy. Nature **23**, 69–70 (1880)
W. Thomson, P.G. Tait, *Treatise on Natural Philosophy* (Cambridge University Press, Cambridge, 1879)
M. Tommasini, O.N. Kirillov, D. Misseroni, D. Bigoni, The destabilizing effect of external damping: singular flutter boundary for the Pflüger column with vanishing external dissipation. J. Mech. Phys. Sol. **91**, 204–215 (2016)
F.E. Udwadia, Stability of dynamical systems with circulatory forces: generalization of the Merkin theorem. AIAA J. **55**(9), 2853–2858 (2017)
A.I. Vesnitskii, A.V. Metrikin, Transition radiation in mechanics. Phys.-Uspekhi **39**(10), 983–1007 (1996)
P. Wu, R. Huang, C. Tischer, A. Jonas, E.-L. Florin, Direct measurement of the nonconservative force field generated by optical tweezers. Phys. Rev. Lett. **103**, 108101 (2009)
V.A. Yakubovich, V.M. Starzinskii, *Linear Differential Equations with Periodic Coefficients*, vols. 1 and 2 (Wiley, New York, 1975)
R. Zhang, H. Qin, R.C. Davidson, J. Liu, J. Xiao, On the structure of the two-stream instability-complex G-Hamiltonian structure and Krein collisions between positive- and negative-action modes. Physics of Plasmas **23**, 072111 (2016)
V.F. Zhuravlev, Decomposition of nonlinear generalized forces into potential and circulatory components. Doklady Phys. **52**, 339–341 (2007)
V.F. Zhuravlev, Analysis of the structure of generalized forces in the Lagrange equations. Mech. Solids **43**, 837–842 (2008)
H. Ziegler, Stabilitätsprobleme bei geraden Stäben und Wellen. Z. angew. Math. Phys. **2**, 265–289 (1951a)
H. Ziegler, Ein nichtkonservatives Stabilitätsproblem. Z. angew. Math. Math. **8**(9), 265–266 (1951b)
H. Ziegler, Die Stabilitätskriterien der Elastomechanik. Arch. Appl. Mech. **20**, 49–56 (1952)
H. Ziegler, Linear elastic stability. A critical analysis of methods. First part. ZAMP Z. angew. Math. Phys. **4**, 89–121 (1953a)
H. Ziegler, Linear elastic stability. A critical analysis of methods, Second part. ZAMP Z. angew. Math. Phys. **4**, 167–185 (1953b)
H. Ziegler, On the concept of elastic stability. Adv. Appl. Mech. **4**, 351–403 (1956)
V.I. Zubov, Canonical structure of the vector force field, in *Problems of Mechanics of Deformable Solid Bodies – Special issue dedicated to the 60th Birthday of Acad. V. V. Novozhilov* (Sudostroenie, Leningrad, 1970), pp. 167–170. [in Russian]